Proceedings of International Conference
Applications of Structural Fire Engineering
Prague, 29 April 2011

Session 6

Fire Testing

PREDICTION OF TEMPERATURE VARIATION IN AN EXPERIMENTAL BUILDING

Xudong Cheng [a,b], Milan Veljkovic [a], Alexandra Byström [a], Naveed Iqbal [a], Joakim Sandström [a,c], Ulf Wickström [a,d]

[a] Division of Structural Engineering –Steel Structures, Luleå University of Technology, Luleå, Sweden
[b] State Key Laboratory of Fire Science, University of Science and Technology of China, Hefei, China
[c] Brandskyddslaget AB, Karlstad Sweden
[d] Swedish National Testing and Research Institute (SP), Borås, Sweden

INTRODUCTION

In view of recent large fires in tall buildings, structures have been observed to have easily lost stability or even collapse during fire. To understand such events, structural behavior under fire loading is more and more of a concern for researchers. Some numerical models have been developed to simulate the behavior of isolated structural components, but lack of validation with full-scale experimental data limit the use of models in fire safety design of structures (Buchanan, 2001 and Usmani et al, 2001). A series of fire resistance tests have been carried out during the last decade. Liu (Liu et al, 2002) and Buchanan (Buchanan, 2003) have completed some fire tests on isolated structural element, e.g. beams, columns and connections, in furnaces to help the development of design models. Some fire tests on reduced scale frame assemblies have also been conducted by Hosam (Hosam et al, 2004) and Yang (Yang et al, 2006). However, many aspects of structural behavior which occur due to the interaction between adjacent members could not be observed and the structural response of reduced scale models may be different from those of a real structure in fire. It is necessary to carry out some large scale fire tests under real nature fire. Dong (Dong et al, 2009) carried out some full-scale fire experiments of steel composite frames under furnace loading. Wade (Wade et al, 2006, Chlouba et al, 2009 and Wade et al, 2009) investigated the global structural behavior of steel-concrete composite frame building during large-scale natural fire tests at the Cardington laboratory and Mittal Steel Ostrava. Due to the high cost of full-scale fire tests and size limitations of existing furnaces, these valuable fire tests are not easy to be conducted frequently.

Two full-scale fire tests to investigate structural behavior under natural fire will be carried out in a two-storey composite frame building in Jilemnice, Czech Repubulic in September 2011 within the RFCS research project COMPFIRE Design of joints to composite columns for improved fire robustness, RFS-PR-08009. It is necessary to conduct some numerical calculation work to simulate the fire development and obtain prediction of fire development before the real fire tests. Fire dynamics simulator (FDS) is a program, which is frequently used by researchers to simulate different fire scenarios (Ryder et al, 2004 and Pope et al, 2006). In this paper, four fire scenarios with different locations of ignition sources for the full-scale fire test are simulated by FDS without mechanical load. The temperature variation of upper hot smoke layer is also obtained, which is important for the behavior of beam and connection. The effect of ignition on fire development was analyzed.

1 FDS MODEL OF FIRE SCENATIOS

FDS is a large eddy simulation (LES) model, which was developed by the National Institute of Standards and Technology (NIST). The primary assumption behind the LES technique is that the larger scale turbulence that carries the majority of the energy of the system, which needs to be directly resolved in order to accurately represent flow (McGrattan et al, 2010). FDS solves numerically a form of the Navier-Stokes equation appropriate for low-speed, thermally-driven flow with an emphasis on smoke and heat transport from fires.

The dimension of the two-storey composite frame building in Jilemnice is 12 m by 9 m by 8 m. There are five composite columns as shown in figure 1. A steel beam is mounted under the ceiling

and included in the FDS model of the fire. None of the structural components are fire protected. A door and a window are located on the wall for natural ventilation during the fire; the total opening area is 14m^2. The fuel consists of 24 timber cribs with the size of 1.0 m by 1.0 m by 0.6 m are uniformly distributed on the floor as shown in figure 2.

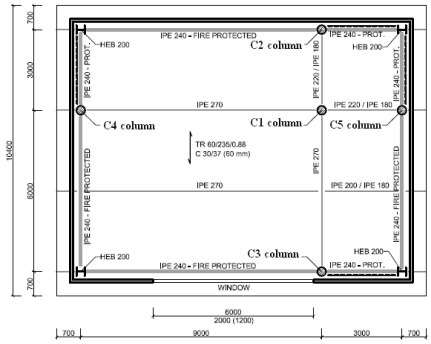

Fig. 1 Ground plan of the building

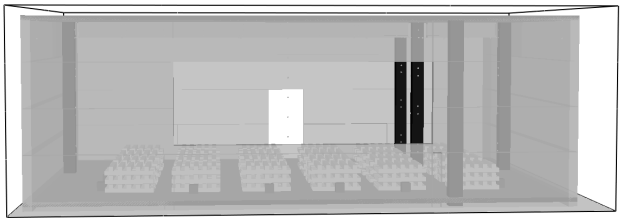

Fig. 2 FDS model of the building (one-storey)

In the FDS model, three different kinds of material are used: concrete, steel and wood. The thermal properties of these materials are shown in table 1, which are assumed to be constant during the fire. The timber crib is ignited by small ignition sources. There are four fire scenarios depending with different locations of the ignition source, such as four sides, center, four corners and one side of the wood fuel stacks. These are named as case1, case2, case3 and case4, respectively, in this paper. The heat release rate of the ignition sources is assumed to be developing in three steps, which linearly increases to the peak at 50 s at first, and keeps that state until 300 s, and at last decreases linearly to zero at 400 s. The approach for describing the pyrolysis here is assuming the solid fuels burn at a specific rate, which is dependent on the properties of the fuel, such as ignition temperature, thickness, heat of vaporization and heat release rate per unit area. The cell size within this model is 0.1 m by 0.1 m by 0.1 m except the area around the steel beam, where it is 0.05 m by 0.05 m by 0.05 m. The computational domain is divided into eight parts, so the parallel FDS calculation is used in these models to save running time.

Tab. 1 Properties of materials used in FDS model

Material	**Density [kg/m^3]**	**Heat conductivity [W/K.m]**	**Specific heat capacity [J/kg.K]**	**Heat of combustion [kJ/kg]**	**Component member**
Wood	400	0.2	1300	18000	fuel
Steel	7850	46.0	460	/	Column, beam
Concrete	2100	2.0	950	/	wall, ceiling, column

2 RESULTS AND DISCUSS

2.1 Heat Release Rate

Figure 3 shows the heat release rate (HRR) curves of the four different fire cases. The natural fire development process included four basic stages: ignition stage, fire growth stage, fully developed stage and decay stage. The fire develops as t-square fire model with different fire growth rates in the four fire cases. There are a series of small ignitions around the wood fuels in case 1, which can be seen from figure 2. The outer timber cribs are ignited at the same time, which probably will be used in real fire test. The fire develops so quickly that flashover appears at about 500 s, and the fire growth rate is about 32 W/s^2. In case 2 and case 3, the fire spreads from center and four corners, respectively, through various directions. There are no obvious differences between these two cases. The fire growth rate is about 5.4 W/s^2. In case 4, the fuels are ignited along one side and the fire travells from left to right. The fire develops very slowly with low fire spread rate. All the fuels are ignited after 3500s, and the fire growth rate of this case is only about 0.2 W/s^2, which is much lower than that of the other three cases because of the initial ignition condition.

The peak values of heat release rate in four cases are almost the same, which are about 26 MW. The period of fully developed stage is about 800 s. During this period, the compartment is nearly full of hot smoke, and the fire is controlled by the ventilation conditions. The peak value of heat release rate could also be calculated by *eq. (1)* (Karlsson et al, 2000), which assumes complete combustion of all the oxygen entering the compartment. The peak value from FDS simulation is a little lower than that from hand calculation, which should be caused by complete combustion assumption of oxygen. The performances of structural components are degraded and most buildings may collapse during this period. As the fuel consuming, the fire turns into the decay stage.

$$Q_{peak} \approx 1500 A_0 \sqrt{H_0} = 1500 \times 14 \times \sqrt{2} kW \approx 29674 kW = 29.67 MW \quad (1)$$

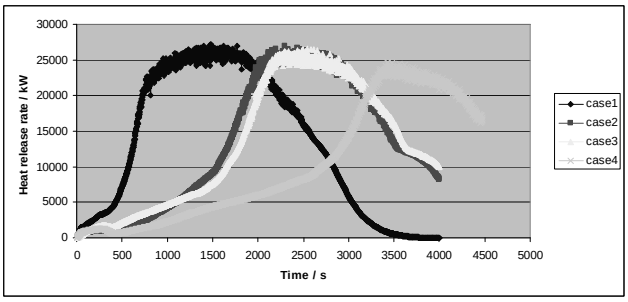

Fig. 3 Heat release rate of four fire cases

2.2 Hot Smoke Temperature

During the fire development, there are two main layers in the compartment: hot smoke layer and cold air layer. The temperature of hot smoke layer is the boundary condition of beam, ceiling, connections and others. Figure 4 gives the results of hot smoke temperatures of the four fire cases. The thermocouple sensor in FDS model is positioned in the center of compartment and 200 mm below the ceiling. The temperature values for the four fire cases reaches to about 600°C before flashover with different increasing rates. During the fully developed stage, hot smoke temperature continues to increase with lower rate. The final peak value reaches to about 900°C, which is similar with the temperature in a standard fire test.

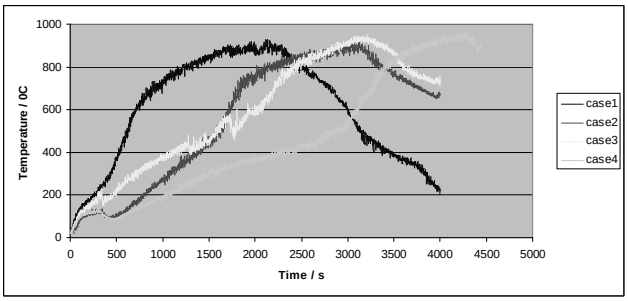

Fig. 4 Hot smoke temperatures in four fire cases (center position)

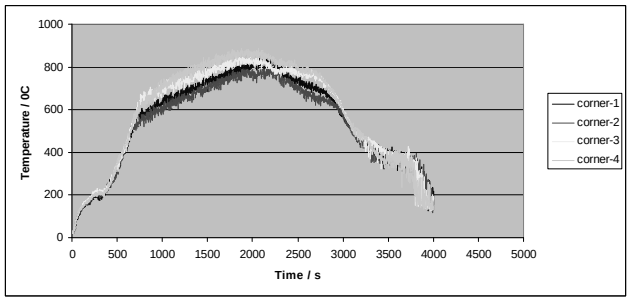

Fig. 5 Smoke temperatures of four corners around the connections (Case 1)

Connections between beams and columns are important structural components with great importance to the robustness of a steel framed structure. The fire gas temperatures around the four corners are also predicted in the FDS model. Figure 5 presents the temperature results around the corners in case 1. In case 1, the uniformly distributed fuel is ignited around four sides, and the temperature distribution is also nearly uniformly. It can be seen that the smoke temperature variation trends around four corners are nearly the same. During the fully developed stage, the peak values reach to about 800 °C, which is close to the temperature in the center position.

The average value of smoke temperature in ventilated enclosure fire could also be approximately estimated by energy balance theory (Karlsson et al, 2000), as shown in *eq. (2)*. The compartment is made up of 200 mm thick concrete blocks, the thermal penetration time of which could be calculated as *eq. (3)*. The calculation time is assumed to 1200 s. The final smoke temperature could

be calculated as *eq. (4) and eq. (5)* shown. The result is about 1000 °C, which is a little higher than the FDS simulation result for using higher heat release rate in hand calculation.

$$Q = m_g c_p \left(T_g - T_a\right) + q_{loss} = m_g c_p \left(T_g - T_a\right) + h_k A_T \left(T_g - T_a\right) \tag{2}$$

$$t_p = \frac{\delta^2}{4\alpha} = \frac{0.2^2}{4 \times 5.7 \times 10^{-7}} \approx 17544s = 292\,\text{min} \tag{3}$$

$$h_k = \sqrt{\frac{k\rho c}{t}} = \sqrt{\frac{2 \times 10^6}{1200}} \approx 40.7W/mK = 0.041kW/mK \tag{4}$$

$$\Delta T = 6.85\left(\frac{Q^2}{A\sqrt{H}h_k A_T}\right)^{1/3} = 6.85 \times \left(\frac{29674^2}{14 \times \sqrt{2} \times 0.041 \times 370}\right)^{1/3} \approx 980K \tag{5}$$

2.3 Ceiling Temperature

The roof of the compartment is made up of concrete. Its top side is exposed to ambient temperature, and the low side to hot smoke. The temperature of ceiling increases during the fire by absorbing radiative heat from the flames and by convection from hot fire gases. The temperature results in the C1 column position from FDS simulation are shown in figure 6. The variation trend is a little different from heat release rate and hot smoke temperature, especially during the fully developed period. During fire growth stage, the temperatures reach to about 500 °C for case2, 3 and 4. But in case 1, the temperature only reaches to 350 °C before flashover due to the limited combustion time. During fully developed stage, the temperature continues to increase until 800 °C because of energy accumulation, except case4 due to the long combustion time. As the fuel consuming, the temperature also decreases gradually.

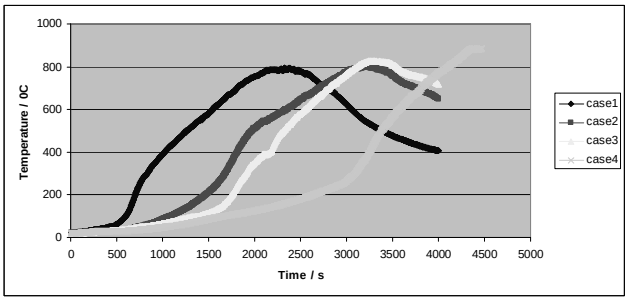

Fig. 6 Ceiling temperature at C1 Column position in four fire cases

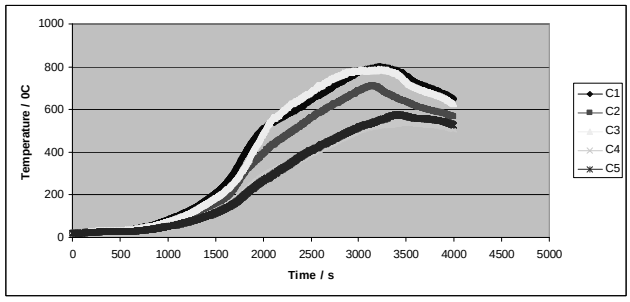

Fig. 7 Ceiling temperature at five column positions (case 2)

In large compartment fire, although the hot smoke nearly fills up the compartment, there are still some differences between ceiling temperature at different positions. Figure 7 gives the ceiling temperatures of five column positions in case 2, in which the ignition sources are in the center. Since the C1 column is positioned near the center and the C3 column is positioned near the big opening, the ceiling temperatures at C1 and C3 column positions are higher than the others, which reaches to about 800 °C. The peak values of ceiling temperature near C4 and C5 columns are less than 600 °C. The assumption of uniform ceiling temperature distribution within the compartment is not very valid. It is good to divide the ceiling into several parts when analyzing the mechanical behavior of ceiling in FEA model.

2.4 Column Temperature

The column in this compartment is made up of steel hollow section filled with concrete. The cross section is assumed as a square shape with dimensions 250 mm by 250 mm, and steel hollow thickness equals to 15 mm. Figure 8 shows the surface temperature of C1 column at the height of 3.5m in these four cases. The temperature of the column increases slowly by absorbing heat from hot smoke and flame. During fully developed period, the temperature still increases with the same rate, which is different from that for the ceiling. The peak value of temperature is about 700°C in

case 1, 2 and 3, but higher in case 4 due to the long combustion time. The mechanical behavior of column would be affected greatly.

Heat transfer inside column is also investigated by FDS, which is a one dimensional heat conduction issue. Figure 9 gives the temperatures at different inside depths of C1 column in case 3. It can be seen that there was a higher temperature gradient near the surface, but lower temperature gradient near the kernel. Most of the heat is absorbed by the steel hollow section. Part of the concrete in contact with the steel hollow section is affected by steel, and the highest temperature reaches to about 500 °C. The temperature inside the concrete is increasing very slowly during the whole period, even when the fire is decreasing.

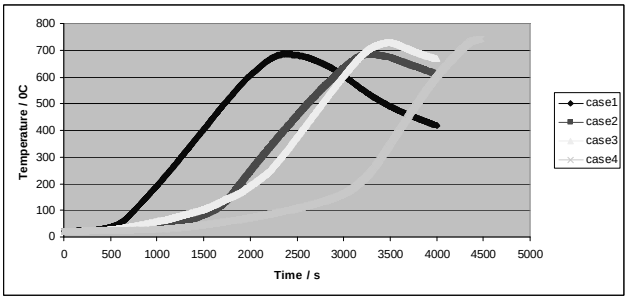

Fig. 8 Surface temperature of C1 column in four fire cases (3.5m high position)

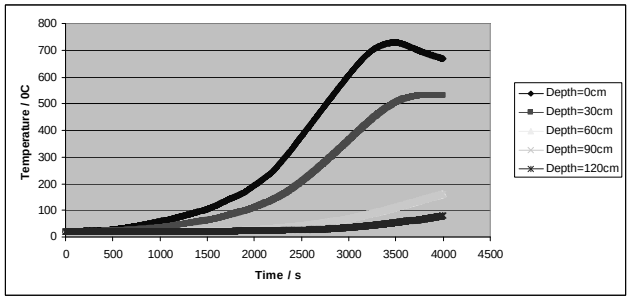

Fig. 9 Temperatures at different inside depths of A1 column (Case 3)

2.5 Beam Temperature

The solid steel beam is positioned between two columns under the ceiling. During the whole fire development, the beam is exposed to the hot smoke completely. The beam temperature increases rapidly as shown in figure 10, which is similar to column temperature due to the same material. The peak values of four cases reaches to about 800 °C, which is very close to the hot smoke temperature. In the fire growth stage, beam temperature is determined by both radiation and convection. As the temperature is increasing, the difference between beam and hot smoke is decreasing gradually. During fully developed period, beam temperature continues to increase with an obvious lower increase rate mainly due to the radiative heat.

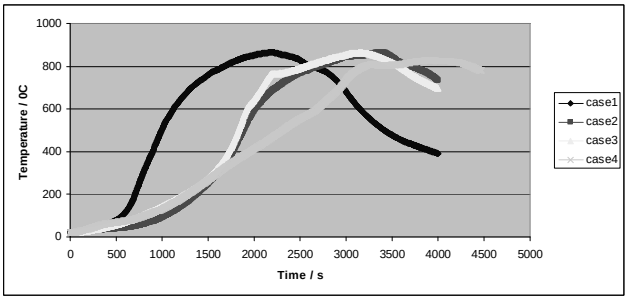

Fig. 10 Beam (left part) temperatures in four cases

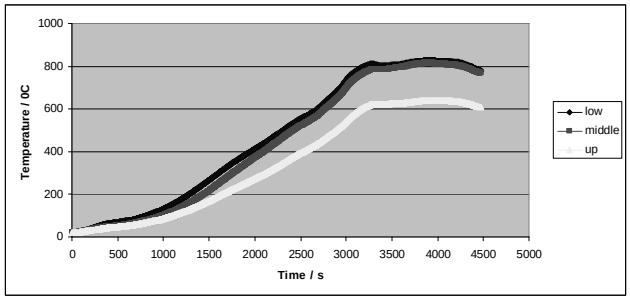

Fig. 11 Beam temperatures of different parts (Case 4)

The steel beam is made up of three thin steel plates. The boundary conditions of bottom flange and middle part are hot smoke, but the top part is just tightly under the ceiling. In FDS model, the environment temperature is assumed to be 20 °C immutably. There is only a one dimensional heat conduction calculation in FDS. Actually the heat conduction effect along the plane is feeble because of the low heat conductivity of concrete. Then the temperature of the top part of the beam is lower than that of the other two parts. Figure 11 gives the temperature variation of different pasts in case 4. There are no differences between the bottom flange and the middle part, because the hot smoke temperatures around them are almost the same. The temperature of the top part increases with a low rate. The peak value of the top part is only 600 °C, which is 200 °C lower than the other parts. The difference should be considered carefully when analyzing the mechanical performance of beam in a fire scenario.

3 CONCLUSION

In this paper, compartment fire scenario with uniformly distributed wood cribs is simulated by FDS. Four different ignition sources were considered. The temperature variations during fire of structural components are obtained from the FDS calculations. Simulation results indicate that the fire growth rate is greatly affected by the position of ignition sources and the peak value of heat release rate during flashover period is controlled by the ventilation condition. The fire development process could be divided into four stages clearly as: ignition, growth, fully developed and decay. The temperature variation trend is mainly determined by heat release rate. The highest temperature of hot smoke reaches to about 900 $^{\circ}$C, which is not uniform at that level. The surface temperature of the concrete ceiling is similar to the smoke temperature, but there are big differences of their values at different positions. The highest temperature of the column surface is about 700 $^{\circ}$C. There is a large temperature gradient along the depth near the surface, but low temperature gradient near the kernel inside the column. The temperature of the beam under the ceiling is also increasing rapidly during the fire, with the same peak value as that of the smoke and the ceiling. The temperature of the top flange of the beam is obviously lower than the other two parts, which should be taken into account in an FE-analysis. Based on these simulation results and the experimental results, further analysis of structural performance in fire using FEA tools will be carried out.

4 ACKNOWLDGMENT

Authors gratefully acknowledge financial support provided by Tillväxtverket project NSS, Nordic Safety and Security and from the European Union (Research Fund for Coal and Steel) under contract grant RFSR-CT-2008-00036", research project COMPFIRE, Design of joints to composite columns for improved fire robustness, RFS-PR-08009.

REFERENCES

A.H. Buchanan, Structural Design for Fire Safety, Wiley, Chichester, 2001.

A.S. Usmani, J.M. Rotter, S. Lamont, A.M. Sanad, M. Gillie, Fundamental principles of structural behaviour under thermal effects, Fire Safety Journal. 36 (8) 721–744, 2001.

Liu, T. C. H. "Experimental investigation of behavior of axially restrained steel beams in fire." J. Constr. Steel Res., 58, 1211–1230, 2002.

Buchanan A. H. Structural design for fire safety John Wiley & Sons, ISBN 0-471-89060-X, 2003.

Hosam, M. A., Senseny, P. E., and Alpert, R. L. "Lateral displacement and collapse of single-story steel frames in uncontrolled fires." Eng. Struct, 26, 593–607, 2004.

Yang, K. C., Lee, H. H., and Chan, O. "Experimental study of fire-resistant steel H-columns at elevated temperature." J. Constr. Steel Res., 62, 544–553, 2006.

Dong Y, Zhu C and Prasad K. Thermal and structural response of two-storey two-bay composite steel frames under furnace loading. Fire Safety Journal, Volume 44, 439–450, 2009.

Wald, F., Simoes da Silva, L., Moore, D.B., Lennon, T., Chladná, M., Santiago, A., Beneš, M. and Borges, L. Experimental behaviour of a steel structure under natural fire. Fire Safety Journal, Volume 41, Issue7, pp. 509-522, 2006.

Chlouba J, Wald F, and Sokol Z. "Temperature of Connections during Fire on Steel Framed Building." Steel Structures 9, 47-55, 2009.

F.Wald, J.Chlouba, A.Uhlir, P.Kallerova, M.Stujberova. Temperatures during fire tests on structure and its prediction according to Eurocodes. Fire Safety Journal 44 135– 146, 2009.

Ryder N L, Sutula J A, Schemel C F, Hamer A J and Brunt V V. Consequence modeling using the fire dynamics simulator. Journal of Hazardous Materials 115 149–154, 2004.

Pope N.D. and Bailey C.G. Quantitative comparison of FDS and parametric fire curves with post-flashover compartment fire test data. Fire Safety Journal 41 99–110, 2006.

McGrattan K, McDermott R, Hostikka S, Floyd J, Fire Dynamics Simulator (Version 5)-User's Guide, NIST Special Publication 1019-5, 2010.

Karlsson B and Quintiere J G. Enclosure fire dynamics. Boca Raton, Florida: CRC Press, 2000, pp. 117-127, 129-132.

EFFECTIVE THERMAL CONDUCTIVITY OF FIRE PROOF MATERIALS
And The Measuring Method

Jun HAN [a], Guo-Qiang LI [b], Guo-Biao LOU [b]

[a] College of Civil Engineering, Tongji University, Shanghai, China
[b] Safe Key Laboratory for Disaster Reduction in Civil Engineering, Tongji University, Shanghai, China

INTRODUCTION

Steel structures have poor fire resistance, due to the great decrease of steel strength as temperature elevate and the high thermal conductivity of steel thereby leading to quick temperature rise. The fire endurance of non-protected steel members is only 15 ~ 20min, so easily destroyed in fire (Li et al., 2006).

Fire proof materials are widely used to provide passive fire protection of steel structures. The basis is preventing direct heat transfer to the steel members from external heat source, thus delaying the steel temperature rise and improving the fire-resistance of steel members (CECS 200: 2006). Therefore, insulation property, commonly characterized with thermal conductivity is the most important parameter to predict steel temperature in fire. However, thermal conductivity of fire proof materials generally has a great change as temperature elevate while steel temperature usually range from room temperature to over 1000℃ in fire. Thus, calculation based on thermal conductivity at room temperature will lead to large errors despite its great convenience in calculation.

Part 11 of *Assessment method of fire protection system applied to structural steel members* (ISO/CD 834) provides a method to calculate thermal conductivity of fire protection materials based on steel components standard fire test and can comprehensively reflect the performance of fire coating in fire. In this method, the thermal conductivity of fire proof materials was calculated directly by iterative formula and non-explicit relationship lies between temperature and thermal conductivity, so manual computation is difficult. In addition, the method proposed the thermal conductivity of fire proof material by every temperature range of 50 ℃, which apparently lead to more accurate result but more complicated calculation in determining the steel temperature in fire. Moreover, the existing furnaces used for standard fire test of steel components are of large sizes, such as the beam and plate furnace sized 3m×4m×1.5m and the column furnace sized 3m×4m×4m, which are extremely time consuming and expensive for small-scaled tests.

In view of this, this paper proposed the concept of effective thermal conductivity and developed measuring method and test setup based on steel components standard fire test, in order to reflect the actual performance of fire insulation in fire. In total, 15 steel specimens with 5 different schemes of layer thickness were fire tested in the new-developed furnace of Tongji University. Comparison of experimental results and theoretical calculations will be presented to show that the effective thermal conductivity can accurately model the performance of steel members protected with fire proof material in fire.

1 THE EFFECTIVE THERMAL CONDUCTIVITY

1.1 Calculation of thermal conductivity

In fire condition, the equilibrium between the heat absorbed by the steel member and the heat transmitted through the insulation can be expressed as (Li et al., 2006; CECS200:2006; EN 1993-1-2,2005)：

$$T_s(t+\Delta t)-T_s(t)=\frac{\alpha}{\rho_s c_s}\cdot\frac{F_i}{V}\cdot[T_g(t+\Delta t)-T_s(t)]\Delta t \quad (1)$$

$$\alpha = \frac{1}{\frac{1}{\alpha_c + \alpha_r} + R_i} \tag{2}$$

$$R_i = \frac{d_i}{\lambda_i} \tag{3}$$

where t time (s);

Δt time intervals (s);

T_s, T_g temperature inside the steel members and ambient temperature (℃);

ρ_s density of steel (kg/m^3);

c_s specific heat of steel (J/kg·K);

F_i cross-sectional area of steel member in unit length (m^2/m);

V volume of steel member in unit length (m^3/m);

R_i thermal resistance of fire insulation (m^2/W·K);

d_i thickness of fire insulation (m);

λ_i thermal conductivity of fire insulation (W/m·K);

α complex heat transfer coefficient (W/m^3·K);

α_c convective heat transfer coefficient, fire to insulation, α_c=25 (W/m^2·K);

α_r radiative heat transfer coefficient, fire to insulation (W/m^2·K)。

Usually, the thermal resistance R_i is much larger than $1/(\alpha_r+\alpha_c)$, so the complex heat transfer coefficient can be expressed approximately as Equation 4.

$$\alpha = \frac{1}{R_i} \tag{4}$$

As a iterative formula, Equation 1 is inconvenient in practice, so Equation 5 was developed as a simple formula of Equation 1 by mathematical fitting approach to determine the temperature of the steel members protected with fire proof material in ISO834 fire.

$$T_s = \left(\sqrt{5\times10^{-5} \times \frac{1}{R_i} \cdot \frac{F_i}{V} + 0.044} - 0.2 \right) t + 20 \tag{5}$$

The comparison between Equation 1 and Equation 5 indicated that the simple formula is close to Equation 1 especially in the temperature zone of 400~700℃, which covers the critical temperature of most steel members, as is shown in Fig.1. The explicit formulation greatly simplifies the calculation of the temperature of steel members.

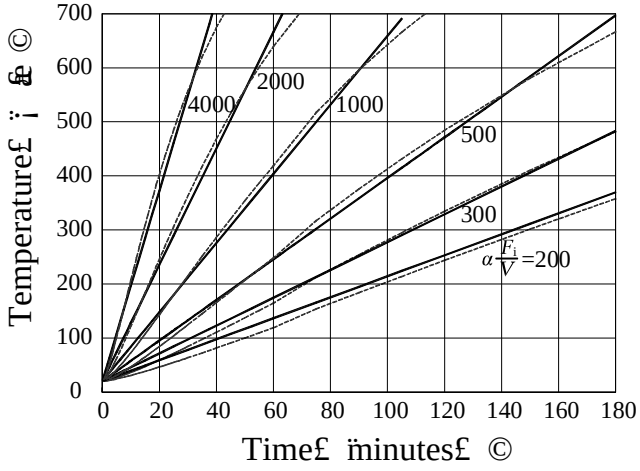

Fig. 1 Comparison between the calculating results of Eq.1 and Eq. 5

Thermal resistance of the fire insulation can be easily obtained, if temperature-time curve is known, as Equation 6 shows. Afterwards, the thermal conductivity of fire insulation can be calculated from Equation 7.

$$R_{\mathrm{i}} = \frac{5\times10^{-5}}{\left(\frac{T_{\mathrm{s}}-20}{t_0}+0.2\right)^2-0.044}\cdot\frac{F_{\mathrm{i}}}{V} \tag{6}$$

$$\lambda_{\mathrm{i}} = \frac{d_{\mathrm{i}}}{R_{\mathrm{i}}} \tag{7}$$

1.2 Definition of effective thermal conductivity

The relationship between thermal conductivity and temperature can be derived from Equation 7 according to the specimen temperature-time curve in steel structures standard fire test. The time-dependent thermal conductivity brings much difficulty to determine the temperature of steel members. Consequently, the concept of effective thermal conductivity is proposed to represent the insulation property of fire proof materials with a constant, and the two definitions of effective thermal conductivity are drawn as follows:

(1) Def.1: the average of the thermal conductivities when the specimen temperature was 400~600℃

The critical temperature of most steel members is in the temperature zone of 400~600℃, in which the calculated temperature should be as close as the measured temperature. The average of thermal conductivities in this temperature zone can accomplish this object.

(2) Def.2: the thermal conductivity when the specimen temperature was 540℃ (1000℉)

In *Standards Test Methods for Fire Tests of Building Construction and Materials* (ASTM E119), the standard fire test will be stopped if the temperature of steel members is higher than 1000℉(538℃), which is defined as the critical temperature. Defining the thermal conductivity of fire proof material when the specimen temperature was 540℃ (1000℉) as the effective thermal conductivity can greatly simplify calculation.

Comparison of the two definitions has been made and detailed below.

2 TEST SETUP AND SPECIMENS

2.1 Test setup

A mini-sized furnace was developed for small-scaled test of fire coating, whose technical specifications are as follows:

1) Furnace size: 1.0m×1.0m×1.2m;

2) Furnace Temperatures: ISO834 fire, Hydrocarbon fire and customized heating curves are available and ISO 834 fire was employed in the experiment;

3) Data Acquisition and Control: the pressure and the temperature of the furnace, loading and unloading, the data acquisition, the secure alarm are all integrally controlled with a computer, so as to reach the convenient operation.

As is shown in Fig.2, four standard specimens can be placed on channel steel [14b with fire protection in the furnace.

a) Furnace

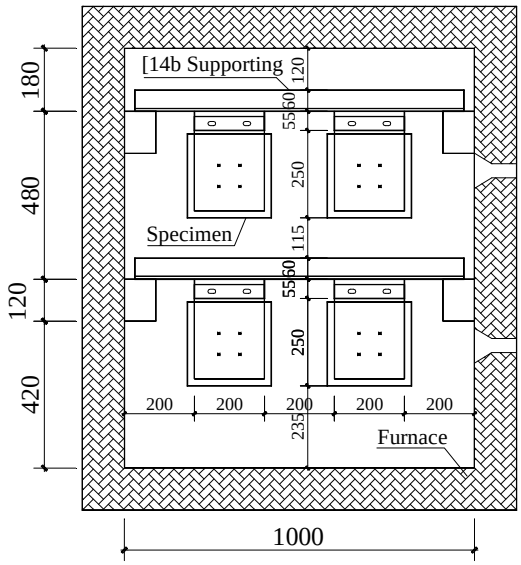

b) The cross-section and the arrangement of specimens

Fig. 2 Testing furnace and the arrangement of specimens

2.2 Test specimens

As shown in Fig. 3, steel plate specimens with dimensions of 16mm×200mm270mm were chosen in the test based on the following considerations:

1) The shape and configuration of specimens should be as simple as possible, so steel plate was selected;

2) The size of the steel plate should be as small as possible to reduce cost but not too small to ensure the uniformity of temperature field of steel plate, which is necessary to simulate one-dimensional heat transfer.

3) The typical thickness of steel plates was chosen as16mm, because steel plates with thickness of 6mm~25mm are usually used in practice. Moreover, shape parameter of the selected specimen is $145m^{-1}$, which is similar with the shape parameter of specimens used in *Fire resistive coating for steel structure* (GB 14907-2002), as is shown in Tab. 1.

4) Specimens with five different thickness (10mm, 17mm, 20mm, 30mm, 40mm) were carried out to determine the effects of layer thickness on the thermal conductivity, and then the appropriate thickness will be select as a typical thickness.

5) Fig. 2 shows three measuring points on every steel plate and the temperature will be measured with thermal couples. Theoretically, the temperatures at point 1 and point 3 are the same, while the small deviation in practice can confirm the uniformity of the temperature field inside the steel plates.

Tab. 1 Shape parameter F_i/V of the specimen used in GB 14907-2002

Specimen Type	Shape Parameter F_i/V (m^{-1})	
	Four sides in fire	Three sides in fire
I36b	142.1	125.6
I40b	137.0	121.7

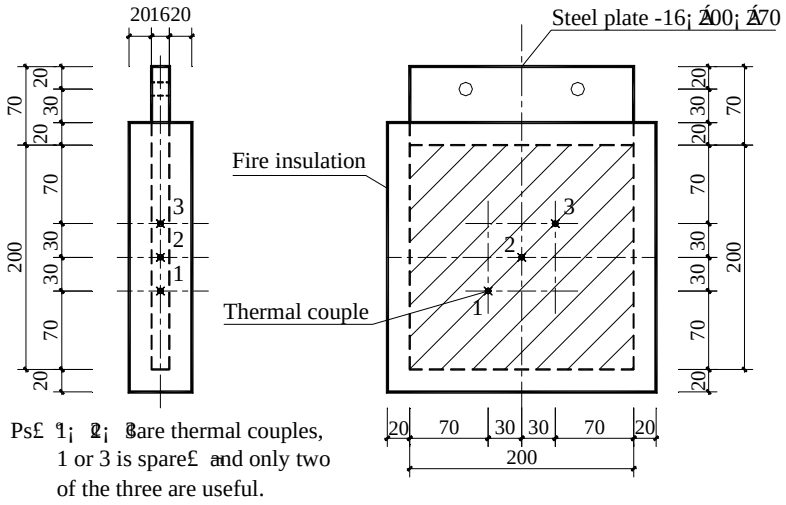

Fig. 3 Dimensions of specimens and arrangement of thermal couples

3 TESTING RESULTS

The fire insulation showed peace performance with no obvious change and the temperature of the steel member rose steadily in fire (Han, 2009). Cracks appeared on the surface of the insulation after fire, as is shown in Fig. 4.

Fig. 4 Reaction of spray coating in fire

Fig. 5 ~ Fig. 8 shows the temperature-time curve of steel members, furnace temperature-time curve and the thermal conductivity of fire insulation (calculated by Equation 7). Tab. 2 shows the comparison between the thermal conductivity calculated by the two definitions indicating that the definitions of effective thermal conductivity are reasonable and available. The following conclusions are derived from the experiments:

1) The thermal conductivity calculated in Equation 7 was at first increased and then decreased and reached peak value when steel temperature was around 540℃ (the largest difference was not over 4% for all the specimens).

2) Calculated temperature matched well with the measured temperature, especially when the steel temperature was higher than 400℃, verifying that the method proposed above are available.

3) The effective thermal conductivities derived by the two definitions are similar. However, the second definition is suggested for its more convenience than the first one.

4) The thickness of fire insulation has little effect on the effective thermal conductivity. 20mm was chosen as typical thickness for its wide use.

Tab. 2 Testing results of effective thermal conductivity

Specimen ID	Design Fire-resistance (h)	Design Thickness (mm)	Actual Thickness (mm)	Shape Parameter F_i/V (m^{-1})	Time of Ts=540℃ (min)	Effective Thermal Conductivity (W/m·K)			
						By Def.1	Average of Def.1	By Def.2	Average of Def.2
1-1	0.5	10	11.2	145	41	0.2271		0.2277	
1-2	0.5	10	11.6	145	39	0.2472	0.2359	0.2448	0.2349
1-3	0.5	10	12.5	145	43	0.2334		0.2323	
2-2	1.0	17	14.2	145	41	0.2827	0.2597	0.2834	0.2604
2-3	1.0	17	14.5	145	47	0.2366		0.2373	
3-1	1.5	20	18.5	145	55	0.2476		0.2498	
3-2	1.5	20	18.0	145	62	0.2031	0.2339	0.2055	0.2366
3-3	1.5	20	18.0	145	53	0.2511		0.2545	
4-1	2.0	30	33.0	145	86	0.2373		0.2456	
4-2	2.0	30	31.0	145	91	0.2050	0.2299	0.2125	0.2374
4-3	2.0	30	31.5	145	81	0.2475		0.2542	
5-1	2.5	40	36.0	145	94	0.2300		0.2378	
5-2	2.5	40	36.0	145	98	0.2182	0.2272	0.2251	0.2342
5-3	2.5	40	36.0	145	94	0.2335		0.2396	

Ps：the steel plates are all sized 16 mm×200 mm×270mm；

Def.1—the average of the thermal conductivity when the specimen temperature was 400~600℃,

Def.2—the thermal conductivity when the specimen temperature was 540℃ (1000℉).

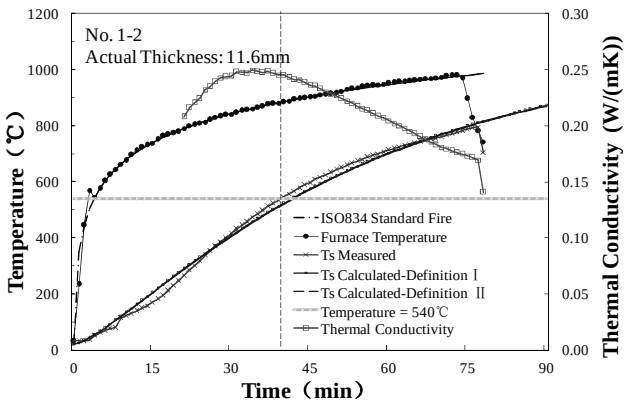

Fig. 5 Comparison between Ts calculated and Ts measured（No.1-2）

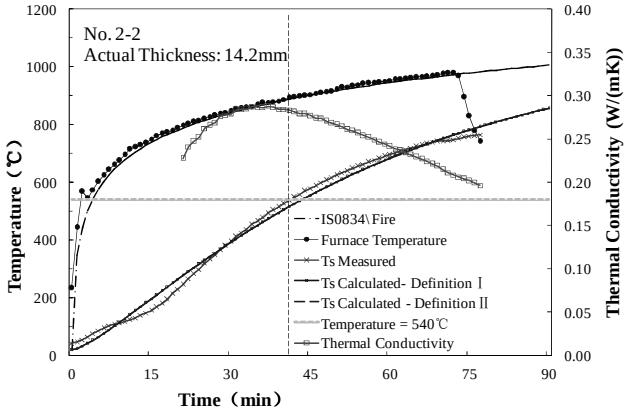

Fig. 6 Comparison between Ts calculated and Ts measured（No.2-2）

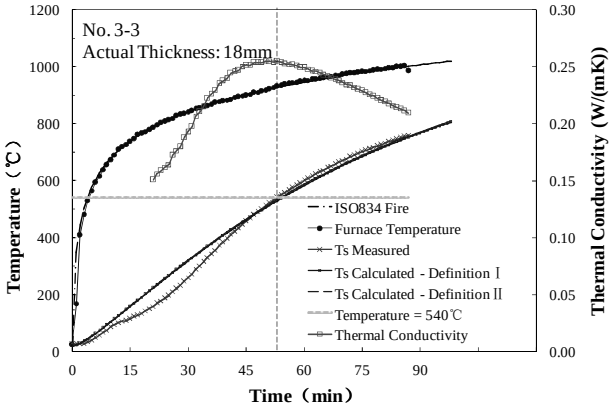

Fig. 7 Comparison between Ts calculated and Ts measured（No.3-3）

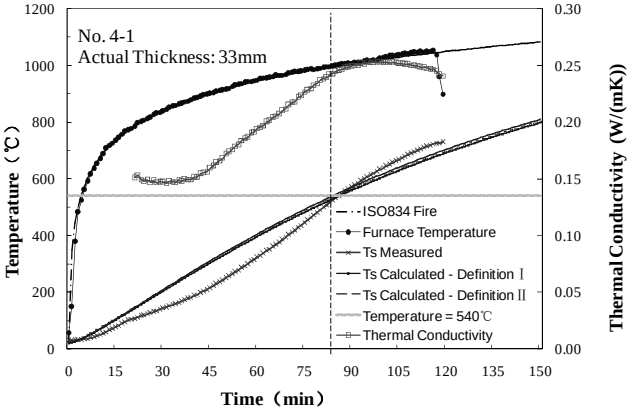

Fig. 8 Comparison between Ts calculated and Ts measured（No.4-1）

3 SUMMARY

The thermal conductivity generally changes a lot with temperature elevate. Therefore, predicting steel temperatures in fire with the thermal conductivity at room temperature brings large errors, while variable thermal conductivity makes calculation complicated. In view of this, this paper proposed the concept of effective thermal conductivity and developed measuring method and test setup based on steel components standard fire test, which represented actual performance of fire proof materials in fire. The deviation between calculated temperature and measured temperature met the engineering requirements, indicating that the test-based method is available. The main work and conclusions may be drawn as follows.

1) Proposed a measuring method suitable for thermal conductivity of fire proof materials and developed the corresponding test setup.

2) Proposed two definitions of thermal conductivity. Def.1: the average of thermal conductivities when the specimen temperature was 400~600℃; Def.2: the thermal conductivity when the specimen temperature was 540℃(1000℉).

3) Verification and comparison of the two definitions were proposed. Comparison between the calculated temperature and the measured temperature indicated that the two definitions met the engineering requirements. In practice, the second definition is suggested for its more convenience than the first one.

4) The thickness of fire insulation has little effect on the effective thermal conductivity. 20mm was chosen as typical thickness taking actual use into consideration.

REFERENCES

Li G. Q., Han L. H., Lou G. B., Jiang S. C., Fire-resistant Design of Steel and steel - concrete composite structure ,China Architecture & Building Press, Beijing, China, 2006

CECS200:2006, Technical code for fire safety of steel structure in buildings, China Association for Engineering Construction Standardization, China Planning Press, Beijing, 2006

ISO/CD 834-11: 2003, MOD. Fire Resistance Tests— Elements of Building Construction, Assessment method of fire protection system applied to structural steel members, International Organization for Standardization, 2003

EN 1993-1-2. Eurocode 3, Design of Steel Structures, Part 1.2: Structural Fire Design, 2005.

ASTM E 119-00a, Standards Test Methods for Fire Tests of Building Construction and Materials, American Society of Testing and Materials (ASTM), July 10, 2000

GB 14907-2002, Fire resistive coating for steel structure, General Administration of Quality Supervision, Inspection and Quarantine of PRC, 2002

HAN, J., Measuring method of fire insulation parameters of steel structures, Bachelor Thesis, Tongji University, Shanghai, China, 2009

FIRE LOAD SURVEY OF COMMERCIAL PREMISES IN FINLAND

Jouni Björkman [a], Veli Autio [a], Heikki Ylihärsilä [a], Peter Grönberg [b], Markku Heinisuo [c]

[a] Seinäjoki University of Applied Sciences, Seinäjoki, Finland
[b] Technical Research Centre of Finland (VTT), Espoo, Finland
[c] Tampere University of Technology, Seinäjoki, Finland

INTRODUCTION

Fire load is the most important parameter to know for different types of enclosures in building fire safety design. Fire load is the integral against time of fire heat release curve, which can be used, when fire development in an enclosure is evaluated by calculations, e.g. numerical simulations. They give temperatures, smoke layer depth and amount of poisonous gases in an enclosure in a building. By using temperatures, the temperatures in structures can be calculated and thereby determine the integrity of structures in case of fire. In Finland and many other European countries the new Eurocodes are being taken into account in building design. The new European standards (Eurocodes) in building engineering will be applied in Finland as of 2011. In the Eurocodes relating to fire safety, the fire load densities are given according to (EN 1991-1-2, 2003). However, the national annex in Finland (NA, EN 1991-1-2, 2007) does not allow applying the above mentioned Eurocode-tables of fire load densities to different room types. The fire loads may vary a lot in shopping malls and shops. Accordingly, this fire load study concentrates on those types of premises. In fire safety related Eurocodes, building fire load densities, growing factor and heat release rates are given according to the use of the building. Design fire load density is then calculated according to the standard (EN 1991-1-2, 2003) by applying a formula, where an average fire load density, efficiency factor, ignition risk according to the enclosure size, ignition risk according to the use and coefficient describing active fire protection arrangements are multiplied together. In this study the fire load density is given in unit MJ/m^2, where the square meters refer to the floor area. Fire loads have been determined since 1920. Traditionally the fire load is determined by surveying the burnable objects in existing buildings and multiplying the masses of those by calorific values of materials. Burning is expected not to be oxygen or fire load restricted. Fire load is divided into movable and fixed fire load. Linings (floor, walls, ceiling) are included into the fixed fire load. Movable fire load is separated according to material type. The total fire load is the sum of all those different fire loads for a space according to the usege. The datapoints are then fitted to some statistical functions. Applied distributions related to the fire load density measurements are normal, logarithmic normal (lognormal), 3-parametric gamma- and Gumbel distributions. In the Eurocodes the Gumbel-distribution has been applied. Design parameters applied are average and the fractiles of 80, 90 and 95 %. In this study fire loads were measured in 30 commercial premises in the Seinäjoki area in Finland and design parameters for Eurocode based fire safety design were derived. We hope that the results of this study, besides the results of former and ongoing other research projects, will give the basis for the Eurocode based fire load density determining in building design.

1 FIRE LOAD

1.1 Fire load calculation

Fire load is divided into movable and fixed fire load. Linings (floor, walls, ceiling) are included into the fixed fire load. Movable fire load is separated according to material type. The total fire load is the sum of all those different fire loads for a space according to the use of space. Fire load is defined as total released heat in full burning in an enclosure where the fire is situated (Sleich & Cajot 2001). Fire load Q can be expressed mathematically as follows

$$Q = \chi \, m \, \Delta H \quad (1)$$

where χ is burning efficiency factor, m mass, H calorific value. According to Eurocodes all movable items and linings are included into fire load. The parts of the burnable material which do not char during the fire do not have to be taken into account in fire load (EN 1991-1-2 Appendix E 2003). According to the Finnish building rules, E1: Building fire safety, the fire load is the total released heat, when the materials in the enclosure burn completely. Bearing, stiffening, separating and other pieces of building as well as movable objects are included in the fire load (E1: Building fire safety 2002). First of all, fire loads are defined according to the use of the building. Many studies dealing with fire loads have been carried out in Finland and worldwide (Autio et al 2011).

2 MEASUREMENTS

The premises investigated were shops with different sizes and types in Seinäjoki and its surroundings in Finland. It was assumed that the geographical situation of a shop does not have any significant meaning. The shops were chosen so that the premises with small as well as big fire load densities could be taken into account in the study. Measurements were carried out in 30 commercial premises and their relating spaces. Those relating spaces were storages and social rooms. The floor area investigated was almost 28000 m^2. The smallest shop was 54 m^2 and the largest one was 4550 m^2 with a 800 m^2 storage. There were shoe shops, textile shops and bookshops as well as furniture shops and nine groceries.

The measuring method given by (Theyvoyen et al 2008) was applied, where burning materials were divided into wood, textiles, plastic, paper and miscellaneous materials. Measurements of the fixed fire load were carried out at the linings without damaging them. Measuring devices such as typical weighers, rulers and laser-systems were used. In small places all materials were weighed and parts of different materials were evaluated. The weight of the bigger items was measured from the volume or just evaluated. In the biggest places parts of the materials were weighed e.g. kg/m^2 and then multiplied by the evaluated dimensions. Into the fixed material all floor, wall and ceiling lining materials were incorporated. The amount of the material was evaluated by measuring the area of material multiplied by the thickness. The gained volume was multiplied by the material density that yielded the mass.

In addition to the fire load data, many other fire safety related things were collected, too. In the premises information about openings, fire safety class, and distance from the fire station, evacuation plans and active fire safety equipment was also collected. A floor plan was also drawn if not already available.

The fire load was calculated by using the Equation 1, by using calorific values of materials from literature (DiNenno et al 2002, EN 1991-1-2, 2003, Kumar & Rao 1995). See Table 1.

Tab. 1 Average calorific values used in calculations

Material	Average calorific value (MJ/kg)
Wood	17,5
Paper	20
Plastic	30
Textiles	20
Food	15

3 RESULTS

3.1 Fire load densities: Shops and associated spaces

Thirty commercial premises with floor area of 54 … 4550 m^2 were analysed. The smallest shops were typically special shops situated in shopping malls. The largest premises were groceries, building material shops and household appliance and furniture shops. The studied types of shops

were: grocery (9), furniture shop (2), decoration shop (1), household appliance shops (2), ironmongers shop (1), video hiring (2), toyshops (1), sports shop (1), draper shop (1), optician (1), book-shop (2), shoe-shops (2), clothing store (3), bag-shop (1) and chemist's shop (1).
Associated spaces relating to the shops were mostly storages (17), social premises (4) and offices (3). Fixed (burnable parts of the building and linings) and movable fire loads in premises were measured. In percentages, the biggest part of the fire load of the shops was movable. In associated premises there were spaces where the amount of fixed fire load was bigger than that of movable. On the other hand, there were associated spaces where the amount of fixed fire load was smaller than in shops at its minimum. The variation of the fire load of associated spaces was bigger than in shops. Movable fire load was divided into five material classes: wood, paper, textile, plastics and miscellaneous. The fire load diversity of certain shop types was very similar. For example in textile shops there were mostly textiles. The share of plastics is the biggest in household appliance and toyshops. In furniture and decoration shops there is a lot of wood in the fire load. Miscellaneous fire load can be found in groceries and at chemist's shops. Paper is a common material, of course, in book shops, but also in shoe shops. (Autio et al 2011)

3.2 Fitting

It has been claimed that the fire load density in buildings is often assumed to follow logarithmic normal (lognormal) (DiNenno at al. 2002) or Gumbel-distribution (Eurocode EN 1991-1-2). In this study the suitability of these two stochastic models to calculated fire load densities was considered. The curves were fitted into the fire load density data collected. The parameter estimates of the biggest probability (MLE) of fitted curves, average value, standard deviation and fractiles of cumulative functions were determined. The fitted density and cumulative functions and their parameters for shops and associated spaces are given in (Autio et al 2011).
In Figure 1 there are the density f(x) and cumulative F(x) functions of fitted distributions with the fire load densities x calculated based on the measured data of shops. It is clearly to be seen that logarithmic normal and Gumbel (maximum) –distributions match the data well.

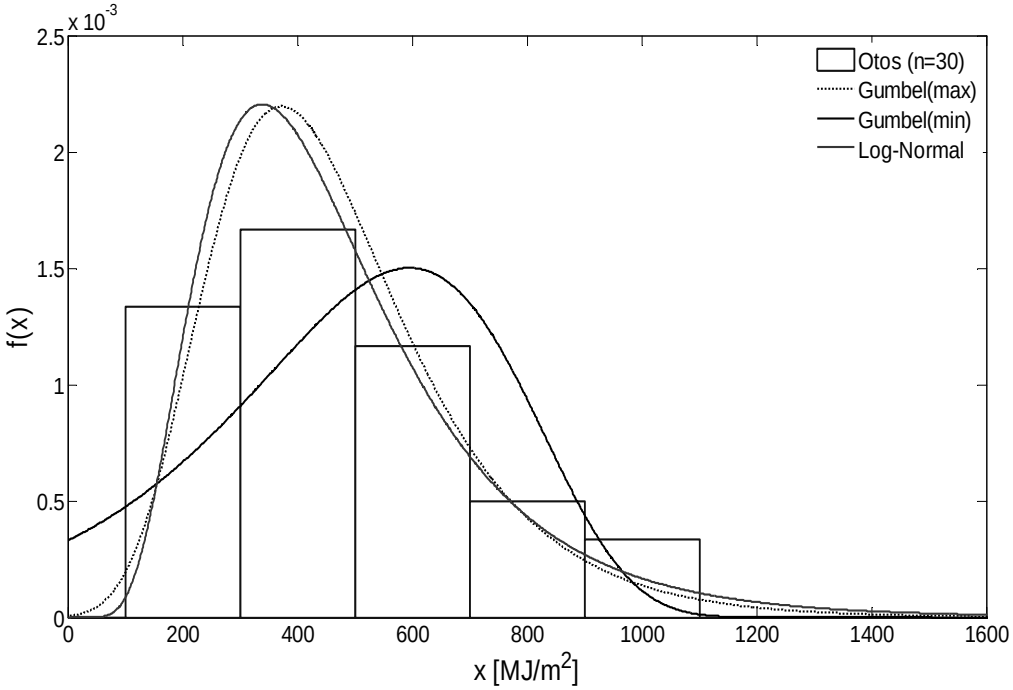

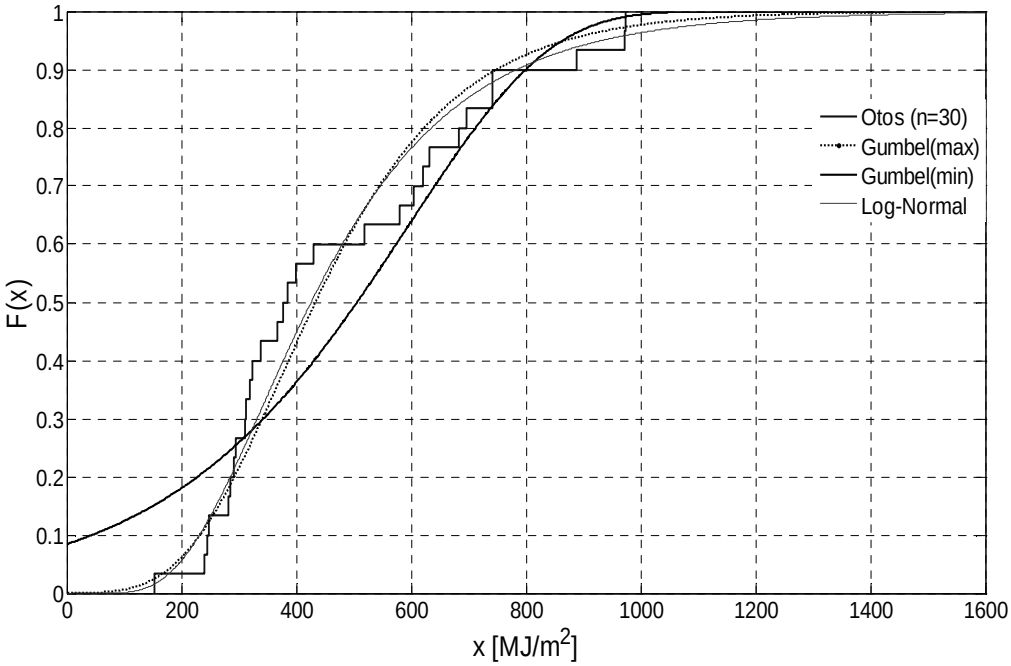

Fig. 1 Fitted density functions and cumulative functions for shops. Measured based fire load densities are expressed by using histograms and the cumulative fire load density by using step curve.

Fitted density functions f(x) and cumulative functions F(x) for associated spaces are in (Autio et al 2011).

It can be seen in figures that the logarithmic normal distribution and the Gumbel (maximum) –distribution fit well with the fire load density histogram and the cumulative step curve.

When looking at the curves of cumulative functions it can be seen that the logarithmic distribution matches best the fire load data. However, evaluation by eye is difficult and uncertain. Accordingly, the quality of fitting was investigated by using χ^2 –test. It was found that measured and calculated fire load density function follows logarithmic normal distribution significantly more reliably than the Gumbel (minimum) –distribution, and a bit more reliably than Gumbel (maximum) –distribution. In the case of associated spaces the results are corresponding.

The final result can be concluded so that the logarithmic normal distribution describes the measurement based fire load densities in the most reliable way. However, in the case of Gumbel (maximum) –distribution, the deviation is not significant.

The results of the additional measurements: Active fire safety arrangements were also investigated in the shops. There was at least one portable extinguisher in every shop. In 10 places there was a rescue plan available. In one place there was none. In 19 places it was not known if a rescue plan was available. Safety and escape illumination was sufficient in 28 shops. Automatic fire detection system was installed in 22 buildings and 12 shops were equipped with an automatic extinguishing system. A smoke exhausting system was installed in 15 shops and a water supply was found in 14 places. In some buildings the water supply may exist somewhere but not in the vicinity of the shops investigated. (Autio et al. 2011)

4 DISCUSSIONS

The inventory in the shops was rather a demanding task. The biggest problem was the large material diversity and material identification. For example, there was a lot of different plastics. They were partly equipped with material data, but some of them were impossible to classify. Almost all items were packed in some way. Thus the mass of an item itself and its packaging material had to be separated. The mass of big items, which could not be weighed, was evaluated based on their volumes. This was especially difficult to accomplish. Accordingly, at the later phase of the work

previously calculated values in the case of items of the same type were used. The most difficult items to evaluate were the items which consisted of many materials.
Fire load densities are typically reported to follow logarithmic normal or Gumbel- distribution. Which one of them suits best requires investigation in every case. Essential factors affecting the suitability and the form of the distributions are the variation coefficient of the measured data set, the structure of the premises i.e. it can be asked if the space is a one- or multi-room space and if the fire load type is fixed or movable as well as what the distribution model itself is.
When the variation coefficient of measured data approaches zero, many distributions converge towards normal distribution. On the other hand, fire load can be assumed to be some kind of sum of masses of burnable materials and specific heats. The fire load of a certain room or building is the sum of fire loads of rooms. It can be assumed that the cumulative process of a fixed fire load is based on different mechanisms from that of a movable fire load. A phenomenon, which is the sum of independent variables which are distributed by different ways, follows normal distribution. A phenomenon which is the product of independent in a different way distributed variables follows lognormal distribution if the ensemble is large. It was found that there is a significantly linear correlation between the fire load and the room volume, which partly may cause lognormal behaviour.

5 SUMMARY AND ACKNOWLEDGEMENTS

In the 30 commercial premises, which were studied, the measured and fitted fire load density follows logarithmic normal distribution significantly more reliably than the Gumbel (minimum) –distribution and slightly more reliably than the Gumbel (maximum) –distribution. On the basis of this study and corresponding foreign studies, it can be claimed that 80 % fractile of the Eurocode of 730 MJ/m^2 is a suitable characteristic value for the fire safety design of commercial premises of shopping malls except for storages and associated rooms. In this study, the fire loads of storages and associated spaces were 1,5 times bigger than in shops. Especially the fire loads in storages may vary a lot and they must be determined according to the type, amount and location of goods. We suggest fire load measurements in theatres, cinemas and libraries and corresponding premises according to the same measuring and analysing methods as in this study.
We are indepted to the students of building engineering of Seinäjoki University of Applied Sciences who assisted in the fire load inventory and the shops who allowed the measurements in their premises. Members of the steering committee and funding by Ministry of Interior (Palosuojelurahasto), Ministry of Environment, Teräsrakenneyhdistys ry, City of Seinäjoki and Tampere University of Technology are highly acknowledged.

REFERENCES

Autio, V., Björkman, J., Grönberg, P., Heinisuo, M. & Ylihärsilä, H. 2011. Fire load survey of buildings. Publications of Seinäjoki University of Applied Sciences. Reports B 47. 65 p. (In Finnish)

DiNenno, P. et al. 2002. Handbook of Fire Protection Engineering. 3. ed. The National Fire Protection Association (NFPA).

E1: Finnish Building Code. Building fire safety. 2002. Ministry of Environment.

EN 1991-1-2. 2003. Eurocode 1: Rakenteiden kuormat: Palolle altistettujen rakenteiden rasitukset. Helsinki: Suomen Standardisoimisliitto. (In Finnish)

Annex NA, EN 1991-1-2, 2007. EN 1991-1-2. 2003. Eurocode 1: Rakenteiden kuormat: Palolle altistettujen rakenteiden rasitukset. Helsinki: Suomen Standardisoimisliitto. (In Finnish)

Kumar, S. & Rao, C.V.S. K. 1995. Fire Loads in Residential Buildings, Building and Environment 30 (2), 29–305.

Schleich, J.B. & Cajot, L-J. 2001. Valorisation project. Natural fire safety concept. Profil Arbed.

Thayvoye, C, Zhao, B, Klein, J & Fontana, M. 2008. Fire load survey and statistical analysis. Fire safety science – Proceedings of the 9th international symposium 991–1002, IAFSS.

SYSTEMATISATION OF DESIGN FIRE LOADS
IN AN INTEGRATED FIRE DESIGN SYSTEM

Markku Heinisuo [a], Mauri Laasonen [a] , Jyri Outinen [b], Jukka Hietaniemi [c]

[a] Tampere University of Technology, Faculty of Built Environment, Tampere, Finland
[b] Rautaruukki Oyj, Vantaa, Finland
[c] Markku Kauriala Ltd, Fire Engineering and Fire Safety Design Consultants, Espoo, Finland

INTRODUCTION

Definition of design fires is the starting point of fire safety engineering. Fire scenarios should be defined with care in close co-operation between the client, the designers and the authorities. Different fires must be taken into account depending on the intended use of the building, as is done when defining the mechanical actions on buildings. In Europe design fires and the corresponding minimum fire loads have been defined in Standard EN 1991-1-2, 2003 based on the occupancies of buildings. However, no standard values exist for many types of fires, such as rack-stored commodity fires and vehicle fires, which requires defining design fires based on literature or tests and analyses. It is also true that the EN standards have not yet been approved by all European countries (Heinisuo et al, 2010) which requires defining design fires in them based on literature or by other means.

It is believed by the authors that fires based on occupancies of buildings, rack-stored commodity fires and vehicle fires are similar across Europe. Rack and vehicle fires depend on the types of stored items and vehicles, but if they are known the fire loads of similar types can be assumed to be the same. In many countries these fires are defined differently even by different local authorities. The standardisation of fire loads is extremely important for the operations of contractors globally. It is also important in creation of design tools for designers.

This paper looks into the systematisation of design fire loads. Systematisation is hoped to lead in the future to the standardisation of fire loads. The implementing environment of the design fire loads of this study is an integrated fire design system developed during the last three years (Heinisuo et al, 2009). Integration starts in BIM (Building Information Model, Tekla Structures) and continues with fire simulations ending with resistance checks of steel members. BIM provides the geometrical entities and required physical properties for defining the fire loads needed to run fire simulations. The fire simulations are done using NIST FDS (Fire Dynamics Simulator). Member resistance checks are done using SCIA Engineering software (Nemetschek) after obtaining the gas temperatures from FDS.

By these means the fire design process can be facilitated and the quality of the simulations improved. Fire simulations can be run taking into account only the conditions of the building to be built in the design phase.

This paper presents the modelling of Eurocode fires based on occupancies of buildings as well as special fires such as rack-stored commodity fires and vehicle fires (Hietaniemi, Mikkola, 2010; Haack, 2001; Shleich, 2010). The effects of sprinklers are also examined. When presenting the Eurocode fires based on occupancy, a so-called chessboard system is utilised which proved to give more reasonable results than applying the fire load of FDS to the entire floor area. Simple rules are included in the definitions of the fire loads to enable sensitivity studies.

1 EUROCODE FIRES BASED ON OCCUPANCIES OF BUILDINGS

During systematisation of the fire loads, idealisations of real fires should be done to put the fire actions into a form readable by computers. The idealisations should be safe and describe all relevant features of the fires. The relevant features depend on the effects we are examining. For example, the most simplified representation of the heat release rate of the fire in Fig. 1 cannot predict the growth

and decay phases of fires which are important in some cases, but may be enough when considering the ultimate resistance of the structures.

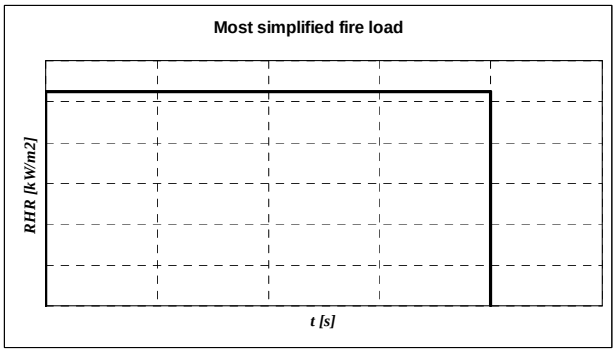

Fig. 1 Simplified fire load

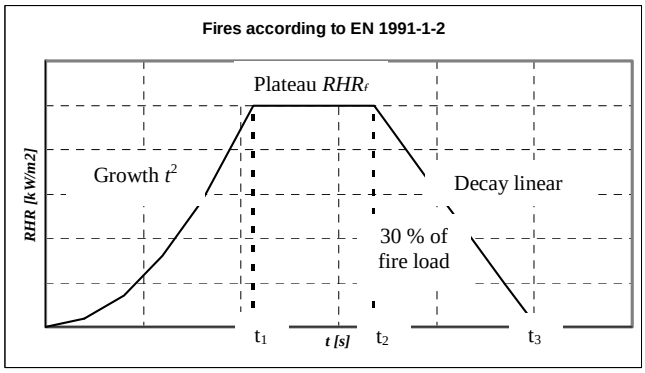

Fig. 2 Eurocode fire loads

Fig. 2 presents the idealisation of the rate of heat release (*RHR*) used in Eurocodes for fires based on occupancies of buildings. The parameters needed to specify the fire of Fig. 2 are:
- RHR_f [kW/m^2], (maximum heat release rate per area, plateau value),
- t_α time to reach 1MW [s] (controls the growth phase of the fire, t^2 rule used),
- $q_{f,k}$ [MJ/m^2], (maximum fire load density per area),
- A_{fi} [m^2], (the maximum area of the fire, which is the fire compartment in case of a uniformly distributed fire load, but which may be smaller in case of a localised fire).

The 30% rule shown in Fig. 2 defines the time t_3 when the fire ends, and this 30% can be considered the parameter given in the Eurocodes. The first three parameters in the Eurocodes are given based on the occupancy of the building. The fourth parameter A_{fi} should be defined by the designer. When these parameters are known, the times t_1, t_2 and t_3 can be calculated using the equations:

$$q_{f,k} = \int_0^\infty RHR_f \; dt \tag{1}$$

$$t_1 = t_\alpha \cdot \sqrt{\frac{RHR_f \cdot A_{fi}}{1MW}} \tag{2}$$

$$q_1 = \int_0^{t_1} \frac{1MW}{A_{fi}} \cdot \left(\frac{t}{t_\alpha}\right)^2 dt = \frac{1}{3} \cdot \left(\frac{1MW}{A_{fi}}\right) \cdot \frac{t_1^3}{t_\alpha^2} \tag{3}$$

$$q_2 = RHR_f \cdot (t_2 - t_1) = q_{f,k} - q_1 - q_3 \Rightarrow t_2 = t_1 + \frac{q_{k,f} - q_1 - 0.3 \cdot q_{f,k}}{RHR_f} \tag{4}$$

$$t_3 = t_2 + \frac{2 \cdot 0.3 \cdot q_{k,f}}{RHR_f} \tag{5}$$

Fig. 3 illustrates all Eurocode fires based on different occupancies for A_{fi} = 200 m^2 using *Eqs. (1)-(5)*.

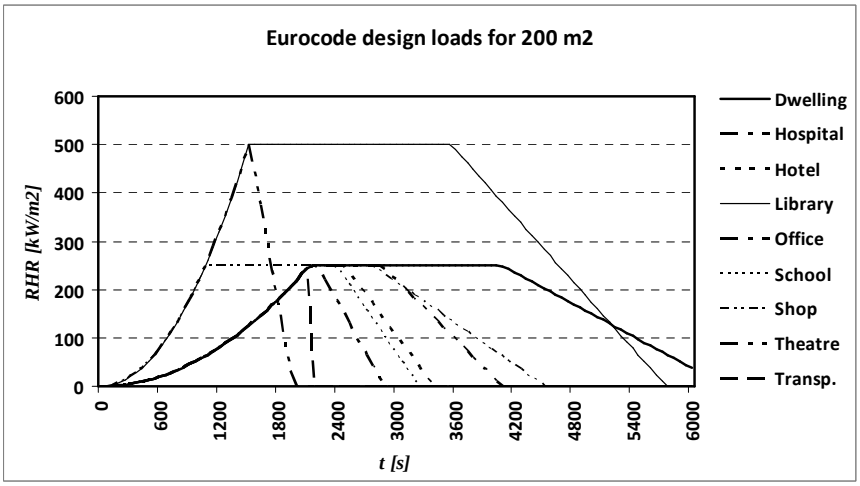

Fig. 3 Eurocode fires based on occupancies

The Eurocodes assume that the fire load is located across the entire floor area. However, when considering e.g. the resistances of roof structures, the fire may be located above floor level. In this study the fire loads are located about 1 m above floor level across about 1x1 m^2 horizontal areas, which are conservatively supposed to ignite simultaneously. Moreover, these fire sources are located randomly at 1 m +/- one grid length in the vertical direction. The exact locations of the fire sources are defined so that they will fit the computational grid. Horizontal distances twice (N=2) the grid size in corresponding directions between the fire sources (chessboard) were found most critical in numerical tests for distances 1, 2, 3 and 4 times grid size. The criteria were the maximum temperatures near the ceiling of the 7x7 m^2 classroom at a height of 3 m. The heat release rates of the chessboard areas should be increased so that the total heat release matches the original.
Fig. 4 shows the FDS result for one classroom simulation and Fig. 5 shows the temperatures near the ceiling, Point 8. The resolution in Fig. 5 is defined in (Heinisuo et al, 2008) and is used to define the proper grid size for the fire simulations. Note, that resolution 7 is much smaller than recommended, but it gave about the same results as using the recommended value in this case.

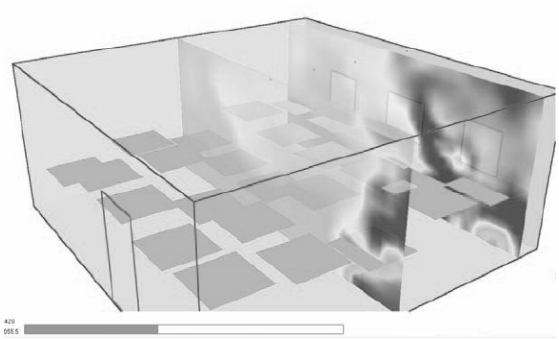

Fig. 4 Classroom FDS model

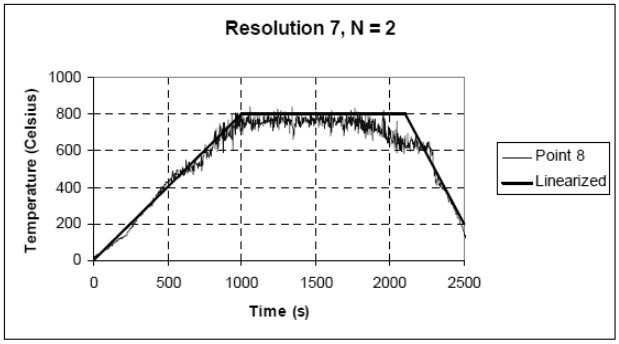

Fig. 5 Gas temperatures near ceiling

Fig. 5 also shows the linearisation of gas temperatures in fire. When defining the resistances of structures, this kind of linearisation is essential to reduce the computing time in post-processing. The exact definition of the linearisation will be considered in further studies.
It is recommended that at least two simulations are done in the case of sensitivity studies. The second run is done by varying the grid size whereby the levels of the fire sources change automatically, because they are defined using random processing. Variation of the grid size is not necessary if the original grid size is defined using the definition of (Heinisuo et al, 2008).
The effects of sprinklers are taken into account based on two scenarios: a local sprinkler fire and a global sprinkler fire. The local sprinkler fire is defined so that the fire ignites just above the broken sprinkler, which is a conservative assumption (Heinisuo et al, 2010). Other sprinklers stop the fire

in other areas and we end up with a local fire without sprinklers. The fire area A_{fi} is defined as the area covered by the broken sprinkler, typically about 3x3 m^2.
The global sprinkler fire is defined by modelling the sprinklers as they are in the FDS analysis while otherwise using the input data given above. This means that the fire is not stopped by sprinklers. They only cool down gas temperatures. In this case we should also assume that some of the sprinklers will not work by reducing the flow rate of the sprinklers by, say, 10% in the input file of the FDS. Typically, a local sprinkler fire is more severe than a global sprinkler fire. The sprinkler data should correspond to the planned properties of the sprinklers of the project.
Fig. 6 shows the critical model (this study used three models corresponding to the three different locations of broken sprinklers) for the local sprinkler fire 3 and the corresponding temperatures at the control points of the 7x7 m^2 classroom in the Eurocode classroom fire. Control points are located near the ceiling and windows. Fig. 7 shows the temperatures at the same control points in the global sprinkler fire. The default K11 sprinklers were located 2.5 m from each other near the ceiling.

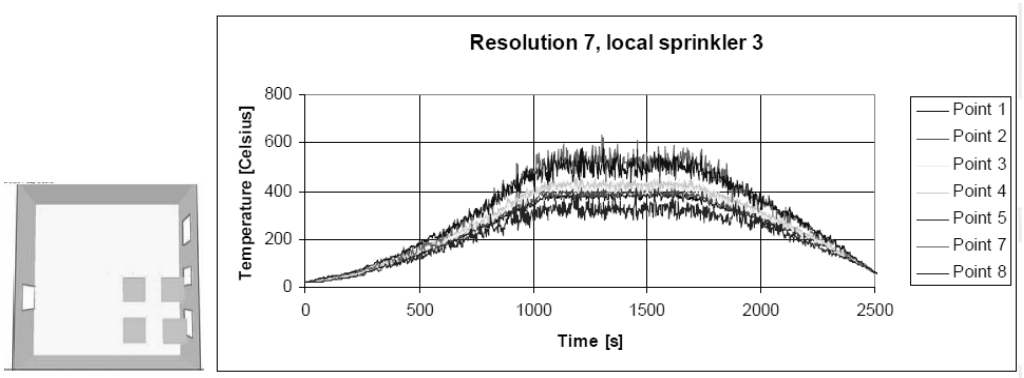

Fig. 6 Critical local sprinkler fire

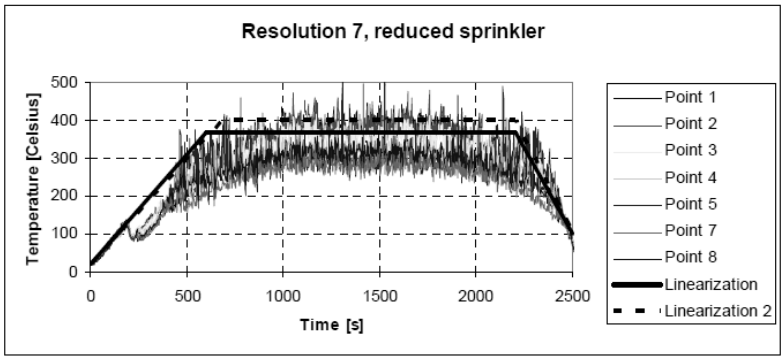

Fig. 7 Global sprinkler fire

The Eurocodes give reduction factors for design fire loads with sprinklers. If an automatic water extinguishing system exists and the number of independent water supplies varies from 0 to 2, then the reduction factors are: at 0 0.61 x 1.00 = 0.61 (load 1), at 1 0.61 x 0.87 = 0.53 (load 2), at 2 0.61 x 0.70 = 0.43 (load 3). The temperatures based on Eurocode reductions for the fire loads with sprinklers were very high (maximum near 800^{o}C) compared to the global sprinkler fire defined above (see Fig. 7).

2 RACK FIRES

Five categories of rack-stored commodity fires are proposed (Hietaniemi, Mikkola, 2010):

1. 150 kW/m^2 which corresponds to a typical fire load of cellulose materials such as wood and paper products.

2. 300 kW/m^2 which corresponds to a typical fire load that may consist of cellulose materials and some fire retardant or otherwise not very highly combustible plastics such as PET, POM, etc. A furniture fire load may fall in this or the next category.

3. 500 kW/m^2 which corresponds to fire loads consisting of mixtures of cellulose materials (major ingredient) and highly combustible plastics such as ABS, PE, PP and PS, or where plastics such as PET, POM, PMMA are the principal ingredient. A furniture fire load may also fall in this category.

4. 1 000 kW/m^2 which corresponds to a typical fire load consisting of significant amounts of non-fire retardant, highly combustible plastics such ABS, PE, PP and PS. The other ingredients may be e.g. cardboard boxes, etc.

5. 2 000 kW/m^2 which corresponds to fire load consisting of a very high percentage of non-fire retardant, highly combustible plastics such ABS, PE, PP and PS. E.g. a boat store fire.

All rack fires are modelled using combinations of basic fuel boxes. The nominal dimensions of the basic box are 100x800x400 mm^3. The actual dimensions of the boxes are fitted to the computational grid of the FDS. The distance between boxes in every direction is one grid length in the direction in question. As many full boxes as possible are fitted in the rack area. The box direction is perpendicular to the rack area direction. In this study the shelves are modelled as non-combustible plates with a nominal thickness of 100 mm. The properties of each box are:
- Ignition temperature 320 °C,
- Density 500 kg/m^3,
- Specific heat 1.5 kJK^{-1}kg^{-1},
- Thermal conductivity 0.2 WK^{-1}m^{-1}.

One box is used for ignition. The others ignite after reaching the ignition temperature. Burn away option of the FDS is used for boxes. An ignition box is located at the bottom and at the top of the rack - both cases should be simulated. Sprinklers are modelled as above, locally or globally. Fig. 9 shows a case of a category 1000 kW/m^2 rack fire without sprinklers with an ignition box at the bottom or at the top.

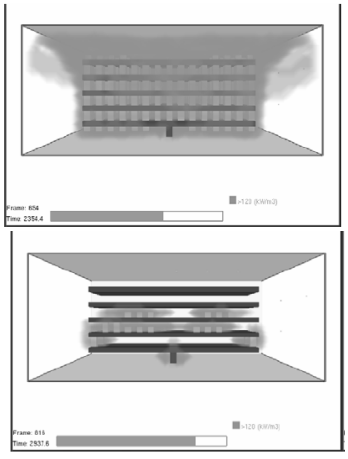

Fig. 9 Ignition bottom

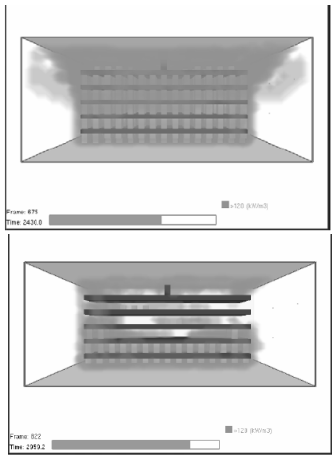

Ignition top

It is recommended that both bottom and top ignition be studied. Moreover, it is recommended that the required resolution factor be used to define the proper grid size for rack fires. A lot of CPU time will unfortunately be required for small heat release rate categories (150 - 300 kW/m^2).

3 VEHICLE FIRES

Based on (Hietaniemi, Mikkola, 2010) and (Haack, 2001) a so-called Type 2 car fire (e.g. Renault Megane) in the case of a 2x5 m^2 floor area was implemented in this study to study fire loads of car parks in Finland. The critical locations of the cars were defined using the rules of (Shleich, 2010).

The heat releases from one and three cars are shown in Fig. 10. The equations for the design curves are given in (Heitaniemi, Mikkola, 2010). An adjacent car ignited 12-15 minutes after a car had started to burn based on tests. The heat release from three Type 2 cars is the sum of the heat releases from three individual cars as shown in Fig. 11 using 12 minute ignition delay.

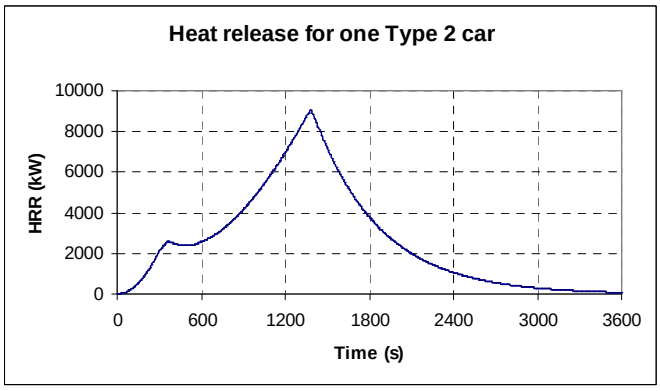

Fig. 10 Heat release for one Type 2 car

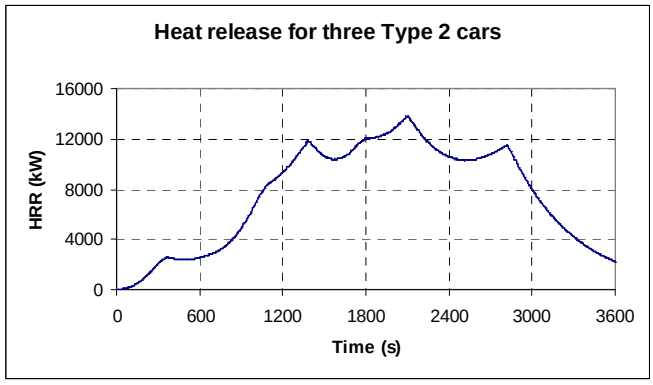

Fig. 11 Heat release for three cars

Heavy goods vehicle (HGV, 40 MW), petrol tank (the most severe 200 MW) and bus fires (20 and 34 MW) were also implemented in this study. HGV and petrol tank design fires (heat release rates, kW/m^2) are presented for the top surface of the geometrical entity shown in (Hietaniemi, Mikkola, 2010). Two bus fires for a 3x10 m^2 area 1 m above the floor level are presented after the definitions of (Hietaniemi, Mikkola, 2010).

4 SUMMARY

Eurocode, rack and vehicle fires were implemented in this study for the integrated fire design system. Comprehensive experimental and theoretical background studies on rack and vehicle fire loads can be found in literature which form a solid basis for the standardisation of these fire loads. Eurocode fires based on occupancies are presently being checked and in the near future they may be revised for use in practical projects.

REFERENCES

EN 1991-1-2, Eurocode 1: Actions on structures, Part 1-2: General actions, Actions on structures exposed to fire, CEN, Bryssels, 2003.

Haack A., Rapporteur, STUVA, Design Fire Scenarios, technical Report – Part 1, Thematic Network, FIT- Fire in Tunnels, Contract no G1RT-CT-2001-05017, WTC, Brussels, 2001.

Heinisuo M., Laasonen M., Hyvärinen T., Berg T. Product modeling in fire safety concept, effects of grid sizes and obstacles to steel temperatures, In: Proc of IABSE Helsinki Conference, 2008.

Heinisuo M., Hietaniemi J., Kaitila O., Laasonen M., Outinen J., Integrated fire engineering of steel skeleton using well established fire sources. In: International Conference, Application of Structural Fire Engineering, Prague, 19-20 February, 2009. pp. 380-385.

Heinisuo M., Laasonen M., Outinen J., Fire design in Europe. in: Cost Action C26, Urban Habitat Constructions under Catastrophic Events, CRC Press/Balkema, London, 2010, pp. 375-402.

Hietaniemi J., Mikkola E., Design Fires for Fire Safety Engineering, VTT Working Papers 139, VTT, 2010.

Shleich J-B, Modern Fire Engineering, Fire Design of Car Parks, Arcelor Profil, Luxembourg Research Centre. (Internet publication), 2010.

A STRUCTURAL FIRE ENGINEERING PREDICTION FOR THE VESELÍ FIRE TESTS, 2011

Shan-Shan Huang[a], Ian Burgess[a] and Buick Davison[a]

[a] The University of Sheffield, Dept. of Civil and Structural Engineering, UK

INTRODUCTION

When a fire occurs in a building the internal forces in the joints change substantially during the course of the fire, even though the external forces applied to the structure remain unchanged. This results mainly from restraint to thermal deformations and degradation of the mechanical properties of the building materials at high temperature. These phenomena were observed in both full-scale tests (Newman *et al*, 2004) and actual fires (NIST 2005, 2008). Because current design methods for connections are solely based on ambient-temperature behaviour, the additional forces and rotations generated in fire are not taken into account. If, at any stage of fire exposure, a connection does not have sufficient resistance to accommodate the large rotations and co-existent forces, fracture will occur. This may lead to extensive damage or progressive failure of the structure. Therefore, how the joints perform in a building fire will be critical to whether it would be able to survive the fire attack.

The Structural Fire Engineering Research Group of the University of Sheffield is participating in the European-funded project COMPFIRE (RFCS 2008), a collaboration between research teams at universities in Manchester, Coimbra, Luleå and Prague, Desmo Ltd in the Czech Republic, and TATA Steel Tubes Europe. The objective of this project is to investigate the behaviour and robustness in fire of practical connections between steel beams (both composite and non-composite) and two types of composite columns - concrete-filled tubular (CFT) and partially-encased H-section columns. Two natural fire tests on a full-scale composite structure are planned to take place in Veselí, in the Czech Republic (Wald 2011). One task of the Sheffield research team has been to predict the structural behaviour of the tests before they are conducted. The assessment was conducted using the specialist structural fire engineering FEA program *Vulcan*, and this paper reports the results of this predictive analysis.

1 TEST DESCRIPTION

The objectives of the Veselí tests are to provide experimental data on the response of composite frames to a natural fire, and to demonstrate the impact of improved detailing of joints on structural robustness in fire. The tests are scheduled to be conducted on the 6th and 15th of September 2011. They have been designed and are to be carried out by the Prague team of COMPFIRE (Department of Steel and Timber Structures of the Czech Technical University) and the Sheffield team has checked the design of the connections. Two fire tests will be performed on the test structure in sequence, one on each storey. During the first test (hereafter referred to as Test 1), the upper storey will be heated without mechanical loading applied on the slab above. This test does not aim to cause failure; the objectives are to observe the heat transfer in the compartment and to measure the temperature distributions in the structure, particularly in the beam-to-column connections. The second test (Test 2) is to be performed in the lower storey, which is subject to both mechanical and fire loading, with the upper floor cool. It aims to collect temperature data and to demonstrate the robustness in fire of the particular types of joints investigated in this project. Failure of the connections is expected.

The test has been set up as a 9m high, 10.4m x 13.4m two-storey office building structure as shown in Figures 1 and 2. The floor system consists of 120mm thick composite slabs with trapezoidal decking and Grade C30 concrete. The slabs act compositely with the steel beams with TRW Nelson 19mm diameter and 100mm height shear connectors in each rib. The slabs are reinforced

with a plain bar mesh, providing a steel area of 196mm^2/m in each direction, situated 20mm below the top of the slab. There is also a ϕ8mm reinforcement bar in each rib, with 20mm cover from the bottom of the slab.

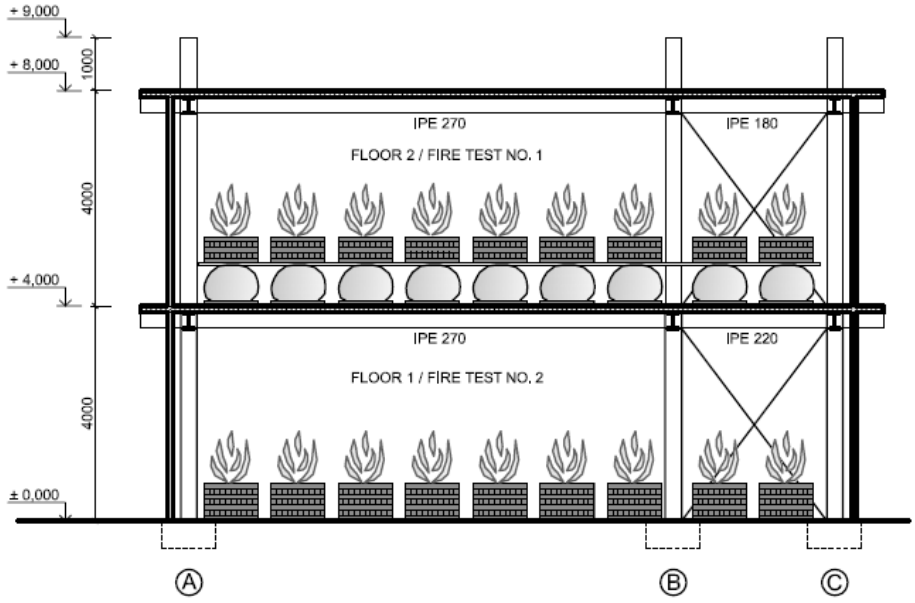

Fig. 1 Test setup (Wald 2011)

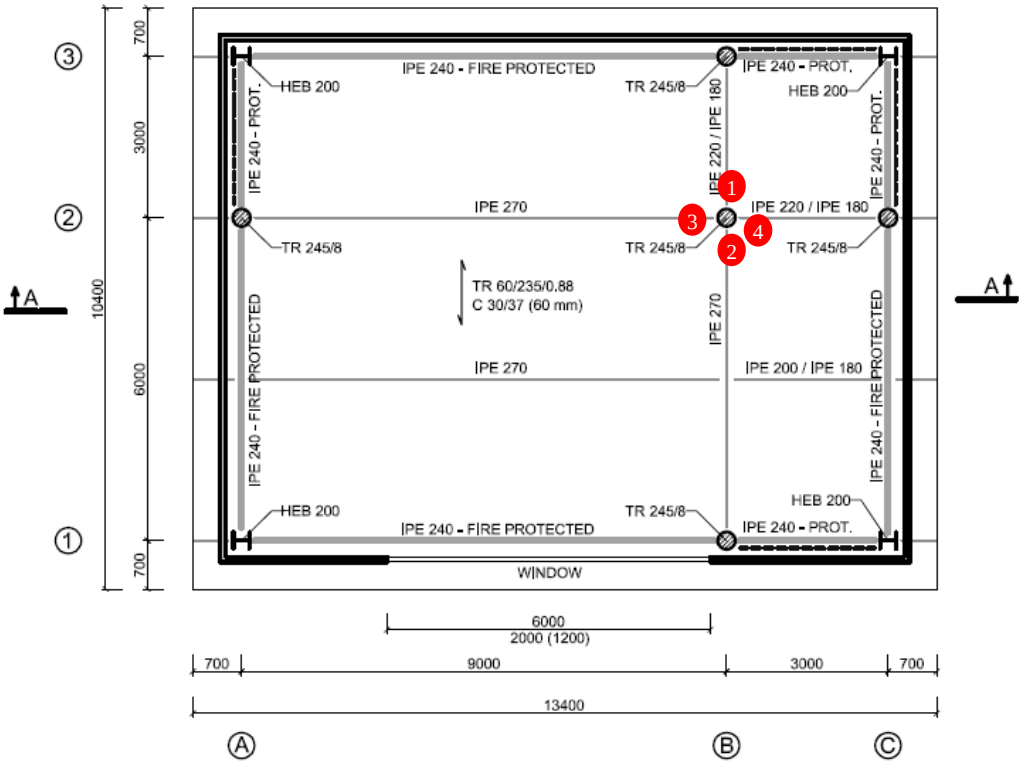

Fig. 2 Floor plan of the test structure (Wald 2011)

The edge beams are all IPE 240, while IPE 270 beams are used for the 9m span interior beams and IPE 220, IPE 200 and IPE 180 are used for the shorter-span ones. The floor arrangement is supported by five circular CFT columns (TR 245/8 filled with Grade C30 concrete) and four HEB 200 steel columns at the corners. All columns and beams are of Grade S355 steel. Two types of connections, reverse-channel and fin-plate, are adopted. The horizontal stiffness of the building is provided by two sets of cross bracing of tubular section in each direction of each floor. The columns, edge beams, bracings and connections in the lower floor are fire-protected to a standard

resistance R60. All the other elements are unprotected. The cladding walls, which are composed of liner trays, mineral wool and external corrugated sheets, form a fire compartment on each floor.
The applied mechanical load has been designed to represent that of a typical office building. The imposed load of 3.0kN/m^2 on the slab is generated by bags filled with gravel and recycled concrete. The self-weight of the floor system (including the slabs and floorings) is 2.85kN/m^2 and that of the partitions is 0.5kN/m^2. The fire load is generated by timber cribs of size 50mm x 50mm x 1000mm to simulate a natural fire in a regular office building. A 2m x 6m unglazed opening in the front wall of each floor provides ventilation to the fire. More details of the test setup can be found in Wald (2011).

2 PRE-TEST MODELLING USING *Vulcan*

This section reports the pre-test predictions of the structural response of the loaded test (Test 2). The modelling was conducted using the structural fire engineering FEA program *Vulcan* (VSL).

2.1 Model setup

Based on the design brief, the model was set up as shown in Figure 3. For simplification the flooring system and the beams of the upper floor were not modelled, but their self-weight (2.85kN/m^2) was applied on the column tops as concentrated loads. The applied load on the slab was 6.35kN/m^2, which is the overall actual (unfactored) load. The column base was assumed to be fixed. Since the frame is braced, the top ends of the upper-floor columns were restrained against lateral movement but free to deform axially, so thermal elongation is unrestrained. All the other elements had neither translational nor rotational restraints. While waiting for the actual temperature data, the first predictions were made by relating the beam, column and slab temperatures to a Eurocode 1: Part 1.2 (CEN 2002) type of fire curve (Figure 4) which reaches 1000°C at 60 minutes and then starts to descend linearly. The upper-floor elements were exempted from this assumption, as they were assumed to remain cool throughout the analysis.

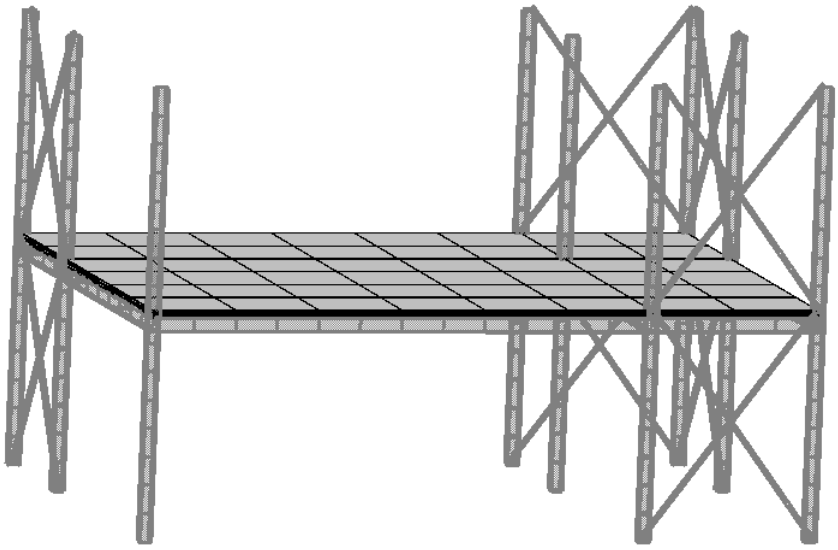

Fig. 3 Vulcan model setup

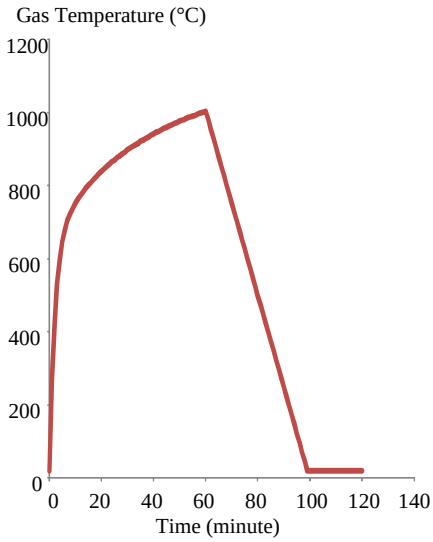

Fig. 4 Fire curve

For the unprotected beams, the temperatures of their bottom flanges and webs were assumed to be 95% of the fire temperature, and the top flanges to be at 80% of the fire temperature. The temperatures of the bottom flanges and webs of the protected beams were assumed to be 50% of the gas temperature, and the top flanges to be at 45% of the fire temperature. The lower-floor columns and bracings, which will be protected, were set as uniformly heated to 50% of the gas temperature. The temperature gradients through the slab depth were represented as a bilinear distribution, in which the slab lower surface was as hot as the fire; the temperature was 50% of the gas temperature 30% into the depth from the bottom, and the top surface reached only 15% of the fire temperature.

After the tests have been conducted, the recorded temperature data will be used as more accurate input data to the *Vulcan* model.

For the diagonal bracing members, RHS 60mm x 60mm x 6mm of Grade S275 steel were assumed in the model. Due to the limitation on mesh shape in *Vulcan*, and the resulting complexity of modelling circular sections, the circular CFT columns were modelled as equivalent (in terms of cross-section area and second moment of area) square columns of 215mm width. The connections were represented using rotational spring elements at this pre-test stage. As a part of the COMPFIRE project, a comprehensive component-based connection element is being established in *Vulcan*; the model will be upgraded using this connection element after the tests. The connections were assumed as rigid, pinned or semi-rigid by varying the rotational stiffnesses of the springs. The orthotropic nature of the slab was accounted for by using the *Vulcan* effective stiffness approach (Huang *et al.* 2000). The full depth of the composite slab was modelled as a flat slab with different bending stiffnesses in the two orthogonal directions to account for the contribution of the ribs. The shear studs connecting the composite slabs and beams, each of which was assumed to have an ultimate shear strength of 350N/mm^2, were modelled using the shear-connector elements embodied in *Vulcan*, providing partial interaction between the slabs and beams.

2.1 Results

The results of the *Vulcan* analyses are summarised in Table 1. Five models with different connection rigidities were analysed by varying the rotational stiffnesses of the spring elements, which were used to model the connections.

Tab. 1 *Vulcan* analysis results

Model No.	Connection Rigidity	Rotational Spring Stiffness (Nmm/rad)	Fire Resistance Period (minutes)	Max. Slab Displacement (mm)	Max. Connection Tying Force (kN)
1	Pinned	100	29	891	118
2	Semi-rigid	$5x10^5$	49	939	119
3	Semi-rigid	$1x10^9$	120	728	268
4	Semi-rigid	$1x10^{10}$	120	666	309
5	Rigid	$1x10^{12}$	120	642	354

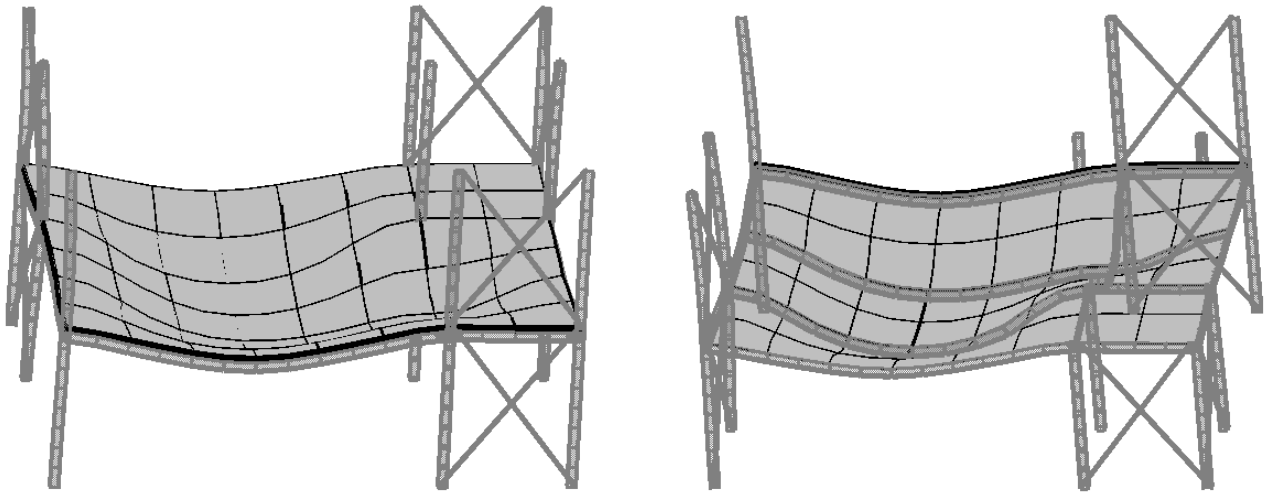

(a) View from top (b) View of slab bottom

Fig. 5 Deformed *Vulcan* model

The model with pinned connections failed at 29 minutes. Unsurprisingly, the fire resistance period was extended with increasing connection rigidity, and Models 3, 4 and 5 survived through the whole course of loading and heating without experiencing failure. The deformed shapes of the models are similar. One example is shown in Figure 5, in which the deflections are magnified three

times. The centre of the slab panel A1-B3 experienced the highest vertical displacement. Figure 6 shows the development of the slab displacement at this point over time for each model, and the maximum displacement which occurred throughout the course of analysis is given in Table 1. The model with rigid connections deflected substantially less than the one with pinned connections, even though it was subject to much higher temperatures. On the other hand, Model 2 (with semi-rigid connections) experienced a larger deflection than Model 1 (with pinned joints), due to its extended fire resistance period compared to that of the latter.

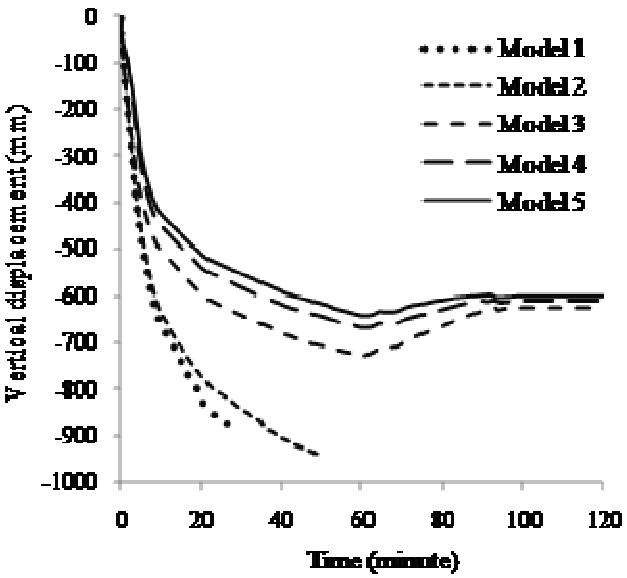

Fig. 6 Maximum displacement of slab

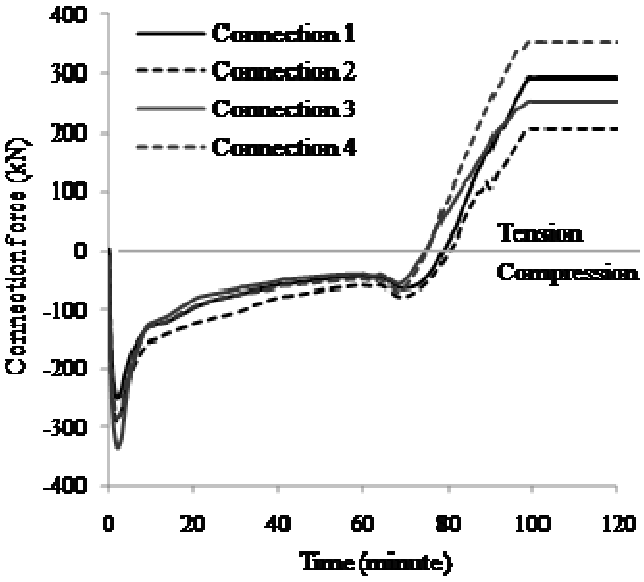

Fig. 7 Connection forces of Model 5

Due to its higher structural continuity and exposure to higher temperatures, the maximum tying force generated in the connections of Model 5 (with rigid connections) was significantly larger than those of the other models, as given in Table 1. The forces in the connections to Column B2 of this model are plotted in Figure 7. The numbering of these connections is marked on the floor plan (Figure 2). The connections were initially in compression due to the restraint to thermal expansion, but as heating continues and the beams deform further, the compressive forces decrease and finally turn into tension during cooling. This phenomenon corresponds closely with the horizontal displacement of Column A2. It can be seen that, after an initial outward movement due to thermal expansion of the structure, this column moved inwards due to pull-in by the vertically-deflecting beams. This observation may prompt speculation about a possible cause of the failure of Models 1 and 2. Further in-depth analyses will be carried out after the tests, in the light of measured temperature and structural data.

3 CONCLUSION

In this paper, an initial prediction has been made of the response to natural fire of the composite structure to be tested later in 2011 at Veselí using the finite element program *Vulcan*. While awaiting precise data (such as the temperature distributions) which will only be confirmed when the tests are performed, conservative assumptions have been made at this pre-test prediction stage. Since the robustness in fire of the connections is of particular interest in these tests, five models of identical setup but different connection rigidities were analysed, and the following behaviour has been observed:

- The deformation shapes of the models are similar;
- Initially, the floor system expanded, which pushed the edge columns outwards and induced high compression in the connections due to restrained thermal expansion;
- This action reversed as the beam deflected further: the columns moved inwards due to pull-in by the deflecting beam, and the connection forces eventually reversed, becoming tensile;

- The effect of connection rigidity on the fire resistance and deformability of the structure is considerable; the fire resistance of the structure is enhanced by increasing the rotational stiffnesses of the connections;
- For the models with more rigid connections, the maximum tying forces in the connections are greatly increased, although the maximum slab displacements are not necessary smaller, since these models experience higher temperatures.

ACKNOWLEDGMENT

The research leading to these results has received funding from the European Community's Research Fund for Coal and Steel (RFCS) under grant agreement n° RFSR-CT-2009-00021.

REFERENCES

European Committee for Standardization (CEN), BS EN 1991-1-2, Eurocode 1. Actions on structures. General actions. Actions on structures exposed to fire, British Standards Institution, UK, 2002.

Huang, Z., Burgess, I. W. and Plank, R. J., Effective Stiffness Modelling of Composite Concrete Slabs in Fire, Engineering Structures, Volume 22(9), pp 1133-1144, 2000.

Newman, G. M., Robinson, J. T. and Bailey, C. G. Fire Safety Design: A New Approach to Multi-Storey Steel-Framed Buildings, The Steel Construction Institute, Ascot, 2004.

NIST, Final Report on the Collapse of the World Trade Center Towers, National Institute of Standards and Technology, USA, 2005.

NIST, Final Report on the Collapse of World Trade Center Building 7, U.S. Department of Commerce and National Institute of Standards and Technology, USA, 2008.

RFCS, Design of Joints to Composite Columns for Improved Fire Robustness, Research Fund for Coal and Steel, Grant agreement n° RFSR-CT-2009-00021, European Commission, Belgium, 2008.

Vulcan Solutions Limited: http://www.vulcan-solutions.com

Wald, F., Demonstration Fire Test on Real Object - Veselí 2011, The Czech Technical University, Czech Republic, 2011.

STRUCTURAL FIRE ENGINEERING IN BUILDING RENOVATION
Application of Natural Fire and Heat transfer Models to guarantee Fire Safety

Tom Molkens [a]

[a] StuBeCo, Engineering Office, Overpelt, Belgium

INTRODUCTION

Till the years seventy or nearly eighties of previous century most of the concrete structures are developed just to resist loads in so far "cold" situations. Due to this reason there rise often problems at the moment of structural renovations. This at two levels; the deformations seems to be unexpected big and the fire resistance of the structural elements are insufficient to guarantee the required level. The deformation problem in the scope of this study no issue.
By the aid of a case study with a problematic concrete floor and cover we want to show the possibilities of software tools to calculate different options which finally must lead to an integrated fire risk management and guaranteed fire stability.
The limitations of this approach don't stop with concrete because this is the main problem in this case study. It seems that also existing wood, masonry and steel structures have the same problems and can be solved on a similar way.

1 DESIGN CONSIDERATIONS

1.1 Juridical

Strictly juridical spoken there is in a lot of cases no need for a proven fire stability. In most of the cases the need for application of a law will be linked to buildings with a building permit request after the publishing date of the law (for example Annexes R.D., 1997). So existing building (or parts) escape, even in rather heavy transformation, to the regulation for new buildings.
For our case study the special Belgian regulation for school buildings (IBN/BIN, 1982) is valid and requests only one half hour of fire stability, with only day-use of the building. Only for buildings/parts with permit requests after 1997, the normal regulations for low buildings are valid which would ask a fire resistance of at least one hour. Because his higher order this regulation is mostly used, but like already said not on application for existing buildings.
Unless this juridical possibilities or call it leaks, the school authority wants to assure in our case-study a higher level of security instead of the half hour (maximum which can be achieved by application of tabulated data). This to be in order with their own conscience. Just for the case if something must happen with the knowledge that there building didn't fit actual regulations.

1.2 Scientific

To solve this conscience problem we presented the school a natural fire with the criterion that the existing structure must withstand the whole duration of the fire. There is no longer an estimated time because we're speaking about a natural fire and not about a comparison criterion like the ISO834 is. Belgian regulation (Annexes R.D., 1997) allows such an approach but the calculations must be approved by the interrogation commission of the ministry of internal affairs.
The advantage for an old building of this approach is that because there is no regulation valid, we can skip this verification by the interrogation commission. This becomes therefore more cost effective because of lesser administration and lesser retarding effects on the building process. This latest is important because mostly the inconvenience comes clear in the demolishing phase just before rebuilding. However in our opinion the missing of verification can be a disadvantage, because such natural fire models can be sensitive for boundary conditions.
With the presence of rather heavy masonry, concrete floors and not a real high amount of windows, it can be estimated that the fire will be smouldered and not very explosive.

1.3 Software use for structural fire engineering

After juridical and scientific considerations we've got to solve the problem and therefore rather easy to use software solutions are available, sometimes even free. For our approach we made use of a 2-zone model (Ozone V2) to determine the fire load. This fire load is introduced in a basic commercial available thermo elastic frame work software called Powerframe. To reduce the problem to a 2D-frame we made a slice of 1 m width. This allows us to regard not only the thermal behaviour of the sections but also to the thermal expansion effects of the structure as whole. With those rather simple "in use" software tools we can obtain much more guarantees about the behaviour of the structure in case of fire as before.

2 DESCRIPTION OF THE CASE STUDY

2.1 Geometry

The involved building part was build in 1939 and in the 50's of previous century extended, the oldest part dates from 1881. The connection between those 3 building phases was partially demolished to create a new entrance with some new facilities. Partial, because a part of the building (with an audience) was protected by the ministry of monuments and sites, this must be kept in his original shape.

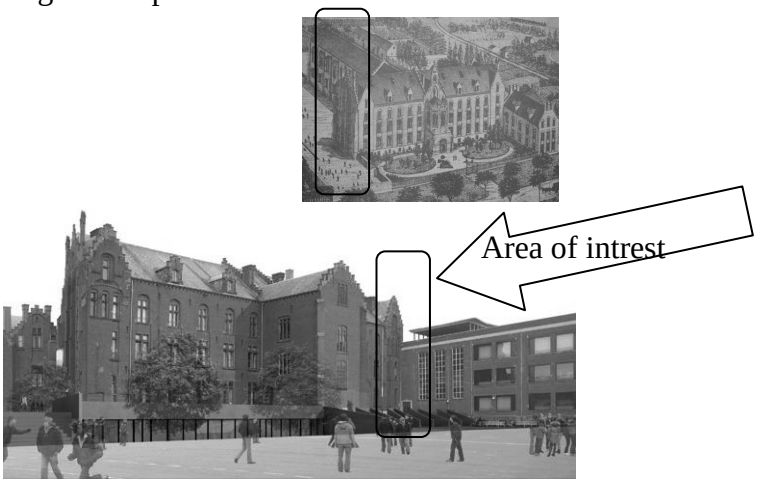

Fig. 1 Elevation views

Fig. 2 View from demolished area

Besides previous images the ground floors and section made by the architect gives a much better idea of the dimensions of the structure.

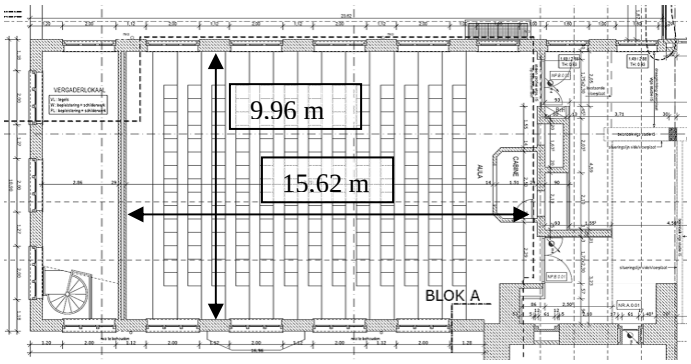

Fig. 3 Ground view; 9,96x15,62 m²

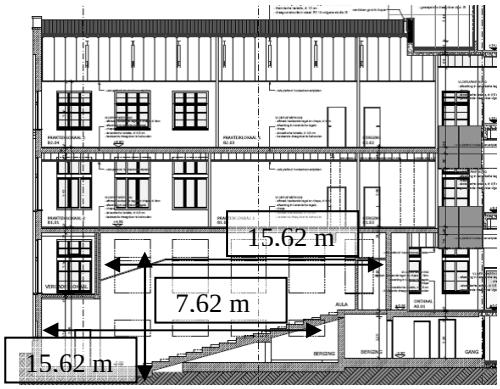

Fig. 4 Section; 7,62 m

The structure exists of bearing masonry and ribbed concrete slabs. The slabs support from elevation to elevation without any intermediate support. Besides the auditorium at 0-level we've also classes at the first and second floor level. Above the second level there are steel truss beams which were in tender foreseen to be protected with anti-combustion painting.

2.2 Materials

All material properties corresponds with the relevant EN-standards for concrete, steel and masonry. We've summarized those in Tab. 1.

Tab. 1 Material properties

Material	ρ [kg/m³]	ΔL/L [mm/mK]	λ [W/mK] at 20°C	c [J/kgK]
Masonry	1600	5	0,70	840
Concrete	2300	10*	1,60*	1000*
Steel	7850	12*	14,6*	450*

* Those values are at 20°C and are only automatically adapted in function of temperature in the frame work model to calculate the mechanical response

3 FIRE LOAD

To limit fire risks it was obtained that each schoolroom or auditorium will be executed as a separated compartment. Only fire doors were not yet foreseen, so the extra cost was not an obstacle. Due to the EN 1991-1-2 the fire load exists of uniformly distributed 347 MJ/m² for a typical schoolroom (tab E.4, 80% fractile). Because of the presence of a wooden false ceiling we raised it for the audience till 511 MJ/m² (+ 21 mm of wood).
For the fire a NFSC fire curve was chosen; fire growth was taken as medium, with a rate of heat release equal to 250 kW/m², danger of activation = 1, reduction for heat detection (0,87), off site brigade (0,78) and raise because of the surface (1,43). The combustion efficiency factor was putted on 0,80 (wood based fire). Because the building can't be air-closed a constant ratio of 2% of the vertical surface is introduced as a kind of natural ventilation factor + windows and doors without REI value of course.

3.1 Audience

Thanks to the software several scenario's where investigated, in particular the influence of the window openings was investigated. Hereby was not only the temperature of importance but also the delay till flash-over. It was mentioned by the school authority that this time must me be as big as possible, at least 10 minutes to be similar with the other existing class rooms. In addition an extra exit bellow the audience seems to be absolutely needed to prevent evacuation problems. We start simulations with the actual situation:

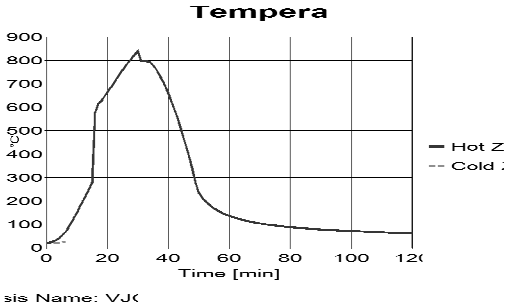

Fig. 5 Gas temperature actual situation

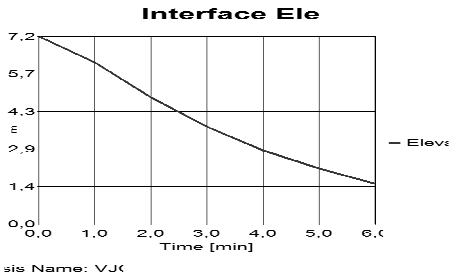

Fig. 6 Cold layer

It is rather clear that after 30 minutes we achieve a temperature which is almost the same as predicted by an ISO 834 conventional fire. But the peak value is only there in a shorter and limited time interval. The switch to one zone happens already after 6 minutes with a cold layer of only 1,54 m = first approximation of smoke free layer.
In the past they closed all window opening, because there is no need for day light in the audience. This avoid entrance of oxygen but also the evacuation of heated smoke. Therefore we did a new calculation with the upper part opened. There is certainly an influence on the temperature decreases from 900 till bellow 600 °C but the time till flash over stays still to big. This figures are not shown.

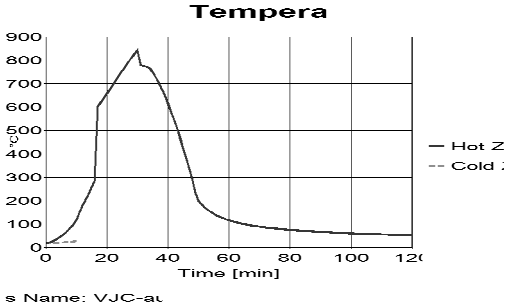

Fig. 9 Gas temperature + S&H system

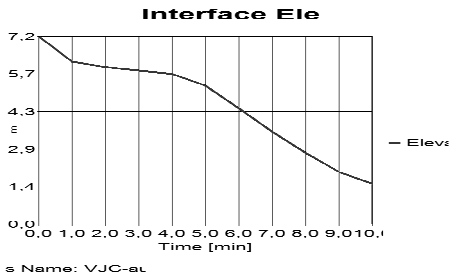

Fig. 10 Cold layer

By changing the ventilation group by a more advanced model which can act as a smoke and heat evacuation system (S&H system with 12 m³/s) we've reached the needed improvement of the time till flash over but the temperature stays still high. By removing the false ceiling (it is a fire load of 347 instead of 511 MJ/m²) only the time interval with higher gas temperatures can be reduced with about 6 minutes. There is no effect on other parameters.

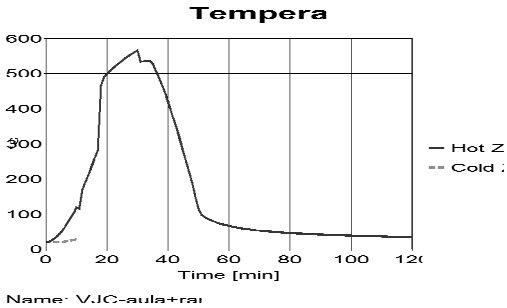

Fig. 11 Gas temperature + S&H system

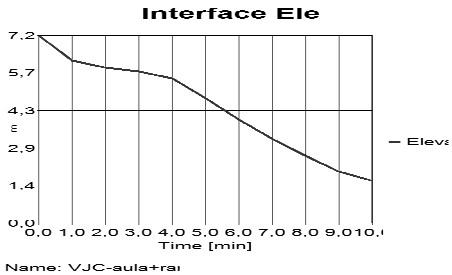

Fig. 12 Cold layer

It seems that a combination of passive (making high openings in masonry) and active equipment (S&H system with 10 m³/s) can lead to low temperature profiles, limited in time and with an acceptable delay till flash over. This option was therefore proposed and chosen.

3.2 Class room at first level

We've looked for the classroom that has the highest ratio window/wall surface to obtain the most worst fire scenario = room 1.01.

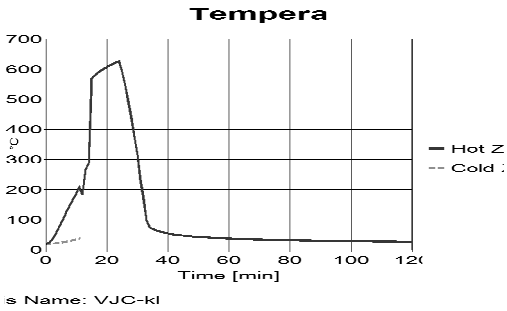

Fig. 13 Gas temperature + S&H system

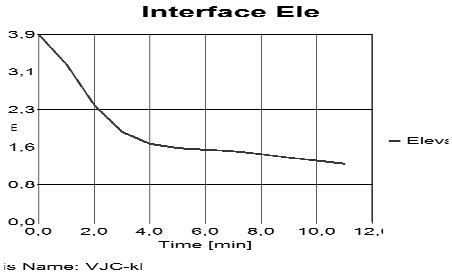

Fig. 14 Smoke layer

Because there are in relation to the elevation surface more opening the temperature rises, due to the limited fire load (347 MJ/m², no wooden false ceiling) the width of curve with higher temperatures is however more limited.

3.3 Class room at second level

As before we made the same exercise but for room 2.04, unfortunately we don't have any more a heavy ceiling but only a plasterboard covering of the steel structure.

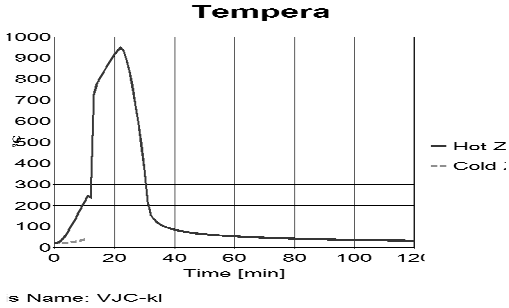

Fig. 15 Gas temperature + S&H system

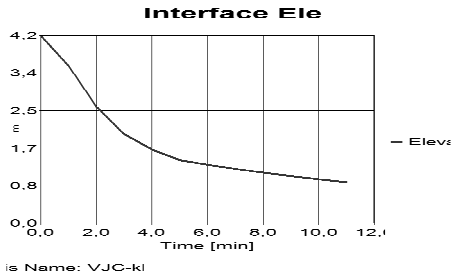

Fig. 16 Smoke layer

The temperature rise higher and quicker as before without “damping” mass

4 REACTION OF THE STRUCTURE

At this moment we’ve calculated several fire loads which are different for each level. Those fire loads are incorporated in a slice-model of the structure. The width is taken equal to 400 mm (= distance between ribs) except at the location of windows where it is limited to the ratio sum of all windows/overall width of the elevation. Spring constants equal to 3EI/L are integrated at the hinges to avoid a mechanism and making a realistic approach of stiffness boundaries.

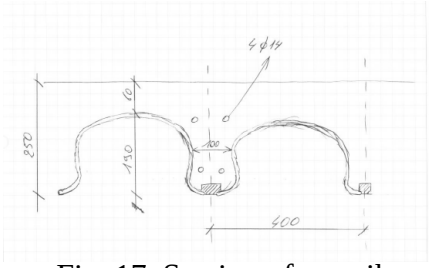

Fig. 17 Section of one rib

Fig. 18 Slice model

For the concrete elements we made a model with only concrete because it was said that the influence of the reinforcement would be of lesser importance, it gives an extra reserve.

4.1 Concrete elements

With the mentioned fire loads above we can calculate following temperature profiles with maximum reinforcement temperature:

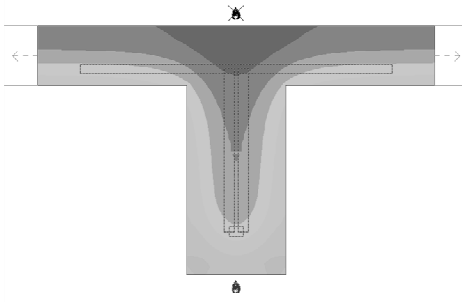

Fig. 19 Audience max after 43 min.

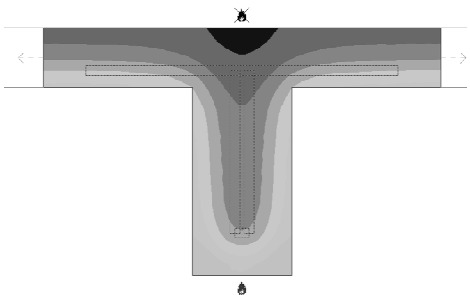

Fig. 20 Class 1.01 max after 31’

At the moment the highest temperatures are reached at the level of the reinforcement the surface subjected to smoke is already in cooling phase. Therefore the natural fires makes that the reinforcement never reaches 500°C, at maximum only about 200°C.

4.2 Steel structure

It seems that also for the steel, thanks to the double layer of gypsum board, the temperature never reaches 500 °C, 150 °C becomes the maximum. This coursed by the very thin peak in the curve.

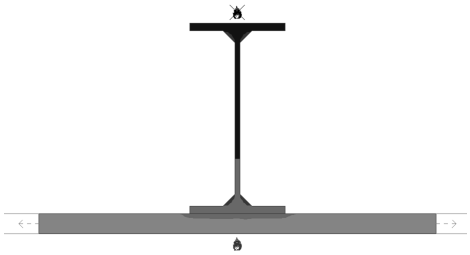

Fig. 21 Steel, max after 55 min.

For the steel is besides the double gypsum board no further protection needed.

4.3 Masonry structure

With the acting bending moments and temperature profiles coming out of the model we could check and confirm on a manual way the bearing capacity of the masonry walls on several levels.

5 CONCLUSIONS

With the aid of easy to use 2-zone models and a thermo elastic stability check we were in the possibility to build up a tailor made solution for this particular problem. This with build in security there were needed, without overkill and perhaps more important without underestimation of some effects.
Some extra costs were needed but otherwise we could realise also some efforts for the steel construction. The proposed solution is approved by the school authority and executed.

REFERENCES

NBN S21-204 Fire protection in buildings – School buildings – general requirements an fire reaction, Belgian standard institute IBN/BIN, 1982.

Annexes to add at the Royal Decree of 19/12/1997, modification of the Royal Decree of 07/07/1994: published the 30/12/1997: Terms and rules for low, medium and high buildings + reaction on fire of materials, Moniteur Belge 1997.

EN 1990:2002+National Annexe NBN EN 1990-ANB:2007, Eurocode 0: Basis of structural design, European Committee for Standardization CEN, 2002.

EN 1991-1-2:2002+National Annex NBN EN 1991-1-2-ANB:2008, Eurocode 1: Actions on structures - Part 1-2: General actions - Actions on structures exposed to fire, European Committee for Standardization CEN.

EN 1992-1-2:2005+Nationale Bijlage NBN EN 1992-1-2-ANB:2010, Eurocode 2: Design of concrete structures - Part 1-2: General rules - Structural fire design, European Committee for Standardization CEN, 2005.

A tool to design steel elements submitted to compartment fires OZone V2. Part 1: pre- and post-flashover compartment fire model, Cadorin J.-F. & Franssen J.-M., Fire Safety Journal, Elsevier, 38 (2003), 395-427, <http://hdl.handle.net/2268/29650> http://hdl.handle.net/2268/29650.

A tool to design steel elements submitted to compartment fires OZone V2.Part 2: Methodology and application, Cadorin J.-F., Pintea D., Dotreppe J.-C. & Franssen J.-M., Fire Safety Journal, Elsevier, 38 (2003), 429-451, <http://hdl.handle.net/2268/29651> http://hdl.handle.net/2268/29651.

PowerFrame version 2010 and Diamonds by BuildSoft, version 2011.

SAFIR. A Thermal/Structural Program Modelling Structures under Fire, Franssen J.-M., Engineering Journal, A.I.S.C., Vol 42, No. 3 (2005), 143-158.

FAILURE PROBABILITY ASSESSMENT FOR FIRE SITUATION WITH A CERTAIN TYPE OF THE NETWORK DIAGRAM
Example of application

Mariusz Maślak [a]

[a] Cracow University of Technology, Faculty of Civil Engineering, Cracow, Poland

INTRODUCTION

Failure probability is usually adopted as an objective measure of the safety level if accidental fire conditions are considered in the analysis. However, estimation of its value, being reliable and precise enough, is not easy. In general such probability depends on a great amount of factors, connected between each other in a complex and intercorrelated network. For this reason, solutions obtained by traditional design methodology not always can be unequivocally interpreted. Moreover, the assessed value will be significantly different from the previous one if further factors influencing the fire safety are additionally considered or even if the order of the occurrence of the examined factors changes. In the presented paper specific and user friendly calculation technique is discussed by the author in detail, helpful for the accurate evaluation of the probability that fire which has already occurred will not be extinguished in any way and, consequently, the failure of the analysed structural member will take place. This approach is based on the study of a certain type of the network diagram, suggested by *R. W. Fitzgerald* (Fitzgerald, 2004). Such diagram contains both AND and OR-type logical gates, which are identified respectively with the conjunction and the alternative of independent and complementary random events. The examined scheme can be extended by the addition of the next level of the analysis if considered fire may expand from one fire compartment to the adjoining one. The proposed design procedure of the assessment of searched failure probability is in the article widely illustrated by a representative numerical example.

1 VARIOUS INTERPRETATIONS OF THE FAILURE PROBABILITY

Application of failure probabilty p_f as a basic safety measure in classical structural analysis made for accidental fire situation explicitly determines the understanding of the limit state phenomenon, danger to some people or to the building structure. This limit state is not reached exactly at the point-in-time when such considered unexpected event really takes place, but earlier, when the probability of its occurrence is no longer possible to accept. Conclusively, the ultimate condition is in general formulated as follows:

$$p_f \leq p_{f,ult} \tag{1}$$

where $p_{f,ult}$ is the maximum value of p_f which can be acceptable to the designer or, more frequently, to the suitable authorities. Values of $p_{f,ult}$, linked with the right side of Eq. (1), are assigned arbitrarily, to be adequate for the assumed reliability class. In the presented paper some aspects of the assesment of the probability p_f, associated with the left side of this inequality, are discussed. However, before the detailed analysis how to correctly evaluate its value will be presented we have to precisely define what kind of the probability is considered. It is crucially important because at least two different interpretations can be distinguished in this field. They are as follows (Maślak, 2005), (Maślak and Domański, 2008):

- probability of failure, caused by fire, if it is known that fire ignition has occurred and; moreover, that this fire has reached the flashover point (it may be described as a fully developed fire) – in further analysis such probability will be marked by the symbol p_f,
- probability of failure, caused by potential fire which can take place; however, it has not yet occurred (so the designer has no information about its ignition and flashover) – let us appoint the symbol p_{ff} for its designation.

Relation between p_f and p_{ff} is given by *T. T. Lie* (Lie, 1972):

$$p_{ff} = p_t p_f \tag{2}$$

where p_t means the probability of fire occurrence (the most frequently not only of fire ignition but also of reaching the flashover point). As we can see, probability p_f should be interpreted as a conditional one with the condition that fire has already occurred and the temperature of exhaust gas in the whole compartment is uniform (the fire is fully developed). Not only qualitative but also quantitative distinction between those both probabilities, p_f and p_{ff}, seems to be very significant. Even if conditional probability p_f is large, probability p_{ff} is usually quite small and does not seem to be apprehensive, because in reality the value of probability p_t is also slight (Maślak, 2005).

2 LOGICAL GATES IN FAILURE PROBABILITY ASSESSMENT

Let us assume, developing the example given by *R. W. Fitzgerald* (Fitzgerald, 2004), that failure (F) in this analysis is connected with the case when fully-developed fire in considered compartment will not be extinguished. Only three ways of its extinction are then specified as possible in real conditions:

- $E1$ - fire will burn out spontaneously,
- $E2$ - fire will be extinguished owing to the working of active fire protection measures (sprinklers, water curtains etc.), without any activity of a fire brigade,
- $E3$ - fire will be extinguished due to the activity of a fire brigade.

Let the symbol $\overline{E}$ denote for each identified way of the extinction the event contrary to event E. It is also the event complementary to E in mathematical sense, so that $P(E) \cup P(\overline{E}) = 1$. It is important that all considered ways of fire extinction have to be understood as independent in statistical sense. For this reason the event, formally possible, that fire is only partially supressed by active fire protection measures, but definitively extinguished only when the fire brigade firefighting action is successfully finished, should be classified explicitly as the $E3$ manner. Finally, the following evaluations can be performed:

- fire which has started will not be extiguished at all if event $\overline{E1}$ AND event $\overline{E2}$ AND also event $\overline{E3}$ occur, so failure probability $P(F)$ can be assessed by the formula:

$$p_f = P(F) = P(\overline{E1}) \cdot P(\overline{E2}) \cdot P(\overline{E3}) = [1 - P(E1)] \cdot [1 - P(E2)] \cdot [1 - P(E3)] \tag{3}$$

- fire which has started will be extinguished as a result EITHER of the occurrence of event $E1$, OR event $E2$, OR event $E3$. Occurrence of only one from those three events is sufficient to cause the extinction of fire. However, in this case the scheme of calculation of searched probability is not so simple. Let us notice that the event $E2$ can occur only if the event $E1$ does not occur (i.e. if the event $\overline{E1}$ occurs). Similarly, the event $E3$ can occur only if the events $E1$ AND $E2$ do not occur previously (i.e. if the events $\overline{E1}$ AND $\overline{E2}$ occur). In conclusion the final formula applied for its calculation has the form:

$$1-p_f = P(\overline{F}) = P(E1) + P(\overline{E1})P(E2) + P(\overline{E1})P(\overline{E2})P(E3) = \\ = P(E1) + [1-P(E1)]P(E2) + [1-P(E1)]\cdot[1-P(E2)]P(E3) \tag{4}$$

which means that the fire will be extinguished only when the event $E1$ occurs, OR when the event $E2$ takes place provided that the event $\overline{E1}$ will have happened previously, OR if the event $E3$ appears in the case when not only the event $\overline{E1}$ but also the event $\overline{E2}$ will have come into being.

As we can see two types of the logical gates are taken into account in such analysis. The first kind is the classical AND-type gate. It is the synonymous with the conjunction of independent random events. Probability $p_f = P(F)$ is in this case calculated as a simple product of component probabilities (see Eq. (3)). The second one is the OR-type gate which can be identified with the alternative of considered random events. This is the reason why the probability $P(\overline{F})$ is estimated as an ordinary sum of component probabilities (see Eq. (4)). Let us notice that also some internal AND-type gates can be identified in the evaluation of the probability $(1-p_f)$. Correctness of the obtained solution may be verified by checking the following equation:

$$P(F) = 1 - P(\overline{F}) \tag{5}$$

If the considered fire is not extinguished in the analysed compartment $\Omega 1$ (i.e. when the event F with respect to Eq. 3 takes place) then it will be the imminence that flames can expand to the adjoining room $\Omega 2$. This case will be possible if the fire-break division (fire-partition or fire-resisting door), being a barrier (*B*) for fire increasing, damages and - as a consequence - it does not fulfil imposed insulating requirements. Such event will be denoted in further analysis by the symbol $\overline{B}$. Let us assume that only two causes may be specified for such disaster (Fitzgerald, 2004):

- $\overline{B1}$ for the situation when the fire isolation limit state is reached,
- $\overline{B2}$ for the alternative situation when the fire tightness limit state is reached.

Consequently, the event marked by the symbol B will concern the case when the barrier is sufficiently strong and it does not admit to expand the fire.

3 THE FITZGERALD'S-TYPE NETWORK DIAGRAM

Application of the network diagram can be very helpful for practical evaluation of failure probability $p_f = P(F)$ with the calculation procedure presented above. Many types of such diagram can be found in the professional literature. In the presented article the author proposes to use in this field the scheme given by *R. W. Fitzgerald* (Fitzgerald, 2004). It is shown in Fig. 1 for the case when fire can expand from one fire compartment to adjoining one. Let us notice that all connections marked with the solid line are always linked with the AND-type logical gates. On the other hand, connections drawn by means of the broken line can be identified with the OR-type logical gates. To describe in detail how to correctly use such assessment methodology the numerical example has been prepared by the author (Maślak, 2008). Its fundamental solutions are presented below.

4 NUMERICAL EXAMPLE

Let us assume that in the fire compartment $\Omega 1$ we have:

$P(E1) = 0{,}4$; $P(E2) = 0{,}8$; $P(E3) = 0{,}7$.

Probability that the considered fire will not be extinguished at all in the fire compartment $\Omega 1$:

$$P(F\Omega 1) = [1-P(E1)]\cdot[1-P(E2)]\cdot[1-P(E3)] = 0{,}6\cdot 0{,}2\cdot 0{,}3 = 0{,}036$$

Probabilty that this fire will be extingished succesfully in the fire compartment $\Omega 1$ in any way:

$$P(\overline{F\Omega 1}) = P(E1) + P(\overline{E1})P(E2) + P(\overline{E1})P(\overline{E2})P(E3) = 0{,}4 + 0{,}6 \cdot 0{,}8 + 0{,}6 \cdot 0{,}2 \cdot 0{,}7 = 0{,}964$$

Formal checking:

$0{,}036 + 0{,}964 = 1{,}0$.

Let us assume that:

$P(B) = 0{,}75$; $P(\overline{B1}) = 0{,}15$; $P(\overline{B2}) = 0{,}10$.

Formal checking:

$P(B) + P(\overline{B1}) + P(\overline{B2}) = 0{,}75 + 0{,}15 + 0{,}10 = 1$.

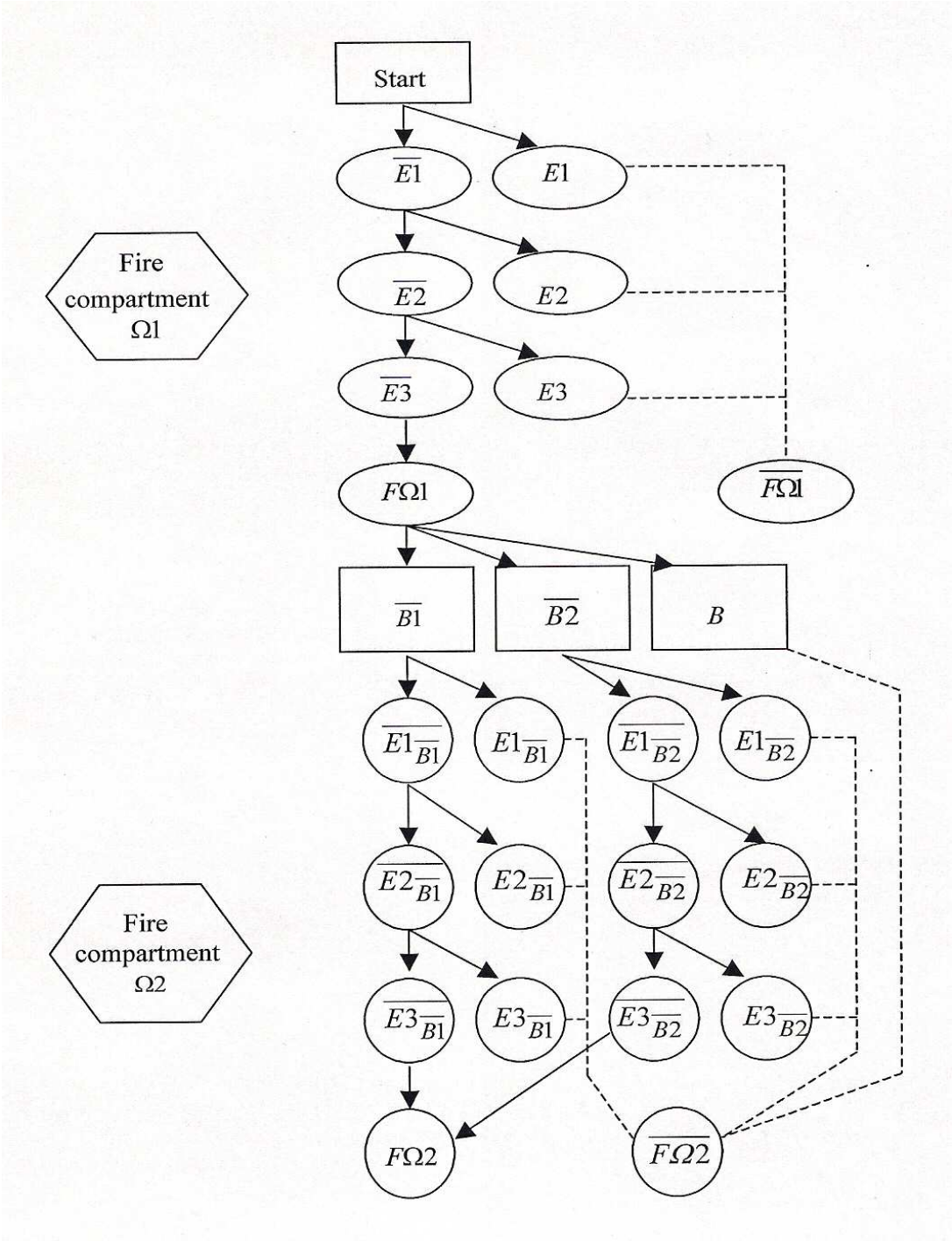

Fig. 1 Network diagram proposed by *R. W. Fitzgerald* (Fitzgerald, 2004) for the case when the considered fire can expand from one fire compartment to adjoining one.

Let, in the fire compartment $\Omega 2$, us have:

$P(E1_{\overline{B1}}) = 0{,}3$; $P(E2_{\overline{B1}}) = 0{,}7$; $P(E3_{\overline{B1}}) = 0{,}9$, $P(E1_{\overline{B2}}) = 0{,}1$; $P(E2_{\overline{B2}}) = 0{,}2$; $P(E3_{\overline{B2}}) = 0{,}3$,

Probability that the fire which has not been extinguished in the fire compartment $\Omega 1$ will not be extinguished also in the adjoining fire compartment $\Omega 2$:

$$P(F\Omega 2_{\overline{B1}}) = P(F\Omega 1)P(\overline{B1})P(\overline{E1_{\overline{B1}}})P(\overline{E2_{\overline{B1}}})P(\overline{E3_{\overline{B1}}}) = 0{,}036 \cdot 0{,}15 \cdot (1-0{,}3)(1-0{,}7)(1-0{,}9) =$$

$$= 1{,}134 \cdot 10^{-4}$$

$$P(F\Omega 2_{\overline{B2}}) = P(F\Omega 1)P(\overline{B2})P(\overline{E1_{\overline{B2}}})P(\overline{E2_{\overline{B2}}})P(\overline{E3_{\overline{B2}}}) = 0{,}036 \cdot 0{,}10 \cdot (1-0{,}1)(1-0{,}2)(1-0{,}3) =$$

$$= 1{,}814 \cdot 10^{-3}$$

$$P(F\Omega 2) = P(F\Omega 2_{\overline{B1}}) + P(F\Omega 2_{\overline{B2}}) = 1{,}134 \cdot 10^{-4} + 1{,}814 \cdot 10^{-3} = 1{,}927 \cdot 10^{-3}$$

Probability that the fire which has not been extinguished in the fire compartment $\Omega 1$ will be extinguished succesfully in the adjoining fire compartment $\Omega 2$:

$$P(\overline{F\Omega 2_{\overline{B1}}}) = P(F\Omega 1)P(\overline{B1}) \cdot \left[P(E1_{\overline{B1}}) + P(\overline{E1_{\overline{B1}}})P(E2_{\overline{B1}}) + P(\overline{E1_{\overline{B1}}})P(\overline{E2_{\overline{B1}}})P(E3_{\overline{B1}})\right] =$$

$$= 0{,}036 \cdot 0{,}15 \cdot [0{,}3 + (1-0{,}3) \cdot 0{,}7 + (1-0{,}3)(1-0{,}7) \cdot 0{,}9] = 5{,}287 \cdot 10^{-3}$$

$$P(\overline{F\Omega 2_{\overline{B2}}}) = P(F\Omega 1)P(\overline{B2}) \cdot \left[P(E1_{\overline{B2}}) + P(\overline{E1_{\overline{B2}}})P(E2_{\overline{B2}}) + P(\overline{E1_{\overline{B2}}})P(\overline{E2_{\overline{B2}}})P(E3_{\overline{B2}})\right] =$$

$$= 0{,}036 \cdot 0{,}10 \cdot [0{,}1 + (1-0{,}1) \cdot 0{,}2 + (1-0{,}1)(1-0{,}2) \cdot 0{,}3] = 1{,}786 \cdot 10^{-3}$$

$$P(\overline{F\Omega 2_B}) = P(F\Omega 1)P(B) = 0{,}036 \cdot 0{,}75 = 0{,}027$$

$$P(\overline{F\Omega 2}) = P(\overline{F\Omega 2_{\overline{B1}}}) + P(\overline{F\Omega 2_{\overline{B2}}}) + P(\overline{F\Omega 2_B}) = 5{,}287 \cdot 10^{-3} + 1{,}786 \cdot 10^{-3} + 0{,}027 =$$

$$= 0{,}03407$$

Hence, the probability that the considered fire will be exinguished at all (in the fire compartment $\Omega 1$ or in the adjoining compartment $\Omega 2$):

$$P(\overline{F}) = P(\overline{F\Omega 1}) + P(\overline{F\Omega 2}) = 0{,}964 + 0{,}03407 = 0{,}99807$$

Formal checking:

$$P(F\Omega 2) + P(\overline{F}) = 1{,}927 \cdot 10^{-3} + 0{,}99807 = 1{,}0$$

5 CONCLUDING REMARKS

Classical calculation technique, used for the evaluation of failure probability in the case when the fully developed fire broke out in considered compartment and when the flames can spread from one room to adjoining one, is usually based on the analysis of typical logical tree, reflecting the hierarchy of all factors influencing the fire safety as well as the internal connection structure between them. Therefore, the methodology of the analysis of complex hierarchical process is suggested to be used to assess its value precisely and reliably enough (Ginda and Maślak, 2006). Mathematical formalism taken from the examination of the so called Markov chains is also very promising in this field. However, the construction and the study of the network diagrams still remains the assessment approach being the most illustrative and imaginative. Such schemes should be less or more adequate for the reality, depending on their complexity and accuracy. The Bayesian networks are implemented the most frequently in the professional literature for this purpose (Holicky and Schleich, 2001). The simple network proposed by *R. W. Fitzgerald* (Fitzgerald, 2004) and discussed in this article seems to be very useful and friendly for practical application when the fire scenario and accompanying circumstances are not very complicated and when they can be explicitly identified.

Consideration of the complementary random events gives the designer the opportunity to apply for the estimation of searched safety level the well known formalism of complete probabilty analysis (Holicky and Schleich, 2001), (Maślak 2008). The logical tree based on such concept can be further developed and complicated, the most frequently through the addition of the next subsequent levels to its internal structure. Let us notice that in such case previously evaluated value of failure probability will change. Therefore, if we want to increase the precision of the probability assessment, and for that reason we take into account in the next step some additional factors influencing the fire safety, then we can easily obtain a value even significantly different from the previous one. The approach presented above is on that score safer for the implementation because the final result of the evaluation does not depend on the order of occurrence of particular component events.

The interpretation of searched probability should be clearly and uneqivocally defined. In clasical structural safety analysis probability p_f, which is conditional with the condition that fire has already ocurred, is usually estimated. However, in many cases we want to evaluate the failure probability related to some people, for example to building occupants who will be able to inhabit in considered compartment if fire ignition and flashover takes place or even to firemen taking part in potential firefighting action. In such context probability p_{ff}, understood in a different way than the previous one (see Eq. 2), is commonly assessed.

6 ACKNOWLEDGMENT

This paper was elaborated with the financial support of the project granted by Polish Ministry of Science and Higher Education (N N506 243938).

REFERENCES

Fitzgerald R. W., Building Fire Performance Analysis, John Wiley & Sons Ltd., Chichester, England, 2004, p. 534.

Ginda G., Maślak M., Assessment of Factors Influencing the Fire Safety for Building Users, Proceedings of IABSE Symposium "Responding to Tommorow's Challenges to Structural Engineering", Budapest, September 13-15, 2006, IABSE Report, vol. 92.

Holicky M., Schleich J. –B., Modelling of a Structure under Permanent and Fire Design Situation, Proceedings of the IABSE International Conference "Safety, Risk, Reliability – Trends in Engineering", Malta, 2001, pp. 1001-1006.

Lie T. T., Optimum Fire Resistance of Structures, Journal of the Structural Division, 98, No. ST1, 1972, pp. 215-232.

Maślak M., Failure Probability of Building Load-bearing Structure under Fire Conditions (in Polish), Czasopismo Techniczne, 12-B/2005, pp. 67-80.

Maślak M., Fire Resistance of Steel Bar Structures (in Polish), Monography No 370, Series "Civil Engineering", Publishers of Cracow University of Technology, Cracow, 2008, p. 203.

Maślak M., Domański T., Safety Factors in Design of Steel Member for Accidental Fire Situation, Proceedings of the International Conference "Design, Fabrication and Economy of Welded Structures", Miskolc, Hungary, Horwood Publishing, Chichester, UK, 2008, pp. 563-570.

APPLICATION OF FIRE SAFETY ENGINEERING FOR OPEN CAR PARKS IN ITALY

Emidio Nigro[a], Anna Ferraro [a], Giuseppe Cefarelli [a], Gaetano Manfredi [a] , Edoardo Cosenza [a]

[a] University of Naples FedericoII, Department of Structural Engineering (D.I.ST.), Naples, Italy

INTRODUCTION

In fire structural design, current Italian and European codes (D.M.14-01-2008, 2008; EN 1991-1-2, 2002; EN 1993-1-2, 2005) allow the use of a performance approach through the concept of Fire Safety Engineering based, among other things, on the mechanical and geometric nonlinear structural response in fire situation. According to ISO/TR 13387-1, the "Fire Safety Engineering" (FSE) is the application of engineering principles, rules and expert judgement based on a scientific assessment of the fire phenomena, the effects of fire and both the reaction and behaviour of peoples, in order to a) save life, protect property and preserve the environment and heritage, b) quantify the hazards and risks of fire and its effects, c) evaluate analytically the optimum protective and prevention measures necessary to limit, within prescribed levels, the consequences of fire.

The Directive 89/106/CEE on Construction Products of the European Community introduced the definition of the requirement of "safety in case of fire" in Europe, which is the base for the application of the Fire Safety Engineering. This requirement, implemented in the National Codes of European member countries, is explained by achieving the following five objectives:

1) the load-bearing capacity of the construction can be assumed for a specific period of time;
2) the generation and spread of both fire and smoke within the works is limited;
3) the spread of fire to neighbouring construction works must be limited;
4) occupants have to be able to leave the works or be rescued by other means;
5) the safety of rescue teams must be taken into consideration.

Focusing on the structural safety, the European codes are established by the "Fire Parts" of Structural Eurocodes. In Italy, the new Technical Code for Constructions has been published in 2008. For the first time in Italy, the fire action is introduced within the definition of the actions on constructions, as an "exceptional load". This document defines the performance safety levels of buildings according to the safety objectives required by the Directive 89/106/CEE. The Italian Technical Code for Constructions defines five safety performance levels depending on the importance of the building, which establish the damage level that can be accepted. These rules define the fire structural performance requirements and they refer to specific technical codes issued by the Italian Ministry of Interior for all activities under the control of the National Fire Brigades.

In this scenario the FSE allows a more precise adjustment of the safety level of the building through qualitative and quantitative criteria (namely acceptance criteria). However, it is important to note that in the current code the performance approach does not replace the prescriptive one, but both the approaches coexist. The technical solutions imposed by the prescriptive approach remain one of the possible ways that the designer may choose for the structural fire design.

The following describes the application of FSE (namely the structural behaviour in fire situation) to the car parks in the new buildings of the "C.A.S.E. Project for L'Aquila". This Project was developed in L'Aquila (province of Abruzzo, Italy), after the seismic event of 06/04/2009, in response to the housing emergency. The car parks, placed at the ground floor of the buildings, are mainly built with steel columns that support the seismically isolated superstructure. The Italian prescriptive code provides, for car parks, a fire resistance class for the load-bearing criterion of 90 minutes in standard fire exposure (R90). However, for obtaining the fire resistance class R90 the adoption of protective coatings of steel columns is needed, for which a continuous and accurate maintenance is required: in fact, there is a high possibility of accidental damage of the protective coatings in case of impact with the cars. Moreover, the possibility of damage becomes elevated when a series of acts of vandalism takes place, for example if the car parks are easily accessible and

not controlled. Because of the uncertainties on the effectiveness of coatings maintenance, in such cases, their use is not recommended.
Therefore, the lack of protective coatings on steel columns and the structural safety during the fire exposure can be evaluated through the application of performance-based approach, which allows to assess, in a more complete and reliable manner, the structural response with reference to the fire scenarios that can realistically occur.

1 FIRE SAFETY ENGINEERING

The performance approach (FSE), as opposed to prescriptive approach, is based on a detailed analysis of the structural behaviour by using advanced analytical models. Therefore, through the engineering method, by following the steps in the layout of Fig. 1, it is possible to evaluate the structural fire safety level. Particularly, it should be defined:
1) the ignition fire hazard according to the purpose of the building (type and amount of fire load, type of users) and if there are active and passive fire protection systems;
2) the design fire scenarios, fire development and the movement and evacuation of smoke, depending on the geometric characteristics and ventilation conditions of the fire compartment and the type and amount of fire design load.

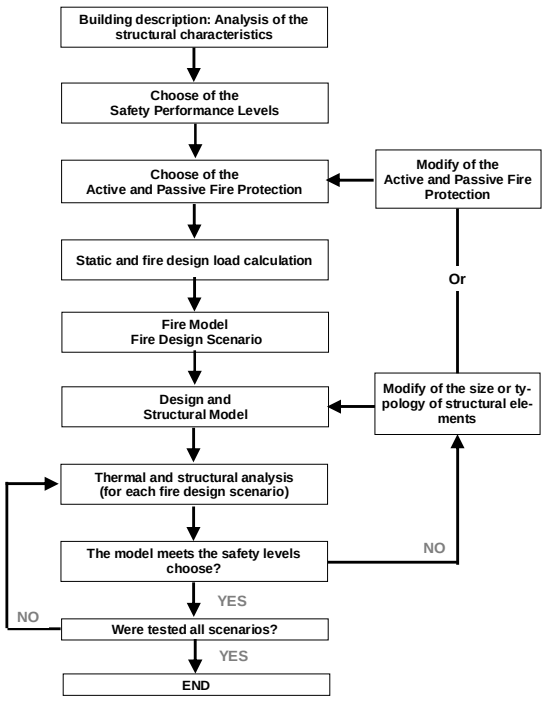

Fig. 1 Fire Safety Engineering: Layout

(a)

(b)

Fig. 2 (a) Tipical building of C.A.S.E. Project for L'Aquila, (b) Parking zone

2 CASE STUDY: CAR PARKS

2.1 Building description: analysis of the structural characteristics

Each residential building is built on a seismically isolated plate, with dimensions equal to $21\times57m^2$ about, capable of supporting a three-storey building with dimensions in plant equal to $12\times48m^2$ about, in addition to the stairs. The buildings (superstructures) are different for architectural and constructive elements; the structures are built with wood materials, reinforced concrete or steel. Each isolated plate (with height of 50cm) is sustained by steel columns (with height of 260cm) by the isolation system. In this area, below each seismically isolated plate, the parking (Figure 2) for about 34 cars are contained. In order to distribute the actions on the reinforced concrete foundation plate the columns are allocated on a 6m×6m grid. The dimensions in plant of the compartment are

equal to 22×58 m^2; in fact the outside walls, when present, are mismatched 50cm with respect to the vertical projection of the edge of the seismically isolated plate.
The steel columns are a circular hollow steel section with a capital at the top; this latter is useful a) for transferring, through the isolator unit, the load between the column and the seismically isolated plate and b) as a structure of contrast to the operations of substitution of the isolator unit. The parking area can be fully open on the four sides or partially closed on one or more sides. Therefore, among the various examined cases are present both open car parks and almost completely closed, as well as several intermediate cases.

2.2 Choice of the active and passive fire protection systems

In this case study, the objective of fire safety design concerns the mechanical resistance and stability, in fire situation, of the primary structural elements in the zone below the seismically isolated plate. In this case a limited damage after the fire exposure has been required. The damage is quantified in terms of relative vertical displacements between the top of two adjacent columns: in order to limit the finishing damage in the superstructure, the relative vertical displacement must not exceed the limit value, chosen cautiously equals to L/200 (5.0 ‰), where L is the distance between two adjacent columns (L=6000mm). Finally, no specific protection systems (active and/or passive) are provided.

2.3 Static and fire design load calculation

The Italian and European codes (NTC, 2008; EN1991-1-2, 2002) classify the fire as an exceptional load, so the fire design load combination is defined by:

$$F_d = A_d + G_{k1} + G_{k2} + \sum_{i=1}^{n} \psi_{2i} \cdot Q_{ki} \quad (1)$$

where G_{k1} is the characteristic value of permanent structural load; G_{k2} is the characteristic value of permanent non structural load; $\psi_{2i} \cdot Q_{ki}$ is the quasi-permanent value of a variable action *i*; A_d is the design value of an exceptional action. Because of the great variability of the superstructure structural type, the fire structural analyses have been carried out, for simplicity and for the benefit of safety, with reference to the maximum combination of exceptional load (maximum axial load on each column equal to 1800 kN).

2.4 Fire model and fire design scenarios.

The fire scenario is significantly affected, among other things, by the geometry and ventilation conditions of the compartment. As regards the evaluation of number of vehicles involved in the fire and the timing of fire initiation by a car to adjacent one, reference is made to the informations from (CEC Agrement, 2001) and the guideline (INERIS, 2001). It is necessary to distinguish the car parks open on all their sides by those partially open (openings limited or absent on one or more sides). The presence of natural ventilation in open car parks does not allow the achievement of the flashover conditions: the phenomenon remains for the entire fire duration of “pre-flashover” type and a limited number of vehicles burn. In partially open car parks, instead, it is possible that the fire involved all of the cars. Therefore, the identification of the more dangerous fire scenarios for the structural stability is to define the position and the number of cars that may be involved in the fire and cause the more dangerous thermal action for the supporting structure building.
By applying the criteria proposed in the aforementioned guidelines to *car parks open on all sides* two localised fire scenarios (L1 and L2) was defined. In this fire scenarios was assumed the presence of cars of category 3, with calorific value equals to 9500 MJ, and only one commercial vehicle (VAN), with total calorific value equals to 19500 MJ (see CEC Agreement 7215-PP/025, 2001). The distribution and number of the cars and the fire propagation times from the VAN (equals to 12 min) are reported in Fig. 3a,b.
For localised fire (Fig. 3a,b), the application of Hasemi’s method (Annex C, EN1991-1-2), with the RHR curve of car of category 3 and VAN (see CEC Agreement 7215-PP/025, 2001), has provide

the heat flux received by steel columns. The heat flux along and around the columns was assumed equal to the heat flux at the top of columns. In Fig. 3c are reported the heat flux on some significant columns.

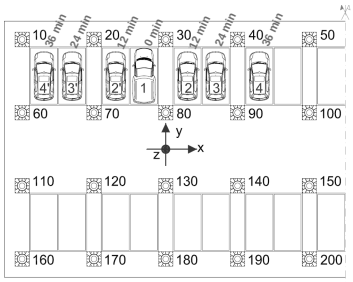

(a) Scenario L1

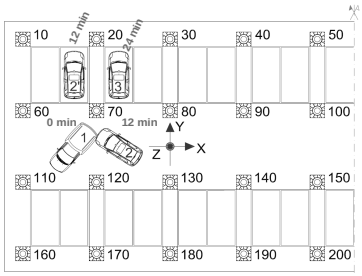

(b) Scenario L2

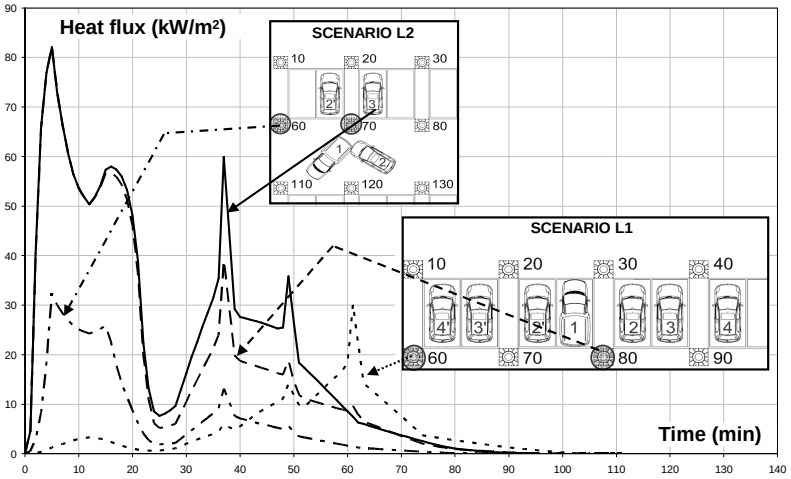

(c) Thermal flux from Hasemi's method

Fig. 3 Fire scenarios

2.5 Structural model and fire safety assessment

In order to limit the analysis time without compromising the accuracy of the results, the thermo-mechanical analyses, for each fire scenario, have been conducted with the reference to the substructure highlighted in Fig. 4 (Nigro et al., 2010). The substructure extension allows assessing in an appropriate way both the thermal field and the hyperstatic effects induced by different thermal expansions of steel columns and bending of the concrete reinforced slab. Along the edge a constraint is introduced for the horizontal movements in the longitudinal direction and for the rotations around transverse axis. This constraint condition, thanks to the structural symmetry, is fully congruent for the analysis in normal temperature conditions and for a generalised fire scenario, while it is on the safe side for the other scenarios (localised fire scenarios), maximizing, thanks to the infinite rotational stiffness, the hyperstatic effects induced on the columns by slab thermal curvature. The steel columns are fixed at the base and linked to the superstructure slab with a hinge.
For each fire scenario, the global thermal-mechanical structural analyses of the substructure in Fig. 4 are conducted by using the non linear software SAFIR2007a (Franssen, 2008), developed at the University of Liege (Belgium), which performs the structural analysis under fire situation. The steel columns are modelled with beam elements with circular cross-section, while the reinforced concrete slab is modelled with shell elements.

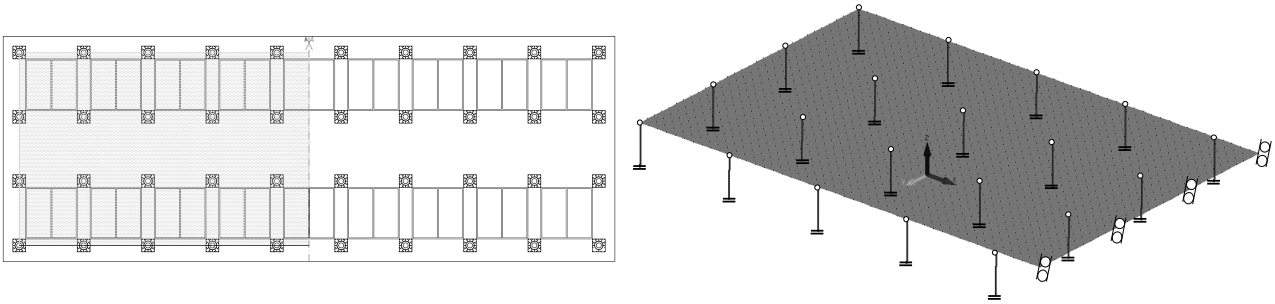

Substructures Static scheme

Fig. 4 Thermo-mechanical model of the structure

In addition to the global analysis, for each fire scenario, in order to calculate more accurately the thermal field and stresses distribution in the capitals above the columns and to assess the possible local buckling, a detailed thermo-mechanical analyses has been conducted with reference to the more stressed and heated column. The 3D modelling (Fig. 5) have been developed with the finite element software ABAQUS/standard (2008). The thermal exposure conditions were considered according to the Fig. 3. The axial load corresponds to the axial load obtained by the global structural analyses.

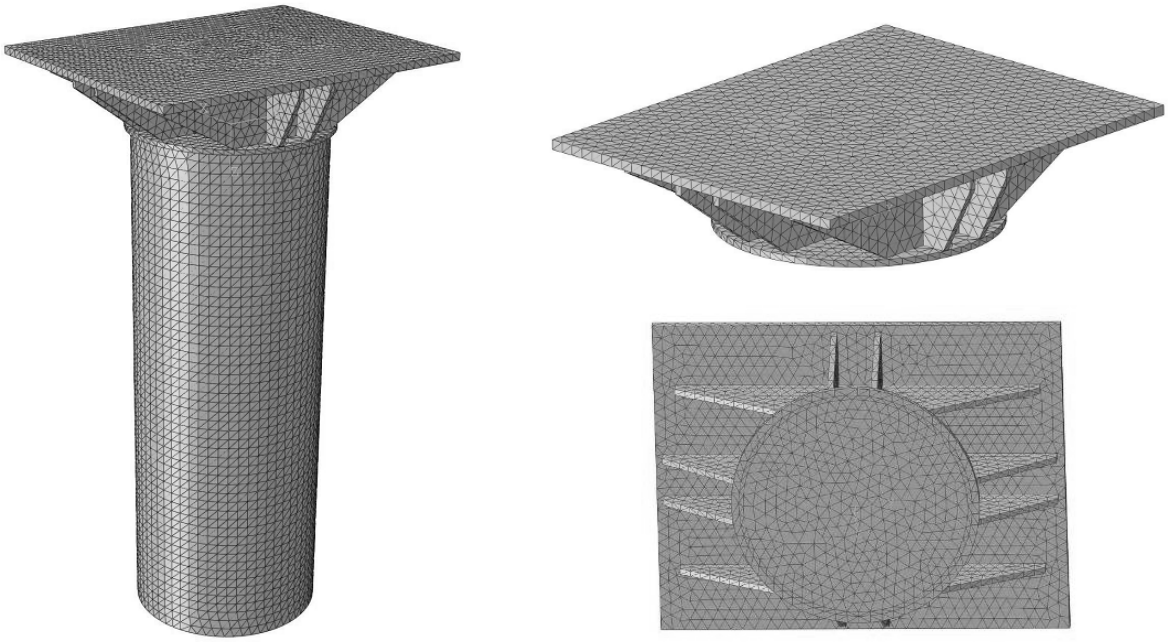

Fig. 5 3D thermo-mechanical model of the column

2.6 Analyses results

In Fig. 6 and in Fig. 7 are sintetized the main strutural results (tempertaures, axial loads, vertical displacements in function of fire exposure time) for scenario L1 and for Scenario L2, respectively. For sake of brevity, the results of structural response in fire situation are reported only with reference to the fire scenario L2, which appears more unfavourable (Fig. 6).

The maximum temperatures reached in the columns do not exceed 600°C (Fig. 6a). The thermal action produces both in the columns and slabs several thermal expansions. Because of the thermal curvature of the slab the columns axial load increases (Fig. 6b). The axial load is further amplified from the differential thermal elongation (Fig. 6c) of columns, exposed to different thermal conditions, which is constrained from slab shear stiffness. The columns displacement reflects, in general, the temperatures trend. However, the reduction of stiffness that the structural elements suffer, if constrained to high temperatures, may lead to a premature reversal development in

displacement respect to the temperature trend. The maximum differential displacement, during the fire exposure, is about 16mm (between the column 120 and column 130) and this value corresponds to 2.6 ‰ below the limit value of 5.0 ‰. Moreover, in Fig. 6d the axial load resistance of the column, evaluated according to EN1993-1-2, is compared with the axial load during the fire exposure. The final displacement is about 5mm in the central area of capital and about 2mm in the tube head: this is due to the plastic strain which has developed in the tube and in the capital (mainly in the zone of load application) during the fire exposure.

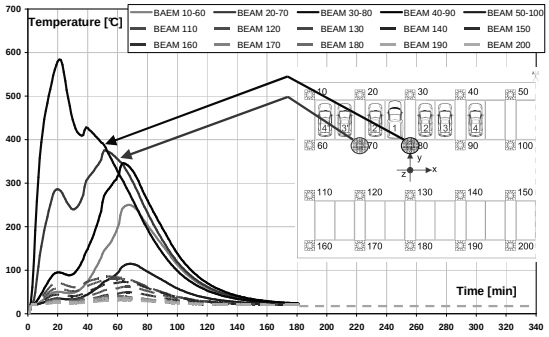

a) Time-temperature curves for the columns

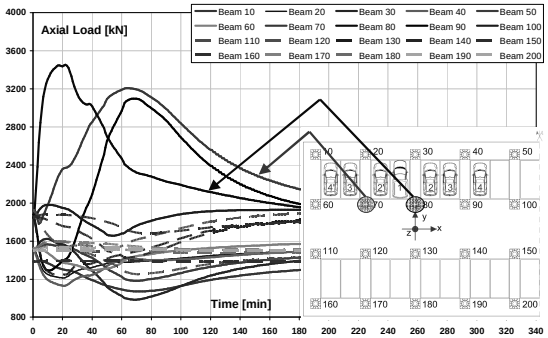

b) Time-axial load curves for the columns

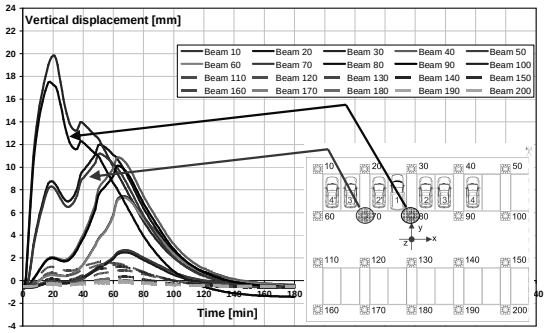

c) Time-displacement curves for the columns' top

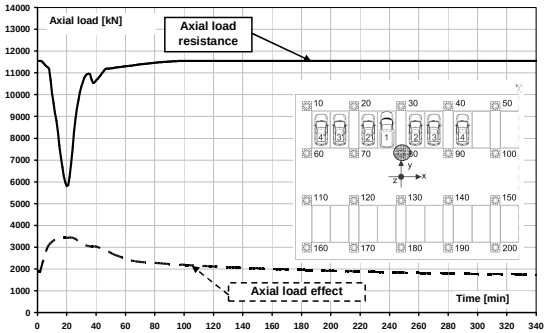

d) Stability check according to EN1993-1-2 (column 70)

Fig. 6 Fire scenario L1

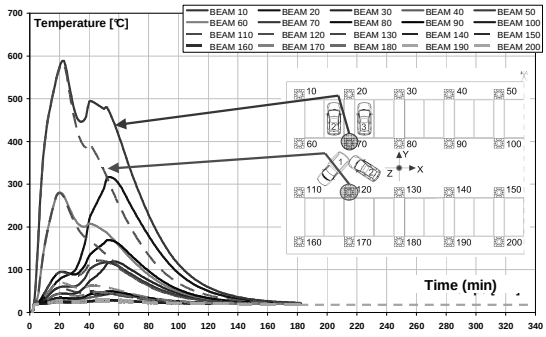

a) Time-temperature curves for the columns

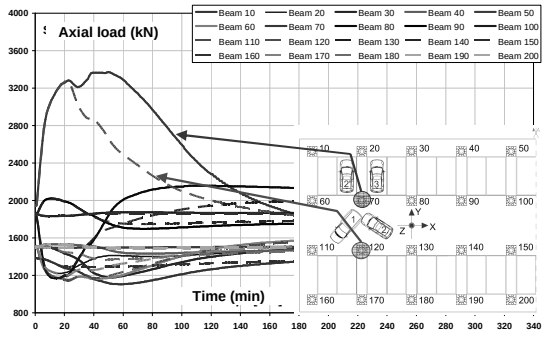

b) Time-axial load curves for the columns

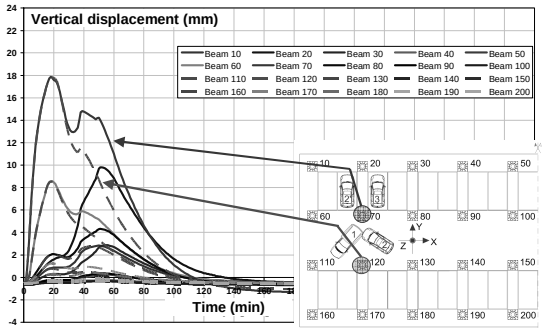

c) Time-displacement curves for the columns' top

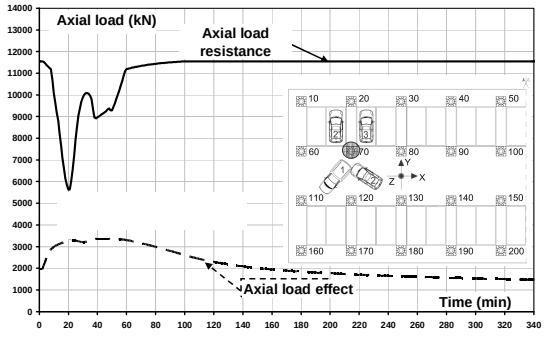

d) Stability check according to EN1993-1-2 (column 70)

Fig. 7 Fire scenario L2

As regards the detailed analysis of the column, the displacement at the head of column is very similar to those obtained in the global structural analyses (Fig. 8). The final displacement is about 5mm in the central area of capital and about 2mm in the tube head: this is due to the plastic strain which has developed in the tube and in the capital (mainly in the zone of load application) during the fire exposure.
Similar considerations are also valid for the other fire scenarios. Therefore it can be concluded that the structure, and in particular the columns in the absence of any protection system against fire, during the design fire exposure perform an adequate load-bearing capacity, including the cooling phase.

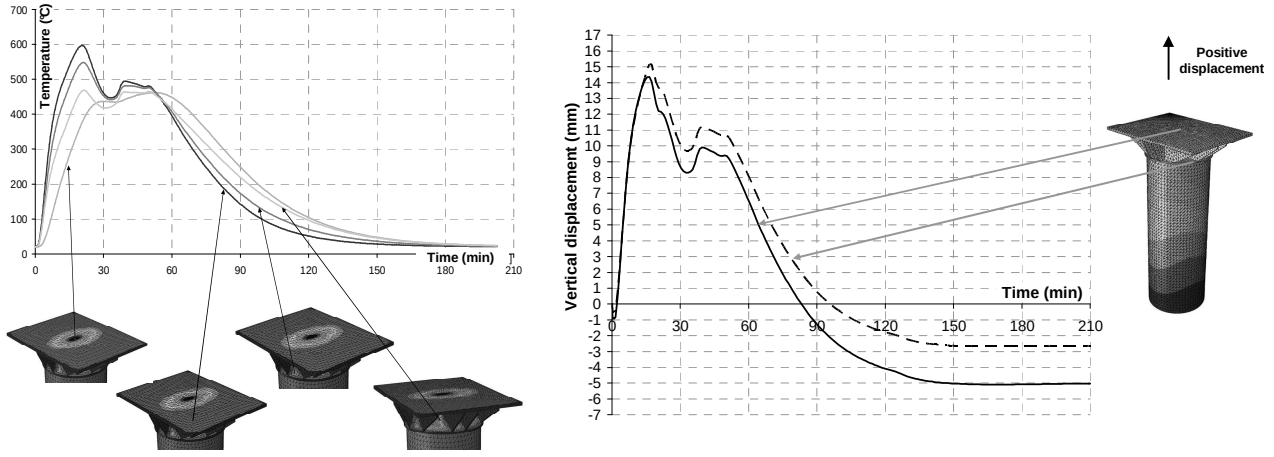

a) Columns time-temperature

b) Columns head time-displacement

Fig. 8 Scenario L2 – Detailed analysis

3 CONCLUSIONS

The Fire Safety Engineering approach, thanks to advanced calculation models both for fire and for thermo-mechanical analysis of the structure, allows simulating the response behaviour of the structure exposed to “natural” fire scenarios. The FSE application to car parks is facilitated by the informations about the possible fire scenarios provided by the European Research Project CEC agreement 7215-PP/025 (2001).
In the described case study, consisting of the car parks located at the ground floor of buildings of the C.A.S.E. Project - L’Aquila, the application of the Fire Safety Engineering has been developed according to the current National Technical Code and Eurocodes, also utilising the fire scenarios suggested by the quoted European Research.
In order to limit the analysis time without compromising the accuracy of the results, the thermo-mechanical analyses, for each fire scenario, have been conducted with the reference to a significant substructure, for which the steel columns are modelled with beam elements with circular cross-section, while the reinforced concrete slab is modelled with shell elements. The substructure extension has allowed assessing in an appropriate way both the thermal field and the hyperstatic effects induced by different thermal expansions of steel columns and bending of the concrete reinforced slab. In addition to the global analysis, for each fire scenario, in order to calculate more accurately the thermal field and stresses distribution in the capitals above the columns and to assess the possible local buckling, a detailed 3D thermo-mechanical analyses has been conducted with reference to the more stressed and heated column.
Finally, the thermo-mechanical analyses in fire situations for the described case study showed that the structures, and in particular the steel columns, considered unprotected, satisfy the performance level set to the design fire scenarios, also thanks to an overstrength in normal condition design.

REFERENCES

ABAQUS Standard/explicit User's Manual (2008), Hibbit Karlsson and Soresen, Inc. Vol 1-2-3, Version 6.7, USA 2008.

CEC Agreement 7215-PP/025, Demonstration of Real Fire Tests in Car Parks and High Buildings, 2001.

EN 1991-1-2, Eurocode 1. Actions on structures - Part 1-2: General actions - actions on structures exposed to fire, November 2002.

EN 1993-1-2, Eurocode 3. Design of steel structures - Part 1-2: General rules - Structural fire design, April 2005.

Franssen J.M., (2008) - User Manual for SAFIR2007a: A Computer Program for Analysis of Structures Submitted to the Fire, University of Liege, Belgium, January.

INERIS, Parcs de stationnement en superstructure largement ventiles. Avis d'expert sur les scénarios d'incendie, Ottobre 2001.

Ministry of Infrastructure and Transport (Italian Government) 2008. Technical Code for the Constructions. G.U. n. 29 of 14/02/2008.

Nigro E., Pustorino S., Cefarelli G., Princi P., Progettazione di strutture in acciaio e composte acciaio-calcestruzzo in caso di incendio (in italian), Ed. Hoepli, Milano, 2009.

Nigro E., Ferraro A., Cefarelli G., Application of FSE approach to the structural fire safety assessment of steel-concrete composite structures, Proceedings of COST Action C26 Conference, 16-18 September 2010, Naples, Italy.

Pustorino S., Princi P., Nigro E., Ferraro A., Caciolai M., Cirillo V., Structural design of open car parks in accordance with the fire safety engineering approach (in Italian). Costruzioni Metalliche, n. 6, Nov/Dic 2010, ACAI, pp. 55-66.

CASE STUDIES OF A NEW SIMPLIFIED NATURAL FIRE MODEL AND SAFETY CONCEPT FOR STRUCTURAL FIRE SAFETY DESIGN

Jochen Zehfuss[a]

[a]hhpberlin fire safety engineers, Hamburg, Germany

INTRODUCTION

The structural fire safety design in most countries is usually carried out on the foundation of the material requirements of the building codes. This prescriptive design bases on the well-known standard temperature-time curve and simplifies the fire exposure to the building elements. Importance such as fire load, ventilation and geometry of the fire compartment are not considered. An alternative design-way is the performance-based design on the basis of natural fires which is especially applied for special complex buildings such as airports, railway stations, big assembly halls etc. The performance based design of construction elements is conducted by Eurocodes and the National Annex. Due to some deficiencies in the methods of the annexes in Eurocode 1-1-2 for the German National Annex a new simplified natural fire model for fully-developed compartment fires was developed.
By means of an example it is shown how to evaluate the relevant fire actions of a natural fire to the structure on the basis of Eurocode 1-1-2 and the German National Annex [DIN, 2010].

1 EUROCODE 1-1-2 ANNEX A

The standard temperature-time curve was developed in the 1930s summarising data from fires in residential, office and commercial buildings. The curve should cover most of the potential courses of fires in common buildings. The standard temperature-time curve is the basis of the prescriptive fire safety design and leads in most cases to an overestimation of the thermal action to the structure. For a performance-based design in Eurocode 1-1-2 natural fire models are available with which the realistic temperature-time development depending on fire load, ventilation conditions and geometry can be obtained.
The simplified natural fire model published inEurocode 1-1-2, annex A however in some cases provides an unrealistic temperature increase and decrease [Zehfuss and Hosser, 2007]. For this reason the annex A-method was not approved in most CEN-countries. The most critical point is that the annex A-method has no temporal connection with the rate of heat release of Eurocode 1-1-2 annex E.This deficiency will be clarified by comparing the parametric temperature-time curve according to Eurocode 1-1-2 with the test results of [Schleich, 2000] (Fig. 1). Obvious is the discrepancy between the temporal course of the parametric temperature-time curve and the rate of heat release according to Eurocode 1-1-2 annex E. The latter achieves its maximum after 30 minutes and declines after 43 minutes. The temperature-time curve and rate of heat release neither match with each other nor are they temporally congruent.

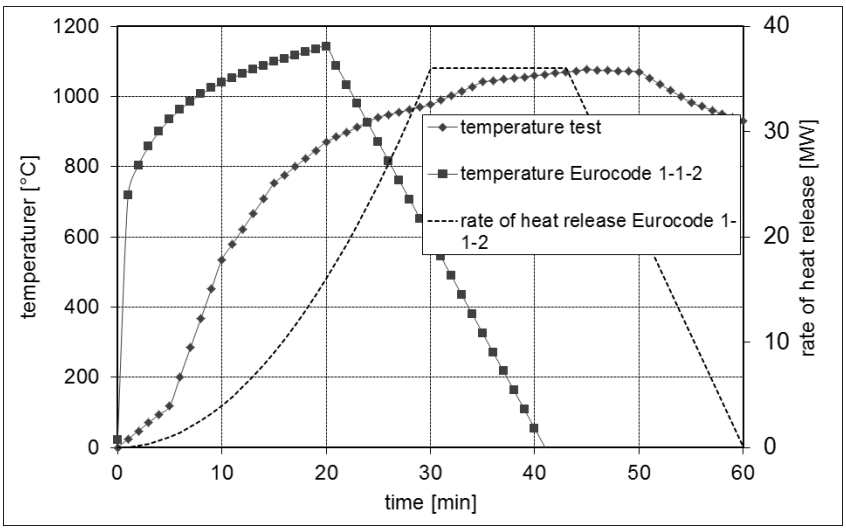

Fig. 1 Temperature-time curve and rate of heat release according to Eurocode 1-1-2

2 NATURAL FIRE MODEL IBMB PARAMETRIC FIRE CURVES

2.1 General

The Eurocode 1-1-2 annex A-method in Germany was not approved by the building authorities due to the mentioned deficiencies. For the reason that in Germany also a simplified natural fire model is provided the new parametric fire curves based on [Zehfuss and Hosser, 2007] were published in the German national annex.

Thenew simplified natural fire modelof the parametric fire curves [Zehfuss and Hosser, 2007], [Zehfuss and Hosser, 2005]is based on the approach of the rate of heat release. The model was derived on simulationswith the zone model CFAST for various boundary conditions vs influencing factors. Fig. 2 shows the qualitative shapes of the rate of heat release due to Eurocode 1-1-2 and the simulated temperature-time curve. The temporal link between these curves is evident.

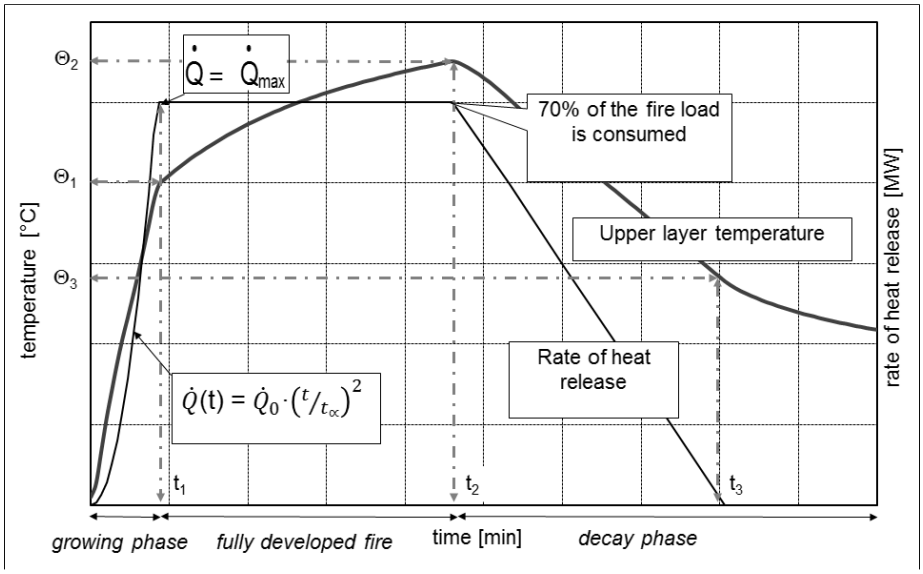

Fig. 2 Approach of heat release and corresponding upper layer temperature (principle)

The parametric fire curves can be divided into three sections (Fig.3). From the beginning of the fire until t_1 the upper layer temperature increases rapidly. At t_1 the maximum of the rate of heat release is achieved and remains constant until t_2. After t_1 the upper layer temperature enhances increases moderately. As 70 % of the fire load is consumed at t_2, the rate of heat release drops off linearly and the upper layer temperature declines. At t_3 the complete fire load is consumed and the rate of heat release decreases to 0. At this time the upper layer temperature-time curve bends and declines to a

lesser extent than before.For the total description of the run of the upper layer temperature-time curve the associated temperatures Θ_1, Θ_2 and $\Theta_3$have to be ascertained (Fig. 3).

2.2 Rate of heat release

The rate of heat release $\dot{Q}$(t) is given by

$\dot{Q}(t) = \dot{m}(t) \cdot \chi \cdot H_{net}$.

Whereby

$\dot{m}(t)$: burning rate [kg/s]

The combustion efficiency χcan be assumed as$\chi = 0.7$ for fire loads in residential and office buildings [DIN, 2010]. The net calorific value can be taken as H_{net} = 17.3 MJ/kg for wooden fire loads and furnishings. The rate of heat release strongly depends on the ventilation conditions and a distinction is made between ventilation-controlled fires and fuel-controlled fires.
In ventilation-controlled fires according to Eurocode 1-1-2 the maximum rate of heat release can be assumed as:
$\dot{m}(t) = 0.1\ A_w\sqrt{h_w}$ [kg/s].
For residential and office buildings in case of a ventilation-controlled fire can be derived by inserting$\chi = 0.7$and H_{net} = 17.3 MJ/kg:
$\dot{Q}_{max,v} = 1.21 A_w\sqrt{h_w}$ [MW].
According to Eurocode 1-1-2 the maximum rate of heat release of residential and office buildings in case of a fuel-controlled fire can be determined as
$\dot{Q}_{max,f} = 0.25 \cdot A_f$[MW].
whereby the maximum burning area A_f[m²] is assumed to be limited to the floor area of the fire compartment.
Fig. 2.illustrates the approach for the rate of heat release [DIN, 2010]. The growth phase is described by the t²-approach:
$\dot{Q}(t) = \dot{Q}_0 \cdot \left(t/t_\alpha\right)^2$
whereby $\dot{Q}_0$= 1.0 MW and the time of fire growth - with a medium fire growth rate in residential and office buildings - can be assumed as t_α = 300 s.
In the fully-developed fire the quadratic increase in the rate of heat release is replaced by a constant value which is taken as the minimum of the two rates of heat release, for fuel-controlled and ventilation-controlled fires [DIN, 2010]:
$\dot{Q}_{max} = \text{MIN}\ (\dot{Q}_{max,v}, \dot{Q}_{max,f})$
When 70 % of the fire load is consumed, the rate of heat release decreases linearly until the fire load is completely burned.

2.3 Parametric fir curves

For a reference fire load density of q = 1300 MJ/m² which is taken as an upper value for residential and office buildings, parametric functions for the temperature-time curve were developed which consider the ventilation conditions, thermal properties of the enclosure and geometry of the compartment. For fire load densities less than the maximum temperature is achieved correspondingly earlier. The appropriate time can be ascertained from the rate of heat release function.

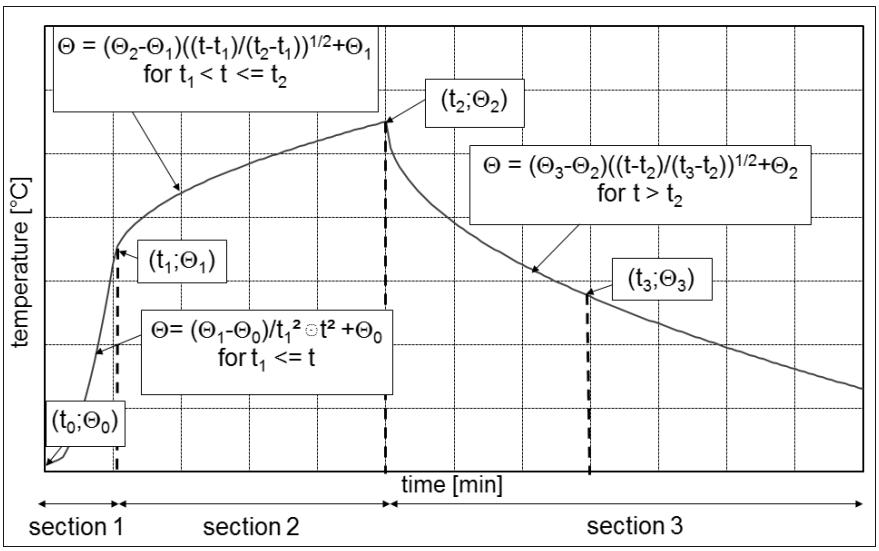

Fig. 3 Mathematical description of the parametric fire curves

A regression analysis for the upper layer temperatures Θ_1, Θ_2 and Θ_3 of ventilation-controlled fires provides the following functions for the reference fire load density of q = 1300 MJ/m² [Zehfuss and Hosser, 2007]:

$\Theta_1 = -8.75 \cdot 1/O - 0.1\ b + 1175$ [°C]

$\Theta_2 = (0.004\ b - 17) \cdot 1/O - 0.4\ b + 2175$ [°C]

$\Theta_3 = -5.0 \cdot 1/O - 0.16\ b + 1060$ [°C]

with

opening factor	$O = A_w\sqrt{h_w} \,/\, A_t$ [$m^{1/2}$],
area of ventilation openings	A_w [m²],
averaged height of ventilation openings	h_w [m],
total area of enclosing components	A_t [m²],
averaged thermal property of enclosure	b [$J/m^2s^{0.5}K$].

For fuel controlled fires the following functions for the reference fire load density of q = 1300 MJ/m² were derived [Zehfuss and Hosser, 2007]:

$\Theta_1 = 24000\ k + 20$ [°C] for $k \leq 0.04$ and $\Theta_1 = 980$°C for $k > 0.04$,

$\Theta_2 = 33000\ k + 20$ [°C] for $k \leq 0.04$ and $\Theta_1 = 1340$°C for $k > 0.04$,

$\Theta_3 = 16000\ k + 20$ [°C] for $k \leq 0.04$ and $\Theta_1 = 660$°C for $k > 0.04$.

with

$$k = \left(\frac{\dot{Q}^2}{A_w \cdot \sqrt{h_w \cdot (A_t - A_w) \cdot b}} \right)^{1/3}$$

maximum rate of heat release $\dot{Q}$ [MW]

The functional form of the parametric fire curves in the three sections is depicted in Fig. 3.

3 EXAMPLE OF APPLICATION

The application of the new simplified natural fire model of German national annex [DIN, 2010] is shown by the example of an office room. The required input data is listed below:

Floor area of fire compartment	$A_f = 16$ m²
Height of fire compartment	H = 3.00 m
Ventilation factor	$A_w\sqrt{h_w} = 12.65$ $m^{3/2}$
Opening factor	O = 0.158 $m^{1/2}$
Total area of the enclosing components	$A_t = 80.0$ m²
Fire load density q_x = 511 MJ/m²	$Q_{511} = 8176$ MJ
averaged thermal property of enclosure	b = 1500 $J/(m^2s^{0,5}K)$

rateof heat release according to Eurocode 1-1-2 and German national annex:

$\dot{Q}_{max}$ = MIN ($\dot{Q}_{max,v}, \dot{Q}_{max,f}$) = MIN ($1.21 \cdot A_w\sqrt{h_w}$;0.25$A_f$) = MIN (15.31; 4.0)
$\dot{Q}_{max}$ = $\dot{Q}_{max,f}$ = 4.0 MW => fuel-controlled fire.
Parametric fire curve for reference fire load density of q = 1300 MJ/m²:
$Q = q \cdot A_f = 1300 \cdot 16.0 = 20800$ MJ,

t_1 = 600 s = 10 min; Q_1 = 800 MJ

Q_2 = 13760 MJ; t_2 = 4040 s ≈ 67 min

Q_3 = 6240 MJ; t_3 = 7160 s ≈ 119 min

forq_x = 511 MJ/m²:

$Q_{2,511}$ =4923 MJ; $t_{2,511}$ = 1831 s ≈ 31 min

$Q_{3,511}$ = 2453 MJ; $t_{3,511}$ = 3057 s ≈ 51 min

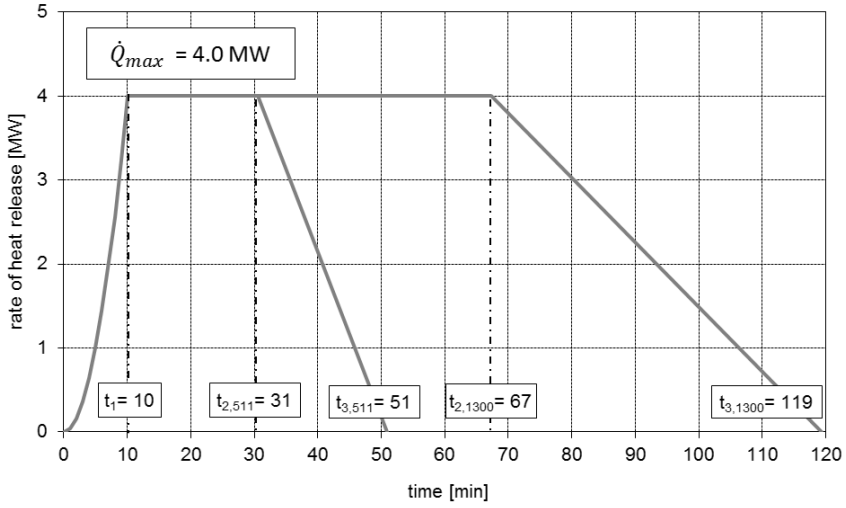

Fig. 4 Rate of heat release example fire in office room

For a fuel-controlled fire it can be derived:

$$k = \left(\frac{\dot{Q}^2}{A_w \cdot \sqrt{h_w \cdot (A_t - A_w) \cdot b}}\right)^{1/3} = 0.0195$$

Θ_1 = 24000 k + 20 = 565°C,
Θ_2 = 33000 k + 20 = 769°C,
Θ_3 = 16000 k + 20 = 383°C.
For the present fire load density q_x = 511 MJ/m² it can be obtained:
$\Theta_{2,511}$ = 689°C,
$\Theta_{3,511}$ = 316°C.
Fig. 5 shows the parametric fire curve compared tothe computed upper layer temperature-time of the advanced natural fire model CFAST and the standard temperature-time curve. The deviation between parametric fire curve and CFAST results are marginal. The new simplified natural fire model of the parametric fire curves can describe the temperature development of a natural fire with a good accuracy.

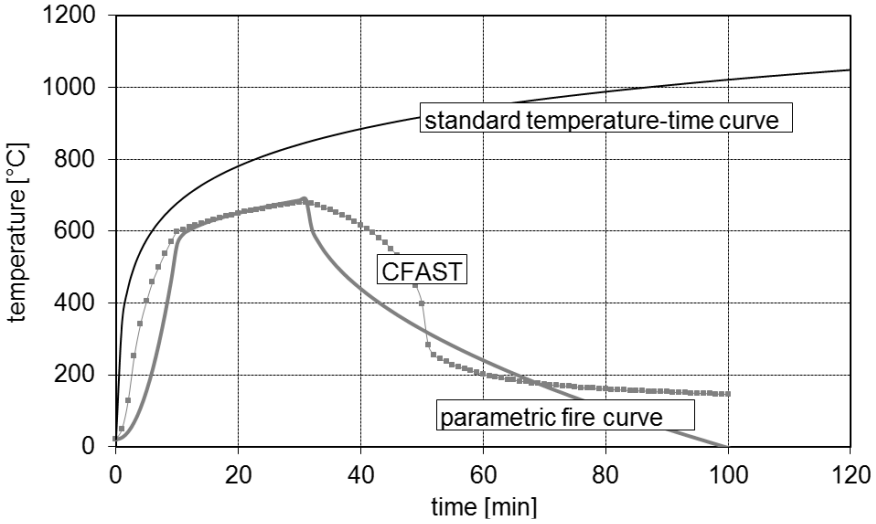

Fig. 5Comparison of parametric fire curves in German national annex with CFAST results and standard temperature-time curve for an office room

REFERENCES

DIN EN 1991-1-2/NA: National Annex – National determined parameter -. Eurocode 1: Actions on structures- Part 1-2: General actions – Actions on structures exposed to fire. DIN (German standard association), 2010.

Schleich J B et al. Natural Fire Safety Concept Full Scale Tests, Implementation in the Eurocodes and Development of anuserfriendly design tool. Technical report No. 6 Period from 01.01.2000 - 30.06.2000.CEC Agreement 7210-PA/PB/PC/PD/PE/PF/PR-060.Esch / Alzette, 2000.

Zehfuss, J, Hosser, D.: A parametric natural fire model for the structural fire design of multi-storey buildings, Fire Safety Journal 42 (2007) 115-126, Elsevier.

Zehfuss, J.; Hosser, D.: Vereinfachtes Naturbrandmodell für die Brandschutzbemessung von Bauteilen und Tragwerken. Bauphysik 27 (2005), Heft 2, S. 79-86 (in German)

FIRE RESISTANCE OF CAST IRON COLUMNS IN VINOHRADY BREVERY

František Wald, Mekonnen Dagefa

Czech Technical University in Prague, Czech Republic

INTRODUCTION

The paper presents a procedure for the structural appraisal of old cast-iron columns exposed to fire. Temperature of the gas during the fire is assumed according to nominal standard fire curve. Transfer of heat is modelled by the FE procedure which allows to take into account not only the hollow section particularity but also of the improvement by filling by concrete and to utilise the intumescent coating protection. The buckling resistance is predicted by generalised column curve formulation modified for the cast iron as well as for the elevated temperature. The results are employed on the case study/worked example of the columns used for reconstruction of the Vinohrady brewery in Prague.

Fig. 1 Reused cast iron columns in a show room at ground floor

Fig. 2 Reused cast iron columns in a design office at the first floor

1 VINOHRADY BREWERY

The building of the Vinohrady Brewery has been reconstructed for residential and business purposes, see (Korunní dvůr, 2008). The cast iron columns were redesigned based on the laboratory test results. The recent photographic information, see Figs 3 and 5, corroborate the reuse of columns as they were in the past much in agreement with the authenticity of the existing historical structures. The column geometry is described at Fig. 4. At level $A = 300$ mm were the average values of external diameter 316,4 mm with thickness 316,4 mm, at level $B = 1000$ mm the external diameter 304,0 mm and thickness 31,4 mm; at level $C = 2100$ mm the external diameter 285,8 mm with

thickness 35,4 mm. The height of the column was measured as D = 2605 mm and average thickness calculated as 32,0 mm with the average internal diameter 238,1 mm and average external diameter 302,1 mm. From the material test of similar columns were derived the design value of the ultimate compressive strength $f_{u,c}$ = 213,1 MPa and the design value of the proof strengths in compression $f_{0,1,c}$ = 29,9 MPa and $f_{0,2,c}$ = 49,1 MPa. n emerges to be 6,0; see (Degefa, 2008).

2 DESIGN RESISTANCE

2.1 Ambient temperature resistance

The design buckling resistance of cast iron column at elevated temperature was detailed studied by Rondal and Rasmussen (2003). Their proposal is based on the generalized column curve formulation. The design buckling resistance of a compression member is taken

$$N_{b,Rd} = \chi_c \, A \, f_{0,2,c} / \gamma_{M1} \tag{1}$$

where $f_{0,2,c}$ is the 0,2 % proof strength of the cast iron in the compression, A is the member area, γ_{M1} is the partial safety factor, and χ_c is the reduction factor, which may be expressed in form

$$\chi_c = \frac{1}{\varphi_c + \sqrt{\varphi_c^2 - \lambda_c^2}} \tag{2}$$

where $\varphi_c = \left(1 + \eta_c + \lambda_c^2\right)/2$; $\lambda_c = \sqrt{f_{0,2,c} / \sigma_{E_0}}$ and $\sigma_{E_0} = \pi^2 E_0 \left(L/r\right)^{-2}$. The imperfection parameter, η_c, is given by

$$\eta_c = \alpha\left(\left(\lambda_c - \lambda_1\right)^{\beta} - \lambda_0\right) A = \frac{\sqrt{\alpha^2}}{\Omega} \cdot e \tag{3}$$

where α, β, λ_0 and λ_1 are functions of the Ramberg Osgood parameters $n = \ln(2)/\ln\left(f_{0,2,c} / f_{0,1,c}\right)$ and $e = f_{0,2,c} / E_{0,c}$, see (Ramberg and Osgood, 1943), where $f_{0,1,c}$ is the 0,1% proof strength for compression. Substituting e = 0,00426 and n = 6, one obtains α = 0,85; β = 0,095; λ_0 = 0,70; λ_1 = 0,5; and η_c = -0,0193 > α with η_c = α = 0,85, see (Rondal and Rasmussen, 2003). For cast iron the 0,2 % proof strength may be approximate as a half of the ultimate compressive strength $f_{0.2,c} = f_{u,c}/2$, see (Blanchard et al, 1997). Cross-section imperfection due to the peculiar eccentricity of the hole to the outer perimeter of a hollow cast iron section is taken into account. It is the result of lifting forces, dislocation and/or deflection of the casting core used for producing the hole of the member during casting.

The eccentricity is given by $g = j\, d_i^2 / (d_e^2 - d_i^2)$ where $j = (d_e - d_i)/2 - t_{\min}$, see Fig. 1. The distance g can be estimated based on the proposal $g / d_e \approx 1/30$. Cast iron being relatively week in tension may lead to possibility of tension failure initiated by fracture developed on one side of the column during overall bending. Tension failure becomes critical for slenderness ratio greater than 80. This is very much greater than the slenderness ratio of the columns used for this analysis 56. Hence this study omits the inclusion of tensile stress analysis in the columns.

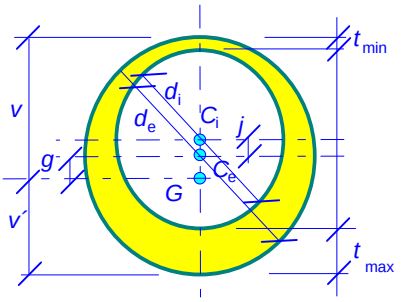

Fig. 5 Cross-section imperfection in hollow cast iron columns, from (Rondal and Rasmussen 2003)

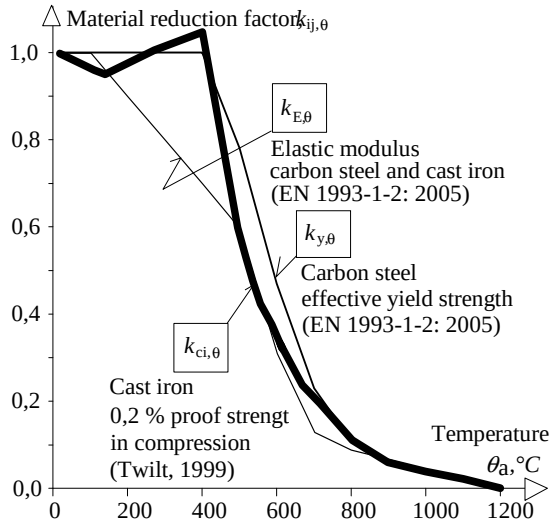

Fig. 6 Reduction factor of 0,2 % proof strength in compression of cast iron $k_{ci,\theta}$ (Twilt, 1999) for effective yield strength steel $k_{y,\theta}$, and for modulus of elasticity $k_{E,\theta}$ (EN 1993-1-2)

1.1 Elevated temperature resistance

The fire design starts with the temperature modelling during the fire. The standard nominal fire curve, see EN 1991-1-2, is the most simple but successful solution for already 120 years. The reduction of material properties was deeply studied in (Twilt, 1999) and Blanchard et al (1997). The results are summarised/compared to EN 1993-1-2: 2005 at Fig. 2.

The integration of Fourier heat transfer equation for non-steady heat conduction inside the member is the general approach to studying the increase of temperature in hollow structural elements exposed to fire. The solution depends on the boundary conditions and in fact numerical solutions, or at least step by step procedure, is necessary. The software SAFIRE (Franssen, 2007), has been used by the idealization of the three dimensional to a two dimensional in those particular model.

As a matter of fact the historical hollow structural cast iron columns have thick cylindrical walls usually falling in the Class 1, see EN 1993-1-1:2005. Hence the design buckling resistance based on the generalized column curve formulation was modified to meet change in properties under elevated temperature

$$N_{b,Rd,\theta} = \frac{\chi_\theta k_{ci,\theta} A\, f_{0,2,c}}{\gamma_{M,\theta}} \tag{4}$$

where χ_θ is the reduction factor for flexural buckling in the fire design situation; $k_{ci,\theta}$ is the reduction factor from Fig. 2 for the 0,2 % proof strength of cast iron as the cast iron temperature θ and $\gamma_{M,\theta}$ is the partial factor for fire condition. The value of χ_θ for the hollow circular column is the same in any direction given by

$$\chi_\theta = \frac{1}{\varphi_\theta + \sqrt{\varphi_\theta^2 - \lambda_\theta^{\,2}}} \tag{5}$$

with $\varphi_\theta = \left(1 + \eta_c + \lambda_\theta^{\,2}\right)/2$. The imperfection parameter, η_c, is given by $\eta_c = \alpha\left(\left(\lambda_c - \lambda_1\right)^\beta - \lambda_0\right)$, neglecting the small variation due to temperature. Where α, β, λ_0 and λ_1 are functions of the parameters n and $e_c = \sigma_{0.2,c}/E_0$. The values are taken from Rasmussen and Rondal (1997) proposal

as $\eta_c = \alpha = 0{,}85$; $\beta = 0{,}095$; $\lambda_0 = 0{,}70$; $\lambda_1 = 0{,}55$. The non-dimensional slenderness λ_θ for the temperature θ,

$$\lambda_\theta = \lambda_c \left[k_{ci,\theta} / k_{Eci,\theta} \right]^{0.5} \tag{6}$$

where $k_{ci,\theta}$ is the reduction factor for the yield strength of cast iron at the cast iron temperature θ and $k_{Eci,\theta}$ is the reduction factor for the modulus of elasticity, $E_{ci,\theta} / E_{ci}$ with $E_{ci,\theta}$ as the modulus of elasticity at temperature θ, see (Wouters and Mollaert, 2002).

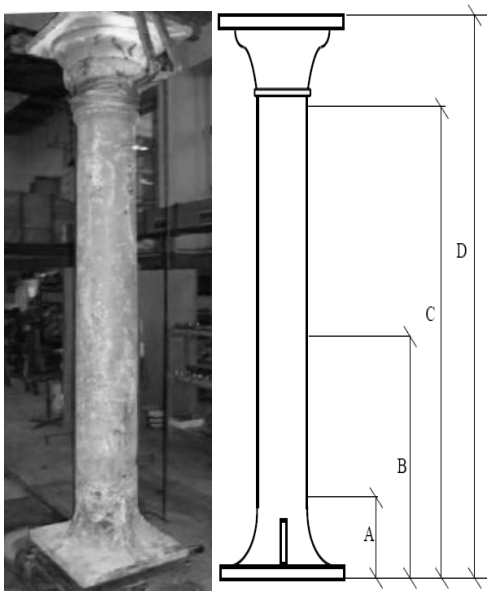

Fig. 5 The laboratory arrangement and geometry of cast iron column

Fig. 6 Failure of base plate during the column test at elevated temperature

3 CASE STUDY

3.1 Ambient temperature verification

The inputs to the procedure described upward are the geometric properties of the column: geometric imperfection $g = 10{,}07$ mm; distance to extreme fibres $G = 161{,}12$ mm; sectional area 27153,41 mm^2; area moment of inertia 251094438,07 mm^4; radius of gyration 96,16 mm and slenderness ratio 27,09. The imperfection parameters may be assumed as $\alpha = \square 0{,}85$; $\beta = 0{,}095$; $\lambda_0 = 0{,}7$; $\lambda_1 = 0{,}55$ The parameters to evaluate the reduction factor χ_c are derived for the slenderness $\lambda_c = 0{,}56$ and $\eta_c = 0{,}85$; $\varphi_c = 1{,}08$. The reduction factors $\chi_c = 0{,}50$ gives the load resistance F_{Rd} of the cast iron column at ambient temperature 4589,5 kN.

Prototype test on two cast iron hollow cylindrical columns of the Vinohrady Brewery of Prague had been conducted at ambient temperature. These are considered typical for the Brewery building. The columns are anticipated to carry service load $N_{\mathrm{Ed,ser}}$ of 1800 kN and load at the ultimate limit state $N_{\mathrm{Ed,ult}}$ of 2700 kN at ambient temperature and $N_{\mathrm{Ed},\theta}$ 1500 kN in fire situation. During the test were reached the the design values of the compression force $N_{\mathrm{Ed,ser}}$ and $N_{\mathrm{Ed,ult}}$. The failure mode was guided by the base plate rupture, see Fig. 5.

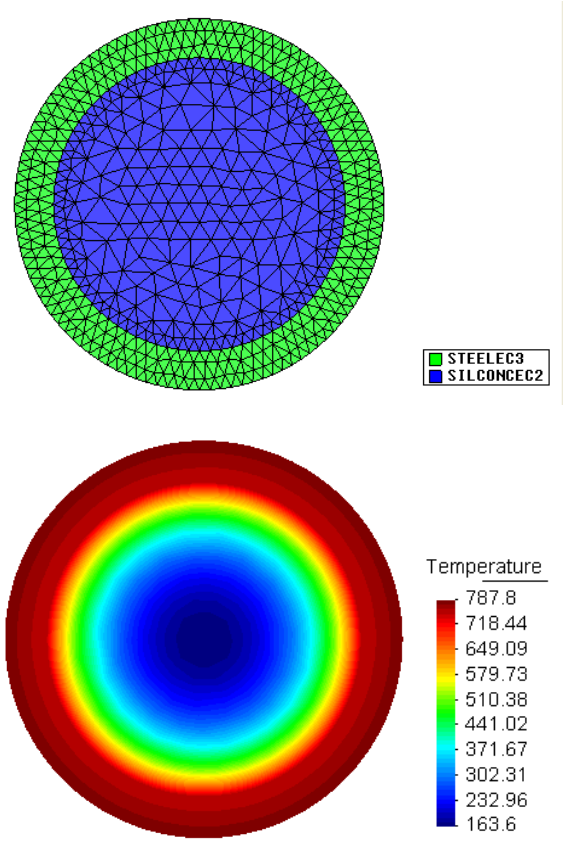

Fig. The meshing and the thermal gradient over the cross section of the concrete infill cast iron column exposed to nominal standard fire curve for 60 min

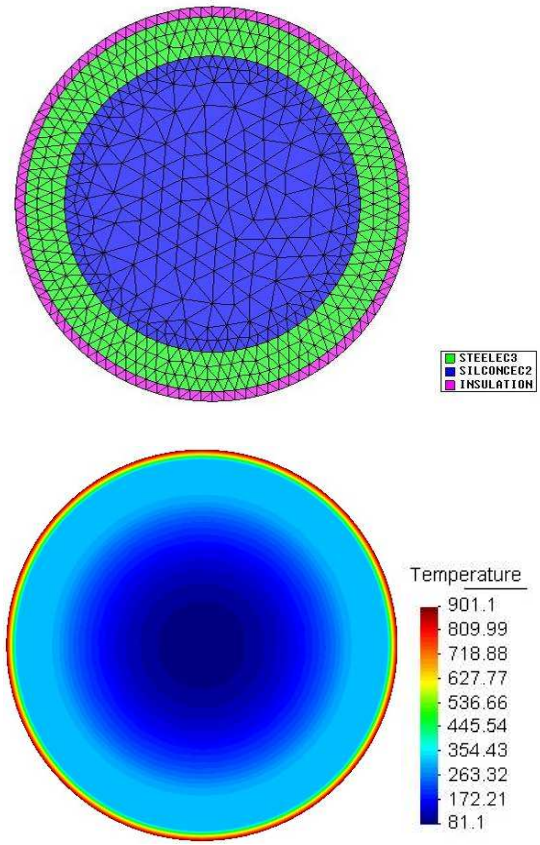

Fig. 8 The meshing and the thermal gradient over the cross section of the concrete infill and intumescent painted cast iron column exposed to nominal standard fire curve for 60 min

3.1 Elevated temperature verification

The transfer of heat was simulated by software SAFIR, see (Franssen, 2007). 2D representation was utilised. The heat induced due to fire is assumed to be uniform around the column meaning it is axi-symmetric like that of the section. Except of fire unprotected column were simulated the column filled by concrete, protected by intumescent coating and filled and protected solution. The geometric properties were taken as: external diameter, d_e = 301,8 mm; internal diameter, d_i = 238,4 mm; thermal conductivity 55 W/mK; specific heat capacity of cast iron at ambient temperature 460 J/kgK. The thermal properties of intumescent coating PROMAPAINT® SC were taken as thermal conductivity 0,2 W/mK; specific heat 1100 J/kgK; specific mass 350 kg/m; relative emissivity 0,8 and the effective thickness 8 mm, see Strejček et al, 2009. The average temperatures of the cast iron wall from the calculation are summarised in Tab. 1. The distribution of the temperature in the column is shown at Fig 7, and 8. The average temperature of the cast iron of the filled unprotected column varies in 60 min of nominal fire from 788 °C till 750 °C, but in case of protection by intumescent coating only from 409 °till 413 °C and with infilling from 354 °C till 274 C. The fire resistance was calculated based on the assumption of the similar imperfection factors as at the ambient temperature, see upward according to Rasmussen and Rondal (1997). The results are summarised at Tab. 1.

Tab. 1 Average temperatures, reduction factors of 0,2 % proof strength in the compression and of modulus elasticity, fire resistance and reduction of resistance for different fire protection of cast-iron column in Vinohrady brewery exposed to 60 min at nominal standard fire

Condition	Temperatures	Factors	R60	Reduction of resistance
Fire unprotected column	864 °C	0,08/0,07	395 kN	8 %
Concrete filled column	769 °C	0,14/0,07	687 kN	15 %
Intumescent coated column	411 °C	1,00/0,67	4530 kN	99 %
Coated plus filled column	314 °C	1,00/0,82	4547 kN	99 %

4 SUMMARY AND ACKNOWLEDGMENT

The procedure of the fire resistance of the columns based on European fire design was completed and applied to a study stay of the reconstruction of Vinohrady brewery. The results of prediction of the fire resistance show a smaller improvement of concrete infilling in R60 as may be expected. The case study recommended applying both protections infilling as well as intumescent coating.

This outcome has been achieved with the financial support of the Czech Ministry of Education, Youth and Sports, project MŠMT CIDEAS No. 1M0579.

REFERENCES

Blanchard J., Bussell M., Marsden, A. and Lewis, D. (1997), Appraisal of Existing Ferrous Metal Structures Stahlbau 66(6).pp. 333 - 345.

Degefa M. (2008), Cast Iron Columns under Ambient and Elevated Temperature, with Vinohrady Brewery's Case Study, Master thesis at Czech Technical University in Prague, p. 64.

Degefa, M., Wald, F., Kolísko, J., Matějka, M., Improvement of Fire Resistance of Cast Iron Columns, v Protection of Historical Buildings PROHITECH 09. London: Taylor & Francis, 2009, vol. 1,2, s. 1378-1391. ISBN 978-0-415-55803-7.

EN 1991-1-2: 2002,. Eurocode 1: Basis of design and actions on structures – Part 2-2: Actions on structures – Actions on structures exposed to fire, CEN, Brussels.

EN 1993-1-1: 2005, Eurocode 3: Design of steel structures – Part 1-1: General rules and rules for buildings, CEN, Brussels.

EN 1993-1-2: 2005, Eurocode 3: Design of steel structures – Part 1-2: General Rules – Structural fire design, CEN, Brussels.

Franssen J. M. (2007), Users Manual for SAFIR 2007. A Computer Program for Analysis of Structures Subjected to Fire. University of Liege.

Korunní dvůr http://www.korunnidvur.cz/lokalita-historie.php.

Ramberg W. and Osgood, W.R. (1943), Description of Stress Strain Curves by Three Parameters. Technical Note No. 902, National Advisory Committee for Aeronautics, Washington DC.

Rondal J. and Rasmussen Kim J.R. (2003), On the Strength of Cast Iron Columns. Research Report No R829. The University of Sydney, Department of Civil Engineering, Sydney.

Strejček M., Cinar R., Stanke V., and Wald F. (2009), Effective parameters of fire protection, in Application for fire engineering, CTU in Prague, pp. 164 - 171, ISBN 987-80-01-04266-3.

Twilt L. (1999), Urban Heritage and Building Maintenance. Problems and Possibilities, in Urban Heritage Building Maintenance – Iron and Steel, Delft University of Technology, The Netherlands.

Wouters I. and Mollaert M. (2002), Evaluation of the Fire Resistance of the 19th Century Iron Framed Buildings, Fire technology, 38, Kluwer Academic Publishers. pp. 383 - 390.

SOFTWARE APPLICATIONS FOR ESTIMATION OF FIRE RESISTANCE OF THE BUILDINGS CONSTRUCTION

Kamil Vargovský [a]

[a] Specialist and engineer of the fire protection, Self-employed No-G/2008/00958-2, Business license 670-16902

ABSTRACT

The aim of this article/paper is the presentation of the practical experiences with projects and their software's applications by the demonstration of the fire resistance of building's constructions for the need of fire engineering with the use of euro codes.
The main part of this work is the judgement of the fire resistance of the particular realized project of the overhead building construction. This project was accepted by Ministry of Interior of the Slovak Republic – Department of Firemen and Rescuers.
The judgement of the fire resistance presents the software outputs as a part of fire resistance proving, by means of "differential method" and "Finite Elements Method" for calculations and simulation.

1. INTRODUCTION

The main subject of this article is an example of fire resistance proving for the particular realized project of concrete building construction. Software's outputs are integral part of fire resistance proving.
An example is the fire resistance test (REI, REW 120) of the building construction by means of the calculation for the ceiling made of load-bearing reinforced concrete hollow panels, for the inside fire actively cooled by Stable Fire Extinguisher (by Sprinklers) and for the outside fire of the object of furniture storehouse extension.
The estimation of fire resistance is processing theoretical-experiment with help of calculations and simulations and by STN EN series 1363, STN EN 1365 a eurocodes series STN 1990, particularly STN EN 199x-1-2.
In the sense of § 8 ministry regulation MI SR č. 94/2004 Z.z., was estimation of fire protection done for the fire resistance of roof construction:

- REI 120D1 (i → o) –interior fire by STN EN 1991-1-2 (zone model);
- REI 120D1 (o → i) –exterior fire by STN EN 1363-2 (standard exterior fire);
- by limiting states of fire resistance – STN EN 1363-1;
- by differential method of unstationary heat conduction;
- by finite element method (FEM);
- by means of results of the fire resistance test - protocol EMI Ltd. (Hungarian), REI 90 by EN 1363-1 (standard interior fire).

2. METHODOLOGY

2.1 Description of construction

Load-bearing reinforced concrete hollow panel forming rectangular section with longitudinal holes. The panels has diameter of 200/1200mm, and the holes diameter is about 155 mm. The panels are like simple beam.

Material:
Concrete C40, steel cable - Ø 12,5 (EN 138-79) protection thickness is 25 mm.

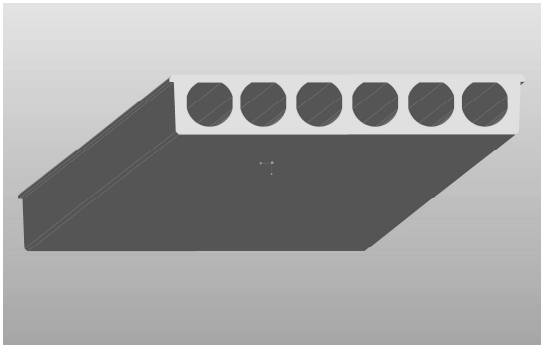

Fig. 2 Loadbearing reinforced concrete hollow panel

2.2 Entrance thermo-technical parameters considered in calculations

In calculations were considered thermo-technical parameters of steel cable by:

Coefficient of the heating conduction	$\lambda = 54 - 0{,}0003\ T$	$[W.m^{-1}.K^{-1}]$,
Volume weight	$\rho = 7850$	$[kg.m^{-3}]$,
Measuring heat	$c = 425 + 0{,}2\ T + 0{,}00038\ T^2$	$[J.kg^{-1}.K^{-1}]$,
Weight humidity	$v = 0$	[%].

In calculations were considered thermo-technical parameters of concrete by:

Coefficient of the heating conduction	$\lambda = 1{,}6 + 0{,}002\ T + 0{,}000000833\ T^2$	$[W.m^{-1}.K^{-1}]$,
Volume weight	$\rho = 2300$	$[kg.m^{-3}]$,
Measuring heat	$c = 1000 + 0{,}667\ T - 0{,}000278\ T^2$	$[J.kg^{-1}.K^{-1}]$,
Weight humidity	$v = 1{,}5$	[%].

2.3 Analysis strategy

Selected strategy: Combination 2Zones - 1 Zone Model
Transition criteria from 2 Zones to 1 Zone
Upper Layer Temperature B 500°C
Combustible in Upper Layer + U.L. Temperature B Combustible Ignition Temperature = 300 °C
Interface Height A 0,2 Compartment Height
Fire Area B 0,25 Floor Area

2.3.1 Parameters

Openings
Radiation Through Closed Openings: 0,8
Bernoulli Coefficient: 0,7
Physical Characteristics of Compartment
Initial Temperature: 293 K
Initial Pressure: 100000 Pa
Calculation Parameters
End of Calculation: 7200 sec
Time Step for Printing Results: 60 sec
Maximum Time Step for Calculation: 5 s.
Air Entrained Model: Mc Caffrey
Temperature Dependent Openings
All openings activated at: 400 °C
Stepwise Variation

Temperature [°C]	% of Total Openings [%]
20	10
400	50
500	100

Linear Variation

Temperature [°C]	% of Total Openings [%]
20	10
400	50
500	100

Time Dependent Openings

Time [sec]	% of Total Openings [%]
0	5
1000	100

2.3.2 Compartment

Form of Compartment:	Rectangular Floor	
Height:	3	m
Depth:	43	m
Length:	40	m
Roof Type:	Flat Roof	

2.3.3 Parametric Interior Fire - STN EN 1991-1-2 (zone model)

Fire Curve:	NFSC Design Fire			
Maximum Fire Area:	1720	$m_{ }$		
Fire Elevation:	0	m		
Fuel Height:	0	m		
Occupancy	Fire Growth Rate	RHRf [kw/$m_{ }$]	Fire Load qf,k [MJ/$m_{ }$]	Danger of Fire Activation
User Defined	75	6000	6186	1,4

Active Measures

Description	Active	Value
Automatic Water Extinguishing System	Yes	$\delta_{n,1} = 0,61$
Independent Water Supplies	1	$\delta_{n,2} = 0,87$
Automatic Fire Detection by Heat	Yes	
Automatic Fire Detection by Smoke	Yes	$\delta_{n,4} = 0,73$
Automatic Alarm Transmission to Fire Brigade	No	$\delta_{n,5} = 1$
Work Fire Brigade	No	
Off Site Fire Brigade	Yes	$\delta_{n,7} = 0,78$
Safe Access Routes	Yes	$\delta_{n,8} = 1$
Staircases Under Overpressure in Fire Alarm	No	
Fire Fighting Devices	Yes	$\delta_{n,9} = 1$
Smoke Exhaust System	Yes	$\delta_{n,10} = 1$
Fire Risk Area:	1720 m	$\delta_{q,1} = 1,83$
Danger of Fire Activation:		$\delta_{q,2} = 1,4$
	$q_{f,d} =$	3831,5 MJ/$m_{ }$
Combustion Heat of Fuel:		40 MJ/kg
Combustion Efficiency Factor:		0,8
Combustion Model:		Extended fire duration

2.3.4 Exterior Fire STN EN 1363-2

By the thermal effort of the sample from the outside is the wall afforded according to STN EN 1363 2 ar. 5.2 line of the outside fire (see the equation)

$$T_N = 660(1 - 0,687e^{-0,32t} - 0,313e^{-3,8t}) + 20 \quad (1)$$

where

T_N – is the average temperature in the oven [°C];

t — is the time from the beginning of the exam in minutes

The calculation of the thermal field -

The calculation of thermal fields of the considering composition of that construction comes out from the Fourier partial differential equation of the unstationary heating conduction that has in differential form this version

$$\frac{dT}{dt} = a \cdot \frac{d^2T}{dx^2} \tag{2}$$

where: dT – is the increase of the temperature [°C];
dt – is the increase of the time [s];
dx – is the thickness of the layer [m];
a – is the coefficient of the heating condution [$m^2.s^{-1}$].

We can express the coefficient of the heating condution by the relation

$$a = \frac{\lambda}{c.\rho} \tag{3}$$

Where: λ – is the coefficient of the heating conduction [$W.m^{-1}.K^{-1}$];
ρ – is the volume weight [$kg.m^{-3}$];
c – is the measuring heat [$J.kg^{-1}.K^{-1}$].

The calculation of the thermal field runs step by step in time intervals dT.
In each time interval are set temperatures in levels separating individual layers. Time interval of the calculation is necessary to set so that for all the materials will be completed the condition

$$dT \leq \frac{dx_i^2}{2.a_i} \tag{4}$$

By the instillation of the thermal technical values from (2) to (3) we gain the condition for the maximal time step

$$dT \leq \frac{dx_i^2.c_i.\rho_i}{2.\lambda_i} \tag{5}$$

Where: dx – is the thickness of the single layer it's type of the material [m];
a_i – is the highest value of the coefficient of the heating conduction is type of the material in the examinated thermal area of 20 °C to 1000 °C [$m^{-2}.s^{-1}$].

3. SUMMARY AND ACKNOWLEDGMENT

3.1 Results for Interior Fire (zone model)

Fire Area: The maximum fire area (1720.00m˛) is greater than 25% of the floor area (1720.00m˛). The fire load is uniformly distributed.
Switch to one zone: Lower layer Height < 20.0% compartment height at time [s] 343.51

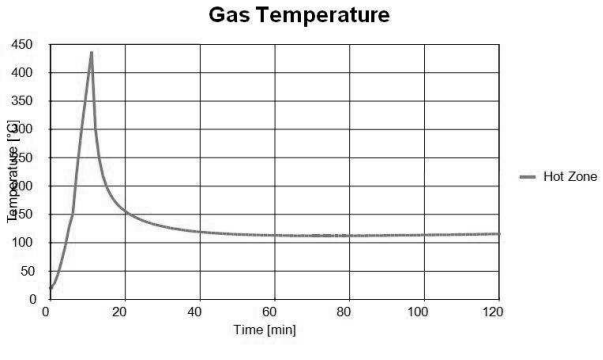

Peak: 437 °C At: 11 min
Fig. 1 Hot Zone Temperature

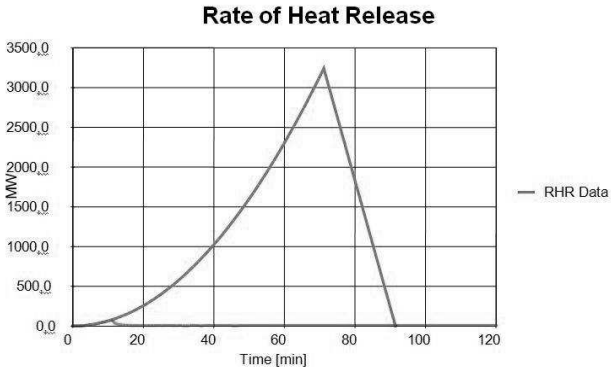

Peak: 3241,41 MW At: 71,2 min
Fig. 2. RHR Data

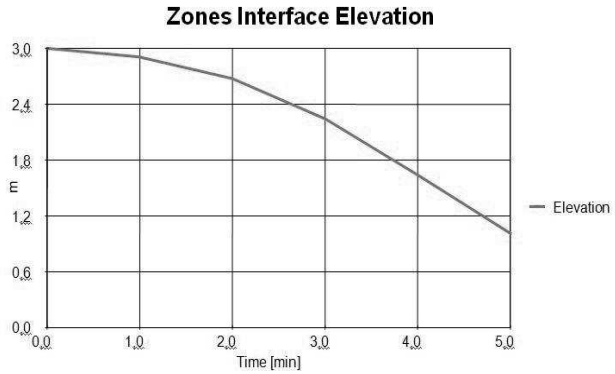

h = 1,00 m At: 5,00 min

Fig. 3 Zones Interface Elevation

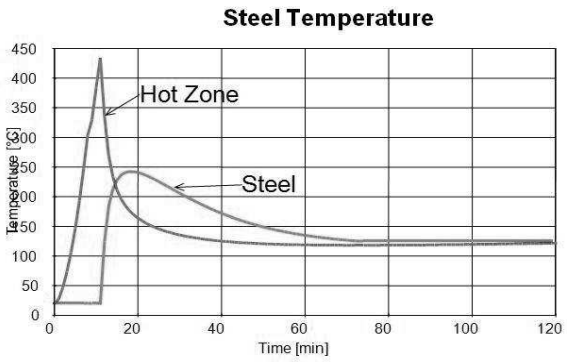

Peak: 434 °C At: 11 min

Fig. 4 Hot Zone and Steel Temperature

STEEL

Protected Section

Catalogue Profile: Steel cable - Ø 12,5 (EN 138-79), coating of steel cable is 25 mm.

Exposed to Fire on: 1 sides

Hollow Encasement

Protection Material: With Constant Values

Protection Thickness: 25 mm

Material Name: Concrete

Unit Mass	Specific Heat	Thermal Conductivity
[kg/mł]	[J/kgK]	[W/mK]
2230	900	1,5

HEATING

Profile heated by: Hot Zone Temperature

Convection coefficient: 35 W/m¸K

Relative emissivity: 0,8

FIRE RESISTANCE

Element Submitted to Bending

Nominal Steel Grade: S 235

Design effect of actions in fire situation

Plastic Redistribution of the Bending Moment

Loading: Uniform Distributed Load - Simple Beam

$P_{fi,\,d} = 13{,}973$ kN/m^2

Span = 8,2 m

Adaptation Factors

Non-uniform Temperature Across the Cross-Section: $k_1 = 0{,}7$

Non-uniform Temperature Along the Beam: $k_2 = 1$

RESULTS

Critical Temperature: 476 °C - by results of the test about fire protection - protocol EMI Ltd. (Hungarian), REI 90 by EN 1363-1 (standard interior fire)

Failure Mode: Flexural Buckling

Class of the Cross Section in Fire: 1

Steel Temperature 242 °**C** At: 18 min

Fire Resistance: (242,0°C < 476 °C) 120,00 min **REW 120 (i →o)**

3.2 Results for standard Exterior Fire

3.2.1 By differential method

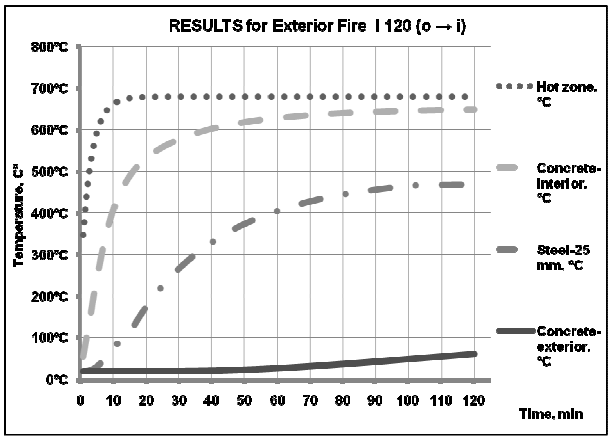

Fig. 5 Graph of the calculation of the unstationary heat conduction

Time, min	Hot zone,°C	Concrete-interior,°C	Steel-25 mm,°C	Concrete-exterior,°C
1	346,1	53,3	20	20
15	676,3	488,6	114,5	20
30	680	577,2	265,3	20,3
45	680	611,4	352,8	22,4
60	680	628,7	405	27,2
90	680	643,9	456,4	42,5
120	680	649,3	469	60,3

Tab. 1 Results of calculation of the unstationary heat conduction

Temperature on interior: 649,3 °C in: 120. minute
Temperature on exterior: 60,3°C in: 120. minute (E,W 120)
Temperature of steel cable: 469,0°C in: 120. minute (R 120)
Critical Temperature: 476 °C
Fire Resistance: (469,0°C < 476 °C) 120,00 min **REW 120 (o →i)**

3.2.3 By finite element method (FEM) for standard Exterior Fire

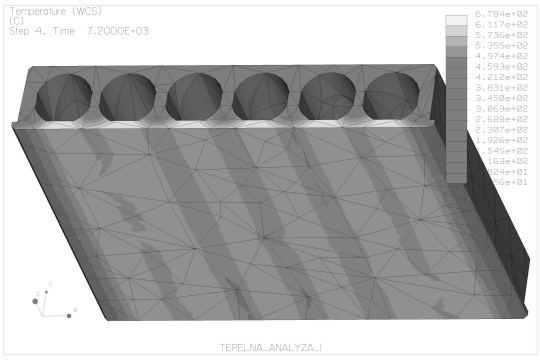

Fig. 6 Results with network analysis by finite element method (FEM) - bottom view.

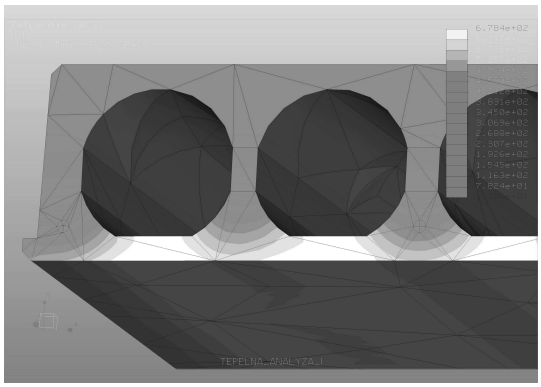

Fig. 7 Results with network analysis by finite element method (FEM) - bottom view.

Temperature on interior: 678 °C in: 120.minute
Temperature on exterior: 78,2 °C in: 120. minute (E,W 120)
Temperature of steel cable: 459,3 °C in: 120. minute (R 120)
Critical Temperature: 476 °C
Fire Resistance: (459,3°C < 476 °C) 120,00 min **REW 120 (o →i)**

3.3 Expert opinion

The subject of this paper was estimation of fire resistance (REI, REW 120) of the building construction by the calculation intended for „load-bearing reinforced concrete hollow panels, roof construction with Sprinkler“, for object storehouse extension.
The judgement was made by theoretical theoretical-experimental with help of calculations and simulations and by STN EN series 1363, STN EN 1365 a eurocodes series STN 1990, particularly STN EN 199x-1-2.

It was proved that: load-bearing reinforced concrete hollow panels, roof construction, for object storehouse extension by the fire exposition from the inside according with Sprinkler to STN EN 1991-1-2 suits to the fire resistance REW 120 (i →o) and from the outside according to STN EN 1363-2 suits to the fire resistance REI 120 (o →i).

REFERENCES

EN 13501-2 Fire classification of construction products and building elements - Part 2: Classification using data from fire resistance tests, except ventilation services.

EN 1363-1 Fire resistance tests – Part 1: Essential requirements.

EN 1363-2 Fire resistance tests – Part 2: Alternative and additional procedures.

EN 1365-1 Fire resistance tests for load-bearing elements– Part 1: Walls.

EN 1990 Eurocode: Principles of construction projection (E)(including Attachment A1: Buildings(S)).

EN 1991-1-2 Eurocode 1: Constructions loading –part 1-2: general loading – construction loading strained by the fire.

EN 1992-1-2 Eurocode 2: Design of concrete structures – Part 1-2: General – Structural fire design.

Protocol by over partial researches fire resistance pro requisites statements deuces, published EMI Kft. (EMI Ltd - society pro quality control and innovation in the building industry), Budapest, April 2005.

Technical and drawing documentation from customer.

THE IMPACT OF FLAME RETARDED TIMBER ON GREEK INDUSTRIES

D.Tsatsoulas [a]

[a] Greek Fire service (Kritis 46 & Martiou, 54008, Thessaloniki)

INTRODUCTION

Wood has many good properties as a construction material. It is heavily used in building construction and building because of its ease of processing, physical and mechanical properties, aesthetic, environmental and health aspects[1][2]. Wood is also used in many industrial applications for purposes such as surface lining material, furniture, flooring, roof, shelves, pallets, wooden scaffolding for both offshore and onshore, packing cases etc[3][4].However with current regulations and standards[5], this is not allowed, as this would significantly add to the fire load within a room in a fire scenario i.e wooden materials in different forms, with the highest percentages, contribute as first ignited materials in fire initiation and spreading and have a major impact in fire losses[3][4][6].The above clearly signals the importance of controlling the ignition resistance, and flammability of Timber as used in different forms in various constructions. Therefore, it is possible to increase the fire performance of wood, with the application of Flame Retardants (possibly intumescent).

There has been a significant but limited amount of work studying the effect of flame retardants for applied on wooden surfaces. Previous research has shown that flame retardants applied to wood have had a positive affect on the burning behaviour of wood, in terms of ignition and the most important variable to describe fire hazard the heat release rate, HRR[1][7]. Intumescent Flame Retardants have also been the subject of study, in their own right. Birgit et al[2] presented comparative test data with fire retardant treated and untreated wood products. The test results show a significant differences between these two groups. The parameters included in the comparison are t_{ig}, HRR (peak and average values) and total HRR. The wood based products tested in different small-scale national fire tests and in the full-scale room fire tests. Fire retardant wood products achieve an improved classification both in present national systems and in possible new systems based on the cone calorimeter and room fire test. D.Tsatsoulas et al[6] used FTIR to investigate toxic emissions of eight species of wood. 'Significant' acrolein peak values are measured for all samples. At low irradiance (i.e., 35kW/m^2), facing types of timber, e.g., MDF, Chipboard, with melamine or maple increases significantly the ignition resistance of MDF and Chipboard by a factor of 1.5 to 2, due to the flame retarding properties of melamine and maple.

In the present work the effect of typical intumescent flame retardant (latest technology) will be examined on representative types of Timber. Analysis involved thermal behavior, and toxic species analysis of the samples.

1 EXPERIMENTAL

The university of Leeds apparatus[4][8-9] used was: I. a standard Cone Calorimeter manufactured in accordance to ISO 5660 (1993) and ASTM E1354 (1992). The tests were carried out in accordance with the test procedure of ISO 5660, II. a 1.56 m^3 enclosed fire test facility, 1.4m x 0.92m x 1.22m, with separate entrained air inlet at floor level and fire product exit at ceiling level, with online effluent gas analysis equipment (FTIR). A TEMET GASMET CR-Series portable FTIR analyzer was used to experiment with virgin samples that were chosen to be painted with flame retardants and for all flame retarded samples. This has a multi-pass, gold-coated sample cell with a 2m path length and volume of 0.22l. A liquid nitrogen cooled MCT detector was used that scans 10 spectra per second and several scans are used to produce a time-averaged spectrum. The instrument was calibrated by the manufacturers for all the species using reference gas concentrations. The response time of the instrument is 5s to reliability resolve all measured toxic species.

A test time duration of 600s was generally adopted, although, in certain flame retardant samples, the duration was extended up to 1000sec, depending on the thermal behavior of the specimen. The reason for that is that the present work aims at examining the development of fires on wooden samples painted or not with fire-retardant paints during the early stage of fire development, and for a period of time up to 10-15 minutes min. This period in real fire conditions, covers the time needed for the evacuation of the industrial plant by its staff, the potential intervention of the fire-safety staff of the plant, and the arrival of the fire department to extinguish the fire[4][6].

2 EXPERIMENTAL FIRES CONFIGURATION

Tests were conducted in the cone calorimeter(small scale) using : substrates were 100mm square and thickness varied from 19mm to 22mm. Three (3) types of wood intumescent flame retardants were used to represent main classes of commercial products i.e. 'Zero Flame' (water based paint), 'Varnish Zero Flame'(varnish water based) and 'Synto Flame' (solvent based paint). This selection of flame retardant was based on its chemical composition, since each one represents a large homogeneous class of products, and also on the applications for which each one has been designed.
The selection of the heat flux is a very important factor when undertaking Cone Calorimeter tests [5].The current tests were carried out in the horizontal orientation at heat fluxes of 35, 50, 65, 80 kW/m^2, to represent a possible range of heat fluxes to be encountered in a developing industrial fire[4]. Also, the aim was to examine all bare, flame retarded samples in the same radiation in order to be able to compare them. Fewer tests have been performed at $80kW/m^2$ because of technical difficulties which did not allow to performed further experiments at such a large value of irradiance. Each test was carried out at least three times, to gain some understanding of test repeatability. Based on the above, eight (8) species of wood which constitute common applications in different forms i.e floor, ceiling, shelves, pallets, packing cases, scaffolding, furniture etc., were chosen for experimental investigation [4][6]. In total 96 tests have been performed in total at various irradiances, in order to determine various flammability characteristics of a range of virgin wood species[4][6]. Three typical types of wood i.e. pine, MDF, blockboard were chosen as representative from those used in virgin form, for painting with the typical types of flame retardants that mentioned above (total performed tests 54). The abbreviations are:, Bb 'Blockboard', ZF 'Zero Flame', SF 'Synto Flame', ZFV 'Zero Flame Varnish', .
Tests were conducted in the enclosed Fire Rig (medium scale) using: I. Untreated wooden crib II. Fully flame retarded wooden cribs III. Partial flame retarded wooden crib. From the various types of wood found in different structures in the industry, pine was selected for medium-scale experimental investigation, since it is one of the most commonly used type of wood is "easy-to-use" and produced in large quantities, especially, from the Mediterranean forests [4]. It was chosen to be tested in form of cribs, because, in real fires there are complex wooden geometries and configurations strongly affecting the "spreading of fires" [4][6]. Thus, a wooden crib, which includes a crossed layer of sticks, simulates complex wooden structures, where the confinement of heat and cross-radiation among the surfaces allows for the efficient burning of wooden surfaces, and the rapid development of fires. Analysis involved thermal behavior, and toxic species analysis of the samples. The experiments were run under controlled airflow conditions. The airflow rate used in the experiment was 75 kg/h, i.e., corresponds to well ventilated fire conditions. The reasons for choosing the above-mentioned high ventilation rate were (i) to reasonably simulate the ventilation conditions in the beginning of most real industrial fires [4], (ii) To allow comparisons with small-scale experimental works in cone calorimeter, where the experimental conditions are also well ventilated.
It should be emphasized, that the objective was not to determine or use the best product in the market, but to establish general patterns of behavior of Timber with or without flame retardant.
Wooden cribs with average fire load equal to 45 kg/m^2(~$765kJ/m^2$) were chosen to perform medium scale tests. In order for the crib to be easily ignited a small volume of ethanol was used in a dish. The ethanol was placed directly below the center of the crib (as "worst" case position) and was ignited using a blow lamp and the crib placed on top. 'Zero-flame' retarded paint was chosen for coating the wooden crib, since it is water-based and especially designed for interior wooden

surfaces, like those simulating the wooden cribs under experimental testing. The following (% flame-retarded % bare) wooden cribs were tested experimentally in order to examine different cases of fire development at the ventilation rate mentioned above.

- 100% flame retarded, where all their surfaces were painted with 'Zero-Flame' retarded paint. Total surface, coated in two (2) layers of flame retarded paint: 0.7 m^2. Overall, three (3) wooden crib tests were performed with 100% flame retarded surfaces. For their quick ignition, 6g ethanol, 20g ethanol, and 30g ethanol were used, respectively, in the manner, described in the case of ignition of virgin crib.
- 50% flame retarded, 50% bare wood, where the first 5 layers (21 sticks) were treated with 'Zero Flame' retarded paint(two(2) coats), and the rest 5 layers (21 sticks) were left untreated. One (1) test was carried out, and 6g ethanol was used as ignition source in the same way described before.
- 60% bare wood, 40% flame retarded wood, where 0.437m^2 were left untreated, i.e 26 sticks in the first 7 layers, while the remaining 0.268 m^2, i.e., 16 sticks, were painted with flame retardant paint(two(2) coats), included in the 7^{th} and 10^{th} (last) layer of wooden crib. Two (2) tests were performed with 6g and 20g ethanol as ignition source, respectively.

The reasons for using the above quantities as ignition sources were: to simulate sources of real fires starting, guided by the statistical analysis of industrial fires[4], and show whether they affect the faster spreading of fires or not. All the above tests using various wooden cribs with different strength of ignition sources give an indication whether the application of flame-retardants at different parts of wooden surfaces located near potential ignition sources (as first or second ignited materials) contribute to suppression or to slower fire developing, and show how they may affect the concentrations of the released toxic gases when the wooden surfaces are burned.

3 THERMAL BEHAVIOR- EXPERIMENTAL RESULTS

Fire development results of small scale experimental work(cone calorimeter) cover: i Time to ignition(s), ii HRR(kW/m^2). All tests were fairly repeatable in terms of the tig and HRR values i.e 2-4% Std.dev.(expresses the standard deviation as a percentage of the average value). Experimental results represent the mean of a minimum of three (3) tests. In all flame treated samples, the intumescent paint swell into a thick, robust foam upon exposure to heat, thus protecting the underlying material from fire by providing a physical barrier to heat and mass transfer.

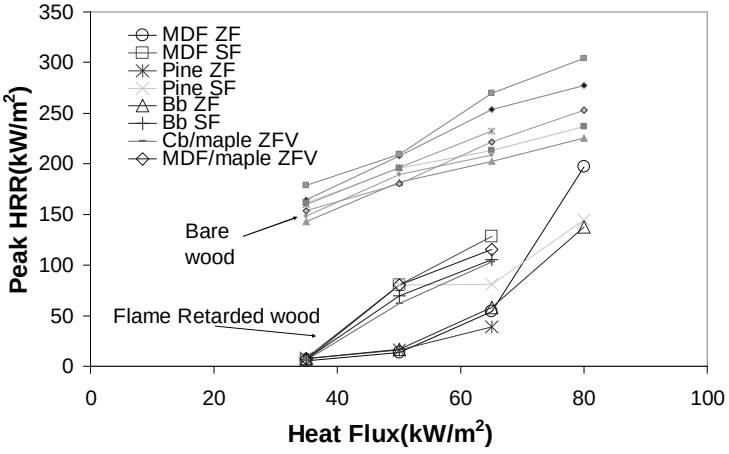

Fig. 1 : Peak HRR(kW/m^2) for various flame retarded samples.

As shown in Figure 1, the peak HRR values increase with increasing in irradiance. First of all, in all cases, the irradiance of 35kW/m^2 did not lead to ignition. At 50 kW/m^2 irradiance some of the samples ignited, particularly those that had been painted with the solvent based ('Synto Flame') retardant. In all cases the ignition delay was very long compared to bare wood data, and this suggests that the ignition process is dominated by the flame retardant coating behavior rather than the substrate. At 65kW/m^2 all samples ignited, however at remarkably longer ignition times than

those observed in the corresponding virgin wood samples, at the same irradiance. At 80kW/m^2 fewer experiments were performed for the reasons mentioned above the HRR was much higher than at lower irradiances, indicative a fully established flame in agreement with the observation. The most effective behaviors are observed in 'Zero Flame', compared to 'Synto Flame' samples; this is attributed to their different chemical composition (water-based versus solvent-based).
Fire development results of medium scale experimental work (fire enclosure) cover: i Time to ignition(s), ii HRR(kW/m^2). One untreated sample was tested using 6g of ethanol as ignition source. The corresponding plot in Figure 2 shows that the untreated sample clearly burned faster. The presence of the FR paint clearly suppressed (either partially or totally) the combustion process. 'No ignition' of the fully treated (100%) crib was detected even when the ignition source was changed from 6g to 30g of ethanol. The fire mass loss as a percentage of the initial mass is shown as function of time in Figure 3. It is obvious that the fire mass loss of flame retarded samples was slower, especially when the treated surfaces are closer to ignition source. It is reminded that % indicates the fraction of the crib (starting from the bottom) that was either flame retarded or untreated

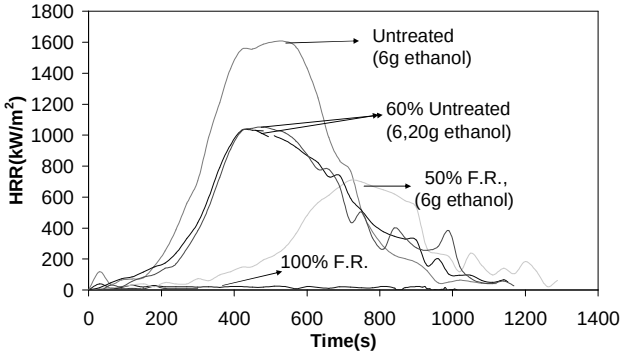

Fig 2: HRR(Kw/m^2) vs time for pine cribs with different FR treatment levels with 75kg/h air flow rate.

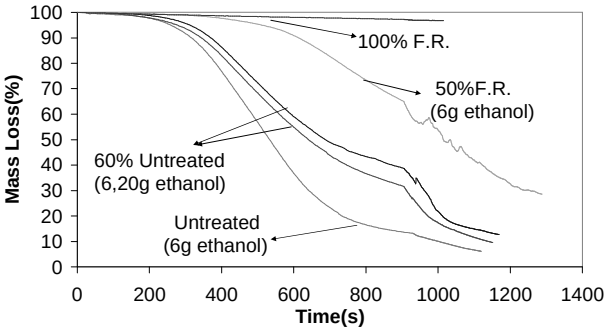

Fig 3: Mass Loss (%) vs time for pine cribs with different FR treatment levels with 75kg/h air flow rate.

An interesting finding evident in Figure 2 is that with regard to the peak HRR the 50% treated test produce about 45% of the untreated peak HRR. However the effectiveness of this partial treatment is in fact far greater when viewed in terms of the '300s average HRR' where it is shown that it is almost as effective as the 100% treated sample (generally less than 15% of the average HRR of the untreated sample).The results clearly show that FR treatment can be very effective and additionally it is not necessary for the whole area to be treated. A partial treatment of the areas nearest to potential ignition sources may be a workable solution which can almost be as effective as the 100% treatment but absolutely much more economical.

4 EMISSIONS - EXPERIMENTAL RESULTS

FTIR analyzer was connected to the Cone Calorimeter for only virgin samples that were chosen to be painted with flame retardants and for all flame retarded samples , at 35, 50, 65 kW/m^2. Figures (4-5) compares CO emissions (ppm) of treated and untreated samples of MDF at 35 and 50 kW/m^2. In cases where 'no ignition' was achieved (i.e. for both flame retardants at 35kW/m^2 and for 'Zero Flame' at 50kW/m^2) the CO emissions maximum levels was approximately half of those of bare MDF. However, when the flame retarded samples were ignited the CO emissions were more than doubled (compared with the Bare MDF) results and more over they appeared to increase with higher heat fluxes . Similar behavior occurred for the other kind of timber that have been tested.

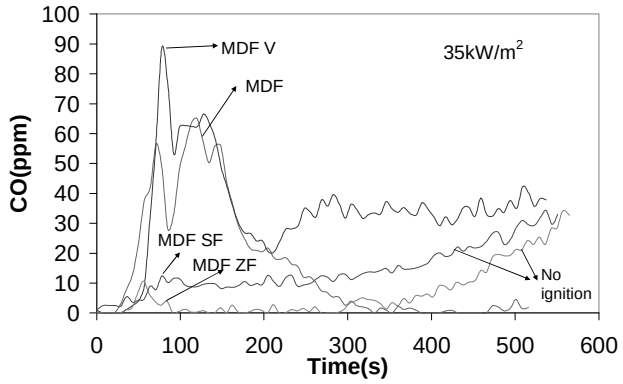

Fig. 4 :CO emissions(ppm) vs time for MDF, varnished MDF, 'Zero Flame' retarded MDF, 'Synto Flame' retarded MDF at 35kW/m^2

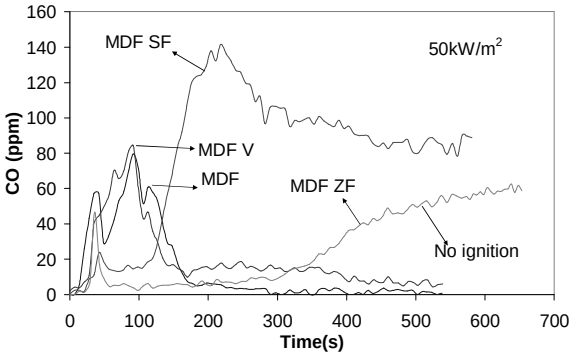

Fig. 5 :CO emissions(ppm) vs time for MDF, varnished MDF, 'Zero Flame' retarded MDF, 'Synto Flame' retarded MDF at 50kW/m

FTIR analyzer was connected to the enclosed fire rig for all the tests. Only measurements of toxic gases that show "significant" concentrations for life safety based on the maximum exposure levels recommended by COSHH for individual combustion products[10] are reported in this work. Toxic yields of main toxic gases were assessed [4] (see Figures 6 and 7) for better comparison of toxic species of wooden samples, untreated or treated in different parts with typical flame retardant.

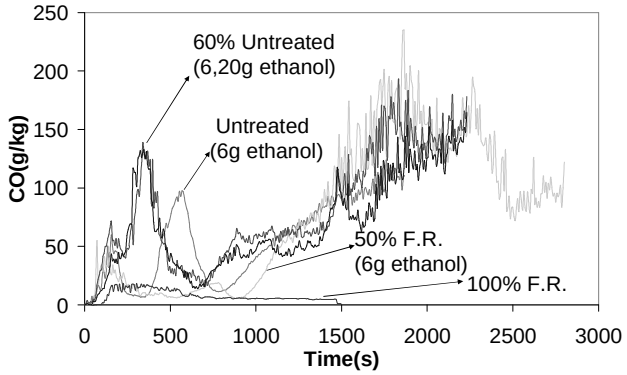

Fig. 6.: C0 mass emissions (g/kg) vs time(s) for various (pine) cribs with 75kg/h air flow rate.

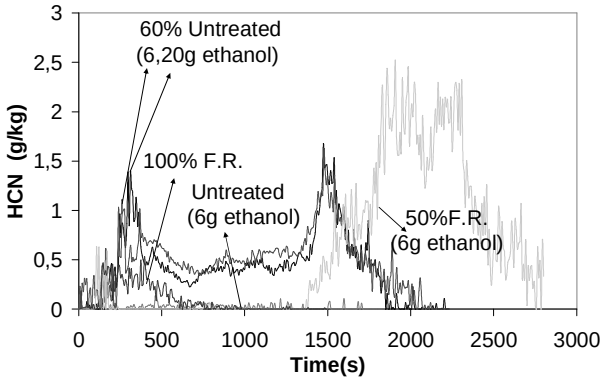

Fig. 7.: HCN mass emissions(g/kg) vs time(s)for various(pine) cribs with 75 kg/h air flow rate.

A direct comparison of the effect of the flame retardant used is achieved by 'Peak $n_{(toxic\ gas)}$ Coefficient Ratio' (P. $n_{(toxic\ gas)}$. R.) (see *Eq.* (1) below).

$$\text{'P.n}_{(toxicgas)}\text{.R.'} = \frac{P.n_{toxicgas}.CoatedSample}{P.n_{toxicgas}.BareSample}, \qquad (1)$$

where $n_{toxic\ gas}$ volumetric (ppm). Therefore, the effects of flame retardant treatment on major toxic emissions compared with the bare samples are shown on the following Table 1.

The effect of FR treatments on major toxic emissions in small scale experimental work compared with the bare samples, are shown in Table 1.In the cases of flame retarded samples, where there was 'no ignition' of the samples (at 35kW/m^2 and 50kW/m^2), there were similar or less toxic emissions compared to the bare samples. At higher irradiance (65kW/m2) the benefit was reduced or reversed due to more involvement of the flame retarded paint in flaming combustion. It should be noted that irradiances of the order of 40kW/m^2 or more are generally associated with the receiver being in close proximity (less than one meter) to a large fire (more than 1MW) or actually engulfed by it. So, in these circumstances, the fire is well established and the data shows that the retardands would be ineffective at this stage.

Tab 1 : Comparative effects of flame retardant treatment on major exhaust emissions (Averaged for all substrates i.e MDF,Blockboard,Pine).

Coated emission / *Bare emission*	35kW/m^2 Heat flux		50kW/m^2 Heat flux		65kW/m^2 Heat flux	
	'Zero Flame'	'Synto Flame'	'Zero Flame'	'Synto Flame'	'Zero Flame'	'Synto Flame'
'Peak **CO**(ppm) Ratio'	⇩	⇩	⇩	⇧	⇧	⇧
'Peak **HCN**(ppm) Ratio'	≈	≈	≈	≈	⇧	⇧
'Peak **Acrolein**(ppm) Ratio'	⇩	⇩	⇩	≈	≈	⇧
'Peak **N0** (ppm)Ratio'	≈	≈	≈	≈	⇧	⇧

The effect of FR treatments on major toxic emissions in medium scale experimental work compared with the bare samples, are shown in Table 2. In most fully-treated (100%) cases, even in the half-treated (50%) cases, lower or almost equal to unity emissions were measured compared with the bare samples. This is due to the fact that, in such cases, due to the in-tumescent action, there was either 'no ignition' of the samples (100%-treated cases), or a considerable delay was seen (50%-treated cases). It is worth noting that 50% treatment is some cases was more effective to reduce toxic emissions compared with 100%-treated cases and, of course, much more inexpensive. This may be attributed to the fact that less flame retardant paint was involved in combustion in these cases. Excessive HCN and N0x occurred in 60% of the untreated cases due to the considerable involvement of the flame retardant paint in flaming combustion, since it contains N in its chemical composition, as mentioned before.

Tab 2 : Comparative effects of flame retardant treatment on major exhaust emissions (during flaming combustion).

Coated emission / *Bare emission*	100%F.R. 6g ethanol	100%F.R. 20g ethanol	100%F.R. 30g ethanol	50%F.R. 6g ethanol	60% Untreated 6g ethanol	60% Untreated 20g ethanol
'Peak **CO**(ppm) Ratio'	⇩⇩⇩	⇩⇩⇩	⇩⇩⇩	⇩⇩	≈	≈
'Peak **HCN**(ppm) Ratio'	⇩⇩	⇩⇩	⇩	⇩	⇧⇧	⇧⇧
'Peak **Acrolein**(ppm) Ratio'	⇩	⇩	⇩	⇩	≈	≈
'Peak **N0x**(ppm) Ratio'	⇩	⇩	≈	≈	⇧⇧	⇧⇧

≈ almost equal to unity.

Each arrow / ⇩ ⇧ indicates decreasing/increaing up to a factor of 2-3. Two arrows together is equivalent to a change by a factor of 3-6.Three arrows together is equivalent to a change by a factor for greater than 6.

5 CONCLUSIONS

- The effect of typical intumescent flame retardants (latest technology) on the most common types of Timber in Greek industries was examined in small and medium scale experiments combined with online effluent gas analysis equipment (FTIR).
- Analysis involved thermal behavior and toxic species analysis of the samples.
- No ignition' and lower toxic emissions compared to untreated samples were observed at 35kW/m2 (small scale).
- The same behavior was observed in those cases where wooden surfaces located next to ignition source had been treated (medium scale).
- It is proposed that the application of intumescent flame retardants on wooden surfaces located close to ignition sources in the most probable areas for a fire to break out, could be a safe and effective approach in reducing fire losses in industries
- The above experimental data (small and medium scale) are compiled in the form of a database that can be used for validation of mathematical fire models and related software applications.

6 SUGGESTIONS

- Performing of more small- and medium – scale experiments, treated with the updated technology of the intumescent paints (different parts of wooden cribs or some other form of samples), and using various ventilation rates to achieve both establishing and documentation of the contribution of intumescent technology in fire suppression.
- Different coatings should be evaluated in terms of durability, impact resistance, weatherability, etc.;

REFERENCES

Shields T.J, Silcock G.W.H, Moghaddam A.Z., Azhakesan M.A,Shang.J. 'Acomparison of fire retarded and non-fire retarded wood-bases wall linings exposed to fire in an enclosure'. Fire and Materials, vol.23:17-25, 1999.

Birgit A-L,Ostman, Lazaros D.T. 'Heat release and classification of fire retardant wood products'. Fire and materials, vol.19:253-258, 1995.

Spearpoint M.J. and Quintiere J.G. 'Predicting the piloted ignition of wood in the Cone calorimeter using an integral model-Effect of species, grain orientation and heat flux'. Fire safety journal, vol 36:391-415,2001.

D. Tsatsoulas. 'Industrial fires in Northern Greece. The influence of Flame retardant on Timber Fires'. Ph.D. Thesis, Leeds (UK) 2008.

D.Drysdale, 'An introduction to fire dynamics',2nd edition. Willey (1999).

D.Tsatsoulas, H.N.Phylaktou and G.Andrews. 'Thermal behaviour and toxic emissions of various timbers in Cone Calorimeter tests'. Third international Conference on Safety and Security Engineering, 1-3July 2009, Rome. In the proceedings of 'First International Conference on Disaster Management and Human Health Risk', pp.181-194, 23 -25 September 2009, New Forest, UK.

Babrauskas V. 'Ten years of heat release research with the cone calorimeter'. Heat release and hazard,vol.1, ppIII-1 to III-8,1993.

D.Tsatsoulas . 'Thermal behaviour and toxic emissions of various timbers in Cone Calorimeter tests' 'International Journal of Safety and Security engineering',*Vol.1, N01(2011)45-64.*

D.Tsatsoulas "Thermal behaviour and toxic emissions of flame retarded timber in Fire Enclosure tests",pp 295-306.Seventh International Conference on 'Risk Analysis 2010', 13-15 September, Algarve, Portugal.

EH 40/2005 workplace exposure limits 'containing the list of workplace exposure limits for use with the Control of Substances Hazardous to Health Regulations 2002 (as amended)', HSE Books, UK Health and Safety Executive.